

PHASE TRANSFORMATION IN SILVER-SELENIDE

by

Mahmood S. Choudry

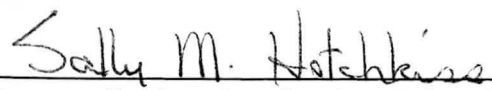
Submitted in partial fulfillment of the requirement
for the Degree of
Master of Science in Engineering
in the
Materials Science Program



Advisor

6/28/90

Date



Dean of the Graduate School

June 29, 1990

Date

YOUNGSTOWN STATE UNIVERSITY

August 1990

WILLIAM F. MAAG LIBRARY
YOUNGSTOWN STATE UNIVERSITY

ABSTRACT**PHASE TRANSFORMATION IN SILVER-SELENIDE**

Mahmood S. Choudry

Master of Science in Engineering

Youngstown State University, 1990

silver-selenide undergoes a phase transformation from α -phase to β -phase on cooling. These two phases have different electrical and thermodynamic properties. In this investigation, it has been attempted to study the characteristics of both phases through resistivity, thermodynamic, metallographic, and X-ray studies. This investigation directly results in the determination of the transformation temperatures upon heating and cooling of the specimen, the enthalpy of phase transformation, the crystal structure of the low temperature phase, the resistivity changes in both phases, and the effect of quenched-in vacancies on the phase transformation kinetics.

ACKNOWLEDGMENTS

The successful completion of the research project is achieved with the grace of The Almighty God.

In this concern I am heartily indebted to Dr. S. Ahmed, Professor of Metallurgy and Materials Science, Department of Materials Engineering, Youngstown State University. His pleasant and precise technical directions, suggestions, and making himself available even at odd times must be recognized.

I would like to express my appreciation to Dr. R. W. Jones, Director, Department of Materials Engineering, Youngstown State University. His kind and wise help in solving baffling problems is very much praised.

I would also like to acknowledge the help of Mrs. Shannon Hopkins, Secretary, Department of Materials Engineering.

TABLE OF CONTENTS

ABSTRACT	ii
ACKNOWLEDGMENTS	iii
TABLE OF CONTENTS	iv
LIST OF FIGURES	v
LIST OF TABLES	ix
CHAPTER	
1. INTRODUCTION	1
2. EXPERIMENTAL PROCEDURE	5
2.1 Sample Preparation	5
2.2 Resistivity Studies	6
2.3 X-ray Studies	7
2.4 Metallographic Studies	7
2.5 Thermodynamic Studies	8
3. EXPERIMENTAL RESULTS AND CALCULATIONS	10
3.1 Resistivity Results	10
3.2 Thermodynamic Results	13
3.3 X-ray Results	14
3.4 Metallographic Results	15
4. DISCUSSION	85
5. CONCLUSION	89
APPENDIX	91
REFERENCES	93

LIST OF FIGURES

FIGURE		PAGE
1	Phase Diagram of Silver-Selenide	27
2	Blue M High Temperature Bath	28
3	Specimen Holder for Point Contact	29
4	Modified Olsen Calorimeter	30
5	Resistivity Versus Temperature Curve for as Annealed Sample	31
6	Resistivity Versus Temperature Curve for 700 °C (973 °K) Quenched Sample	32
6a	Resistivity Versus Temperature Curve for 700 °C (973 °K) Quenched Sample	33
7	Resistivity Versus Temperature Curve for 500 °C (773 °K) Quenched Sample	34
7a	Resistivity Versus Temperature Curve for 500 °C (773 °K) Quenched Sample	35
8	Resistivity Versus Temperature Curve for 500 °C (773 °K) Quenched Sample	36
8a	Resistivity Versus Temperature Curve for 500 °C (773 °K) Quenched Sample	37
9	Resistivity Versus Temperature Curve for 500 °C (773 °K) Quenched Sample	38
9a	Resistivity Versus Temperature Curve for 500 °C (773 °K) Quenched Sample	39
10	Resistivity Versus Temperature Curve for 300 °C (573 °K) Quenched Sample	40
10a	Resistivity Versus Temperature Curve for 300 °C (573 °K) Quenched Sample	41

LIST OF FIGURES (cont'd)

FIGURE		PAGE
11	Resistivity Versus Temperature Curve for 300 °C (573 °K) Quenched Sample	42
11a	Resistivity Versus Temperature Curve for 300 °C (573 °K) Quenched Sample	43
12	Resistivity Versus Temperature Curve for 300 °C (573 °K) Quenched Sample	44
12a	Resistivity Versus Temperature Curve for 300 °C (573 °K) Quenched Sample	45
13	Resistivity Versus Temperature Curve for as Annealed Sample	46
14	Resistivity Versus Temperature Curve for as Annealed Sample	47
15	Resistivity Versus Temperature Curve for as Annealed Sample	48
16	Resistivity Versus Temperature Curve for 300 °C (573 °K) Quenched Sample	49
17	Resistivity Versus Temperature Curve for 300 °C (573 °K) Quenched Sample	50
18	Resistivity Versus Temperature Curve for 500 °C (773 °K) Quenched Sample	51
19	Resistivity Versus Temperature Curve for 700 °C (973 °K) Quenched Sample	52
20	Resistivity Versus Temperature Curve for 700 °C (973 °K) Quenched Sample	53
21	Resistivity Versus Temperature Curve for 700 °C (973 °K) Quenched Sample	54

LIST OF FIGURES (cont'd)

FIGURE		PAGE
22	Resistivity Versus Temperature Curve for as Annealed Sample	55
22a	Resistivity Versus Temperature Curve for as Annealed Sample	56
23	Resistivity Versus Temperature Curve for as Annealed Sample	57
23a	Resistivity Versus Temperature Curve for as Annealed Sample	58
24	Resistivity Versus Temperature Curve for 300 °C (573 °K) Quenched Sample	59
24a	Resistivity Versus Temperature Curve for 300 °C (573 °K) Quenched Sample	60
25	Resistivity Versus Temperature Curve for 300 °C (573 °K) Quenched Sample	61
25a	Resistivity Versus Temperature Curve for 300 °C (573 °K) Quenched Sample	62
26	Resistivity Versus Temperature Curve for 500 °C (773 °K) Quenched Sample	63
26a	Resistivity Versus Temperature Curve for 300 °C (573 °K) Quenched Sample	64
27	Resistivity Versus Temperature Curve for 500 °C (773 °K) Quenched Sample	65
27a	Resistivity Versus Temperature Curve for 500 °C (773 °K) Quenched Sample	66
28	Resistivity Versus Temperature Curve for 700 °C (973 °K) Quenched Sample	67

LIST OF FIGURES (cont'd)

FIGURE		PAGE
28a	Resistivity Versus Temperature Curve for 700 °C (973 °K) Quenched Sample	68
29	Resistivity Versus Temperature Curve for 700 °C (973 °K) Quenched Sample	69
29a	Resistivity Versus Temperature Curve for 700 °C (973 °K) Quenched Sample	70
30	Resistivity Versus Temperature Curve for 700 °C (973 °K) Quenched Sample	71
30a	Resistivity Versus Temperature Curve for 700 °C (973 °K) Quenched Sample	72
31	ΔH Versus Temperature Curve for Silver-Selenide	73
32	X-ray Diffraction Pattern of α -Ag ₂ Se	74
33	Photomicrograph of Sample 3	75
34	Photomicrograph of Sample 3	76
35	Photomicrograph of Sample 3	77
36	Photomicrograph of Sample 4	78
37	Photomicrograph of Sample 4	79
38	Photomicrograph of Sample 5	80
39	Photomicrograph of Sample 5	81
40	Photomicrograph of Sample 5	82
41	Photomicrograph of Sample 5	83
42	Photomicrograph of Sample 5	84

LIST OF TABLES

TABLE		PAGE
1	Resistivity Data for Sample 3	17
2	resistivity Data for Sample 4	18
3	Resistivity Data for Sample 5	19
4	History Between Various Runs and Treatments for Sample 3	21
5	History Between Various Runs and Treatments for Sample 4	22
6	History Between Various Runs and Treatments for Sample 5	23
7	X-Ray Data for α -Ag ₂ Se	24
8	Thermodynamic Data for Silver-Selenide	25
9	Thermodynamic Data for Silver-Selenide	26

CHAPTER I

INTRODUCTION

Silver-selenide (Ag_2Se) is an intermetallic compound containing 33 at. % Se. The melting point of this compound is approximately 900°C (1173°K) (figure 1) (1). It has been reported that this compound exists in two crystal modifications (2-11). The low temperature phase, the α -phase, transforms to the high temperature phase, the β -phase. The transformation temperature ranges from 122°C to 130°C (394 to 396°K). α - Ag_2Se has an orthorhombic form of the space group $\text{P}2_12_12_1$ with $a = 4.333^\circ\text{A}$, $b = 7.062^\circ\text{A}$, and $c = 7.764^\circ\text{A}$ (15). The low temperature α -Phase, in addition to having interesting electrical and thermodynamic properties, also has unusual ductility for a semiconductor and can be machined with no damage to the material. The high temperature β -Phase has a cubic structure with $a = 4.993^\circ\text{A}$.

Controversy exists regarding the exact transformation temperature and the crystal structures, particularly those of low temperature phase. Results of different investigators are discussed in the following paragraphs.

It is interesting to note that the mineral known as Naumannite found on the earth's surface is the silver-selenide compound in its low temperature modification (2). J. W. Earley (2) in 1950 reported that the

transformation of $\alpha \rightarrow \beta$ phase takes place between 122 °C to 130 °C (394-396 °K) at atmospheric pressure. He speculated that the β -phase is cubic and the low temperature α -phase has different undetermined structure other than monoclinic. Subsequently in 1955, A. G. Boettcher (3) determined the low temperature phase to be tetragonal with $a = 7.06$ °A, and $c = 4.98$ °A. These results were further confirmed by P. Junod (4).

In 1960, the research results of J. B. Conn (5) disagreed with both Junod and Boettcher (4). He speculated that the low temperature phase, i.e., tetragonal, was a metastable transition phase. He determined that the low temperature phase is orthorhombic with $a = 7.79$ °A, $b = 7.111$ °A, and $c = 7.790$ °A. He further attempted to substantiate the crystallography by forming Ag_2Se directly out of aqueous solution of Silveroxide in Potassium cyanide ($\text{K}_3\text{Ag}(\text{CN})_4$) and potassium selenide. The product formed at room temperature was Ag_2Se , identified as orthorhombic with $a = 8.630$ °A, $b = 14.130$ °A, and $c = 7.820$ °A, containing four molecules of Ag_2Se per unit cell. However, the investigations by C. L. Cho (6), Z. G. Pinsker (7), and S. K. Sharma (8) found the low temperature phase of silver selenide to be orthorhombic with slightly different lattice parameters: $a = 7.05$ °A, $b = 4.325$ °A, and $c = 7.82$ °A. Later, K. Akiyama (9) found the structure of low temperature phase to be orthorhombic with completely different lattice parameters: $a = 5.5$ °A, $b = 4.35$ °A, and $c = 3.57$ °A.

The most comprehensive investigation was done by

B. W. G. Wyckoff (10). He reported the transformation temperature to be 133°C (406°K). This finding was also confirmed by Conn (5). Later, G. Pellini (11) found the transition temperature to be 122°C (395°K).

The low temperature phase of silver-selenide exhibited semi-conducting properties while the high temperature phase had metallic properties. Silver-selenide exhibited non-degenerate semi-conducting characteristics in resistivity which decrease with increasing temperature from -183°C (93°K) up to the transformation temperature. At transformation temperature, there is a sudden increase in resistivity, indicating the Phase Transformation (5). However, the above results do not agree with Junod who found a decrease in resistivity at transformation temperature (4).

The thermodynamic property was first reported by M. Bellati, et al. (12) in 1888 and subsequently by several investigators including P. N. Walsh (13), Y. Bear (14), and R. Roy (16). The low temperature values found by these investigators are in good agreement with those of the pioneering work of 1888. The equilibrium transformation temperature reported by these investigators was between 128°C to 133°C (401°K to 406°K), the selected value being 133°C (406°K) (1). The enthalpy of phase transformation reported was between 559 to 730 Cal/Mole, the selected value being 560 Cal/Mole (1). Bear, et al. (14) further suggested the existence of second phase transformation of unknown origin from an anomaly which increases by about 5%. Hultgreen (1) concluded that the structure is relatively

ordered from the good agreement of the entropy values obtained from independent property evaluations.

The purpose of this investigation has been to determine the characteristics of the high temperature and the low temperature phases by studying resistivity properties, thermodynamic properties, the characteristic transformation temperatures on heating and cooling, the crystal structure of low temperature phase, and the resistivity change accompanying the phase transformation of annealed and quenched samples. The transformation kinetics of quenched samples have been interpreted in terms of the release of the transformation induced volumetric strain energy by the quenched-in defects.

CHAPTER II

EXPERIMENTAL PROCEDURE

2.1 SAMPLE PREPARATION:

Silver and Selenium both were obtained in 99.999% purity from Aldrich Chemical Company. All samples of Ag-Se (33 at. % Se) were prepared in 4mm ID Quartz tube. The Quartz tubes were first cleaned with aqua regia, then with water, and finally with acetone. Both silver and selenium were accurately weighed using a Mettler electronic balance accurate to four decimal places.

The materials were encapsulated in quartz tubes and sealed under a vacuum of about 10^{-5} mm Hg. After homogenizing the mixture on oxy-acetylene flame, the tubes were quickly put in the furnace pre-heated to 300 °C (573 °K). The temperature of the furnace was raised to 1000 °C (1273 °K) and maintained for 72 hours. The furnace was then cooled to 900 °C (1173 °K) and the sample was given a diffusion anneal for 48 hours. The tubes were then allowed to cool down to room temperature. All quartz tubes containing the sample were found broken due to the volume change accompanying the phase transformation. The surfaces of the samples were cleaned with fine sand paper and then with acetone. The alloy samples thus prepared were approximately 80 mm long. The average weight of the samples

was 8.0 grams. Three samples thus obtained were used for resistivity study only.

The sample used for thermodynamic study was prepared in a 15 mm ID quartz tube by following the same procedure. The alloy sample prepared for thermodynamic study was approximately 24 mm long and the weight of the sample was 26.258 grams.

2.2 RESISTIVITY STUDIES:

The resistivity measurements in this research work were carried out in the temperature range 25-165 °C (298-425 °K). All of the measurements were done in a Blue M constant high temperature bath (figure 2).

A glass container was fitted with electric resistance heating elements. The temperature of the bath was controlled by an automatic temperature controller ($\pm 3K$). This container was also fitted with cooling water circulating tubes. The bath was approximately half filled with Paraffin oil. An electric stirrer was fitted in the bath to ensure uniform distribution of temperature throughout the container. A precision type-T thermocouple was fitted in the bath to measure the temperature.

The resistance measurements were performed with a rod sample. These resistance versus temperature measurements were made at atmospheric pressure by a four lead method. Rod sample was placed in four similar holders (figure 3) specially designed for point contact. The rod sample placed in holders was hung in the center of the liquid bath. The

resistance of the sample was measured by using a Rubicon double Kelvin bridge. The output of the thermocouple was recorded on a Millivolt Potentiometer. The resistivity values were calculated from the results by using the standard equation.

2.3 X-RAY STUDIES:

X-ray studies were carried out on a Norelco diffractometer using copper radiation and Ni filter. Powdered samples for X-ray studies were made by filing the samples used for resistivity studies. These samples were put in the sample holder specially designed for this machine. The diffraction patterns were taken on a strip chart in the range $10^{\circ} < 2\theta < 100^{\circ}$ with a chart speed of one inch per minute and a scan rate of one degree per minute. The two theta values obtained from the strip chart were finally used to determine the crystal structure and lattice parameter of $\text{-Ag}_2\text{Se}$.

2.4 METALLOGRAPHIC INVESTIGATION:

Specimens for microscopic investigation were cut from rod samples used for resistivity study and also from the sample used for thermodynamic study. These samples were mounted by using a Primo Press mounting machine. After grinding on 200, 320, 600, and 1200 grid silicon carbide paper, the mounted samples were finally polished to obtain a scratch-free surface.

The etching reagent used consisted of 20 ml of aqueous

solution of $K_2Cr_2O_7$ with one drop of H_2SO_4 . Etching time was approximately 7 seconds for all samples. After etching, the samples were examined under a Ziess optical microscope and microphotographs were taken at different magnification.

2.5 THERMODYNAMIC INVESTIGATION:

The study of thermodynamic properties was done in a modified Olsen calorimeter (Figure 4). The sample held by a thermocouple was contained in a water-tight copper jacket. This jacket was placed in the calorimeter medium contained in a Dewar's flask which in turn was surrounded by an adiabatic jacket. A Teflon block was used to cover the flask.

Temperature measurement of the medium was done by a thermopile consisting of seven precision thermopiles connected in series. The thermocouples were introduced through the Teflon block. The cold junction of the thermocouple was maintained at $0^\circ C$ with the use of a precision electronic cold junction.

The calorimeter medium was kept agitated with the use of a magnetic stirrer unit placed under the calorimeter assembly.

Spectroquality isopropyl alcohol was used as the calorimeter medium. A measured amount of isopropyl alcohol was weighed in a clean Dewar's flask. After careful weighing, the magnetic stirrer was placed in the flask.

The sample was placed on the thermocouple and lowered into the furnace which had been maintained at $300^\circ C$ ($573^\circ K$). As soon as the sample reached the temperature of

200 °C (473 °K), it was quickly removed from the furnace. It was then capped and lowered into the calorimeter.

The temperature of the sample and the medium was simultaneously recorded using an X-Y recorder and a quartz digital thermometer with an accuracy of 0.0001 °C.

CHAPTER III

EXPERIMENTAL RESULTS AND CALCULATIONS

3.1 RESISTIVITY RESULTS:

The resistivity results for samples 3, 4, and 5 are listed in tables 1 through 6 and graphs are shown in figures 5 through 30. The resistivity results consist of the resistance value as a function of temperature. From these results the resistivity values are obtained from sample diameter and length. In all samples the phase transformation was observed either upon heating or cooling or both. In general the transformation upon heating or cooling starts at a definite temperature T_s and ends at a definite temperature T_f . The mean transformation temperature upon heating (T_h) or cooling (T_c) is obtained by the following equation.

$$T_h \text{ or } T_c = (T_s + T_f) / 2$$

The results near the phase transformation region during cooling cycle allow direct determination of T_s , T_f , and $\Delta\epsilon_{tc}$. The experimental results of all three samples are listed below.

SAMPLE 3:

The experimental results of sample 3 are listed in

table 1 and graphs are shown in figures 5 through 12. The quenching sequence used was 700 °C (973 °K), 500 °C (773 °K), and 300 °C (573 °K) respectively.

No phase transformation was observed during the heating cycle in all cases but a definite change in slope around 135 °C (408 °K) to 140 °C (413 °K) was noted during the heating cycle. In an annealed sample no transformation was observed during the heating cycle and no results were available for the cooling cycle.

Upon quenching from 700 °C (973 °K), 500 °C (773 °K), and 300 °C (573 °K) respectively, the results indicate the same change in resistivity ($\Delta\rho_{TC} = 57$ through $50 \mu\text{Ohm-cm}$). Upon cycling the specimen (i.e., heating and cooling) after 500 °C (773 °K) quench $\Delta\rho_{TC}$ had essentially the same value in all cycles. Upon holding the specimen at 145 °C (418 °K) for five hours after 300 °C (573 °K) quench, the decrease in $\Delta\rho_{TC}$ is almost 50% (figure 7).

The transformation temperature did not change much in all heat treatment cases. It ranged from 121 °C (394 °K) to 123 °C (396 °K). Upon holding the sample at 130 °C (403 °K) for one hour, after 300 °C (573 °K) quench, there was no phase transformation observed while during the heating or the cooling cycles (figure 12). The history of sample 3 between various heat treatments and runs is listed in table 4.

SAMPLE 4:

The experimental results of sample 4 are listed in

table 2 and graphs are shown in figures 13 through 21. The quenching sequence used was 300 °C (573 °K), 500 °C (773 °K), and 700 °C (973 °K) respectively. Phase transformation was observed during the heating and cooling cycles in all cases. During the cooling cycle there was a sharp decrease in resistivity at the transformation temperature followed by gradual increase in all cases. For samples 3 and 5 a sharp increase in resistivity at transformation temperature was observed during cooling cycle.

For an annealed sample in their 1st, 6th, and 7th run, the change in resistivity $\Delta\rho_{tc}$ ranged from 570 to 450 $\mu\text{Ohm-cm}$ in the cooling cycle and from 590 to 485 $\mu\text{Ohm-cm}$ in the heating cycle. The results indicate a gradual decrease in resistivity ($\Delta\rho_{tc} = 470$ to $275 \mu\text{Ohm-cm}$) for samples quenched from 300 °C (573 °K), 500 °C (773 °K), and 700 °C (973 °K) respectively in the heating and cooling cycles. Upon holding the sample at 145 °C (418 °K) for 10 minutes after 700 °C (973 °K) quench, the decrease in resistivity is almost 50%. There was not much change in $\Delta\rho_{tc}$ for the same sample held at 100 °C (373 °K) for 10 minutes. The history of sample 4 is listed in table 5.

SAMPLE 5:

The resistivity results of sample 5 are listed in table 2 and graphs are shown in figures 22 through 30. The quenching sequence used was 300 °C (573 °K), 500 °C (773 °K), and 700 °C (973 °K) respectively.

For annealed and quenched samples, the transformation

temperature is almost in the same range (i.e., from 122 °C (395 °K), to 124 °C (397 °K). There is no phase transformation observed for the heating cycle in all cases, but there is a definite change in the slope around 135 °C (408 °K) to 140 °C (413 °K). The same kind of results were seen for sample 3. Samples quenched from 300 °C (573 °K), 500 °C (773 °K), and 700 °C (973 °K) respectively, in their first and second run, exhibited change in ΔQ_{TC} to be almost within the same range as observed for sample 3. Upon holding the sample, re-quenched from 700 °C (973 °K), at 145 °C (418 °K) for 10 minutes the decrease in ΔQ_{TC} is almost 50% (figure 17). There is not much change in ΔQ_{TC} for the same sample held at 100 °C (373 °K) for 10 minutes. The history of sample 5 between various heat treatments and runs is listed in table 6.

3.2 THERMODYNAMICS RESULTS:

The thermodynamic results consist of continuous change in the temperature of the calorimeter medium as a function of the change in the temperature of the sample. From these results the values of enthalpy change " ΔH " are calculated by using the following equation

$$\Delta H = WC_p \Delta T$$

Where $\Delta H = H_T - H_{454}^{\circ} K$

W = The weight of the calorimeter medium

C_p = The specific heat of calorimeter medium at T K

ΔT = The change in the calorimeter temperature with respect to the reference point at 181 °C (454 °K)

The experimental results are shown in figure 31 and values are listed in table 8. Also, from the above results, the values of specific heat " C_p " are determined at different temperatures by using the following equation.

$$C_p = dH/dT$$

Where dH = Enthalpy change over small interval

dT = Temperature change over small interval

The values of the Specific heat " C_p " are listed in table 9. The experimental results shown in figure 31 allow direct determination of the enthalpy change of the phase transformation.

3.3 X-RAY RESULTS:

X-ray studies involve the determination of crystal structure of α -Ag₂Se and also the determination of lattice parameters. The diffraction pattern obtained for α -Ag₂Se is shown in figure 32.

The region of $20^\circ < 2\theta < 120^\circ$ was used to evaluate the crystal structure and lattice parameters. The results in the X-ray diffraction data consist of 2θ values and the relative intensities. From these 2θ values the $\sin^2\theta$ values were obtained by following the standard analytical approaches. It was attempted to index the pattern on the basis of an

orthorhombic, tetragonal, and cubic systems by following the analytical method. The crystal structure was found to be orthorhombic with lattice parameters $a = 4.333 \text{ \AA}$, $b = 7.062 \text{ \AA}$, and $c = 7.764 \text{ \AA}$. The values are tabulated in table 8 and calculations are given below.

The general equation for orthorhombic structure is

$$\sin^2\theta = \frac{\lambda^2}{4a^2}(h^2) + \frac{\lambda^2}{4b^2}(k^2) + \frac{\lambda^2}{4c^2}(l^2) \quad \text{-----(1)}$$

Where $a, b, c =$ Lattice parameters

$h, k, l =$ Indices

$\lambda =$ Wavelength of Cu radiation

Or we can write

$$\sin^2\theta = A(h^2) + B(k^2) + C(l^2) \quad \text{-----(2)}$$

Where $A = \frac{\lambda^2}{4a^2}$

$B = \frac{\lambda^2}{4b^2}$

$C = \frac{\lambda^2}{4c^2}$

The constants A, B, and C were found to be

$$A = 0.0316 \quad B = 0.0119 \quad C = 0.00986$$

From the above constants, the values of lattice parameters and cell volume can be obtained

$$a = 4.333 \text{ \AA}, \quad b = 7.062 \text{ \AA}, \quad c = 7.764 \text{ \AA}$$

$$\text{Cell volume} = 237.57 (\text{\AA})^3$$

3.4 METALLOGRAPHIC RESULTS:

The photomicrographs of samples 3, 4, and 5 are shown in figures 33 through 42.

The metallographic study reveals that the transformation product upon cooling consists of twin lamaellae with secondary twins between the lamaellae (figure 33). Figure 34 shows twin related transformation product with adjoining "midrib". Figures 37, 38, 39, and 42 show traces of twin lamaellae with adjoining "midrib". Figures 35, 40, and 41 show both twin traces and the needle shaped transformation product.

TABLE 1

RESISTIVITY RESULTS

SPECIMEN: Ag_2Se (33 at.% Se)
 SAMPLE NO: 3²

Run No.	Cycle No.	Treatment	T _{os} °K	T _{of} °K	T _{co} OR T _h °K	$\Delta\rho_{tc}$ OR $\Delta\rho_{th}$ Micro OHM-CM
1	Heating	As annealed	-	-	-	-
	Cooling		-	-	-	-
1	Heating	973°K Quench	-	-	-	-
	Cooling		395	388	391	57.0
1	Heating	773°K Quench	-	-	-	-
	Cooling		395	388	391	55.0
2*	Heating	773°K Quench	-	-	-	-
	Cooling		395	388	391	54.0
	Heating		-	-	-	-
	Cooling		394	387	390	53.0
3**	Heating	773°K Quench	-	-	-	-
	Cooling		398	384	391	63.0
1	Heating	573°K Quench	-	-	-	-
	Cooling		395	388	391	50.0
2***	Heating	573°K Quench	-	-	-	-
	Cooling		396	389	391	30.0

* Sample was held at 150°C(423°K) for 15 minutes

** Sample was held at 150°C(423°K) for one hour

*** Sample was held at 145°C(418°K) for five Hours

Table 1 continued

Run No.	Cycle No.	Treatment	T_{os} K	T_{of} K	T_{co} OR T_h K	$\Delta\rho_{tc}$ OR $\Delta\rho_{th}$ Micro OHM-CM
3****	Heating	573°K Quench	-	-	-	-
	Cooling		-	-	-	-
	Heating		-	-	-	-
	Cooling		-	-	-	-

**** Sample was held at 130°C(403°K) for one hour

TABLE 2

RESISTIVITY RESULTS

SPECIMEN: Ag_2Se (33 at.% Se)
 SAMPLE NO: 4

Run No.	Cycle No.	Treatment	T_{os} K	T_{of} K	T_{co} OR T_h K	$\Delta \rho_{tc}$ OR $\Delta \rho_{th}$ Micro OHM-CM
1	Heating	As annealed	405	414	409.5	590.0
	Cooling		398	392	395.0	570.0
6	Heating	As annealed	411	415	413.0	570.0
	Cooling		396	386	391.0	590.0
7	Heating	As annealed	407	415	411.0	485.0
	Cooling		396	389	392.5	450.0
1	Heating	573°K Quench	405	414	409.5	470.0
	Cooling		397	390	393.5	435.0
2	Heating	573°K Quench	405	411	408.0	440.0
	Cooling		396	390	393.0	420.0
1	Heating	773°K Quench	407	412	409.0	320.0
	Cooling		396	387	391.0	310.0
1	Heating	973°K Quench	401	412	406.5	258.0
	Cooling		399	386	392.5	275.0
2*	Heating	973°K Quench	402	413	407.5	205.0
	Cooling		400	389	394.0	245.0
1**	Heating	973°K Quench	403	416	409.5	200.0
	Cooling		397	388	392.5	185.0

* Specimen was held at 100°C(373°K) for 10 minutes

** Specimen was held at 145°C(418°K) for 10 minutes

TABLE 3
RESISTIVITY RESULTS

SPECIMEN: Ag_2Se (33 at.% Se)
SAMPLE NO: 5

Run No.	Cycle No.	Treatment	T_{on} °K	T_{off} °K	T_{co} OR T_{h} °K	$\Delta\rho_{\text{Micro}}$ OR $\Delta\rho_{\text{OHM-CM}}$
1	Heating	As annealed	-	-	-	-
	Cooling		397	386	391.5	59.0
2	Heating	As annealed	-	-	-	-
	Cooling		397	385	391.0	57.0
1	Heating	573°K Quench	-	-	-	-
	Cooling		397	387	392.0	49.0
2	Heating	573°K Quench	-	-	-	-
	Cooling		397	386	391.5	50.0
1	Heating	773°K Quench	-	-	-	-
	Cooling		395	388	391.5	56.0
2	Heating	773°K Quench	-	-	-	-
	Cooling		397	388	392.5	56.0
1	Heating	973°K Quench	-	-	-	-
	Cooling		396	388	391.5	57.0
2*	Heating	973°K Quench	-	-	-	-
	Cooling		396	390	393.0	57.0
1**	Heating	973°K Quench	-	-	-	-
	Cooling		396	383	389.0	34.0

* Specimen was held at 100°C(373°K) for 10 minutes

** Specimen was held at 145°C(418°K) for 10 minutes

TABLE 4

History of sample 3 between various runs and treatments.

RUN	TREATMENT	HISTORY
1	As annealed	After 1st run (as annealed) the Sample was held for one day at room temperature.
1	973 ^o K Quench	After 1st run (973 ^o K quench) the sample was held for 3 days at room temperature.
1	773 ^o K Quench	After 1st run (773 ^o K quench) the sample was held for 3 days at room temperature.
2	773 ^o K Quench	after 2nd run (773 ^o K quench) the sample was held for 2 hours at room temperature.
3	773 ^o K Quench	After 3rd run (773 ^o K quench) the sample was held for one day at room temperature.
1	573 ^o K Quench	After 1st run (573 ^o K quench) the sample was held for eight days at room temperature.
2	573 ^o K Quench	After 2nd run (573 ^o K quench) the sample was held for 2 hours at room temperature.
3	573 ^o K Quench	after 3rd run (573 ^o K quench) the sample was held for one day at room temperature.

TABLE 5

History of sample 4 between various runs and treatments.

RUN	TREATMENT	HISTORY
1	As annealed	After 1st run (as annealed) the Sample was held for nine days at room temperature.
6	As annealed	After 6th run (as annealed) the sample was held for 3 days at room temperature.
7	As annealed	After 7th run (as annealed) the sample was held for one day at room temperature.
1	573 ^o K Quench	after 1st run (573 ^o K quench) the sample was held for 2 hours at room temperature.
2	573 ^o K Quench	After 2nd run (573 ^o K quench) the sample held for four days at room temperature.
1	773 ^o K Quench	After 1st run (773 ^o K quench) the sample was held for 19 days at room temperature.
1	973 ^o K Quench	After 1st run (973 ^o K quench) the sample was held for one day at room temperature.
2	973 ^o K Quench	After 2nd run (973 ^o K quench) the sample was held for one day at room temperature.
3	973 ^o K Quench	After 3rd run (973 ^o K quench) the sample was held for one day at room temperature

TABLE 6

History of sample 5 between various runs and treatments.

RUN	TREATMENT	HISTORY
1	As annealed	After 1st run (as annealed) the Sample was held for five days at room temperature.
2	As annealed	After 2nd run (as annealed) the sample was held for five days at room temperature.
1	573 ^o K quench	After 1st run (573 ^o K quench) the sample held for one day at room temperature.
2	573 ^o K Quench	after 2nd run (573 ^o K quench) the sample was held for one day at room temperature.
1	773 ^o K Quench	After 1st run (773 ^o K quench) the sample was held for two hours at room temperature.
2	773 ^o K Quench	After 2nd run (773 ^o K quench) the sample was held for five days at room temperature.
1	973 ^o K Quench	After 1st run (973 ^o K quench) the sample was held for two days at room temperature.
2	973 ^o K Quench	After 2nd run (973 ^o K quench) the sample was held for one day at room temperature.
3	973 ^o K Quench	After 3rd run (973 ^o K quench) the sample was held for six days at room temperature.

TABLE 7

X-RAY RESULTS

SPECIMEN: Ag_2Se (33 at.% Se)
 Temperature of measurement: 25°C (298°K)

Line No	I/I_0	2θ	θ	$\sin^2\theta$	hkl	dA°
1	12	26.72	13.36	.05339	111	3.336
2	20	30.92	15.46	.07106	102	2.892
3	20	32.71	16.35	.07929	120	2.737
4	100	33.49	16.75	.08301	112	2.675
5	91	34.75	17.38	.08918	121	2.581
6	35	36.97	18.49	.10052	013	2.431
7	34	40.02	20.01	.11709	031	2.252
8	31	42.65	21.33	.13225	113	2.119
9	27	43.30	21.65	.13611	023	2.089
10	12	43.70	21.85	.13852	210	2.071
11	25	45.00	22.50	.14645	032	2.014
12	8	46.77	23.39	.15754	004	1.942
13	12	48.65	24.33	.16967	014	1.871
14	6	49.92	24.96	.17807	212	1.826
15	2	53.31	26.66	.20126	114	1.718
16	1	55.00	27.50	.21321	222	1.669
17	3	59.09	29.55	.24315	231	1.563
18	6	65.70	32.85	.29424	310	1.421
19	6	69.53	34.76	.32514	302	1.352
20	5	71.15	35.58	.33845	312	1.324
21	6	72.61	36.13	.34765	044	1.306
22	6	76.61	38.61	.38421	313	1.242
23	5	79.02	39.51	.40477	243	1.211

Crystal Structure : Orthorhombic

Average Lattice Parameter :
 $a = 4.333 \text{ \AA}$
 $b = 7.062 \text{ \AA}$
 $c = 7.764 \text{ \AA}$

Volume of orthorhombic phase = $237.5756 (\text{\AA})^3$

TABLE 8

THERMODYNAMIC RESULTS

SPECIMEN: Ag₂Se (33 at.% Se)
 CALORIMETER MEDIA: Isopropyl Alcohol
 WEIGHT OF CALORIMETER MEDIA: 1161 grams
 MEDIA TEMPERATURE: -28.3°C(244.7°K)
 ROOM TEMPERATURE: 25°C(298°K)

Temperature of sample °K	Δ H Cals/Mole	Δ H Joules/Mole
454.54	0.00	0.00
433.25	1148.47	4800.60
421.33	1556.22	6504.99
408.47	1923.40	8039.81
397.42	2217.00	9267.06
397.42	2495.21	10429.97
396.69	2567.37	10731.60
396.69	2640.21	11036.07
396.69	2772.96	11590.97
396.69	2835.08	11850.50
396.69	2930.10	12247.81
396.69	3020.13	12624.14
396.20	3077.98	12865.95
394.25	3252.27	13594.48
392.54	3389.48	14168.02
390.10	3473.11	14517.59
387.66	3554.56	14858.06
385.23	3563.88	14897.01
383.29	3662.49	15309.20
380.86	3739.71	15631.98
377.95	3821.19	15972.57
374.32	3899.95	16301.79
369.49	4026.53	16830.89
365.15	4131.64	17270.25
361.53	4204.59	17575.18
357.88	4304.13	17991.26
353.83	4402.85	18403.91
349.49	4473.66	18699.89

TABLE 9

SAMPLE: Ag_2Se (33 at.% Se)

Temperature $^{\circ}\text{K}$	Specific Heat C_P Cals/ $^{\circ}\text{K}$ -Mole	Specific Heat C_P Joules/ $^{\circ}\text{K}$ -Mole
444.00	5.11	21.37
403.00	14.59	60.98
395.00	19.07	79.71
374.00	6.48	27.08
354.00	5.39	22.53

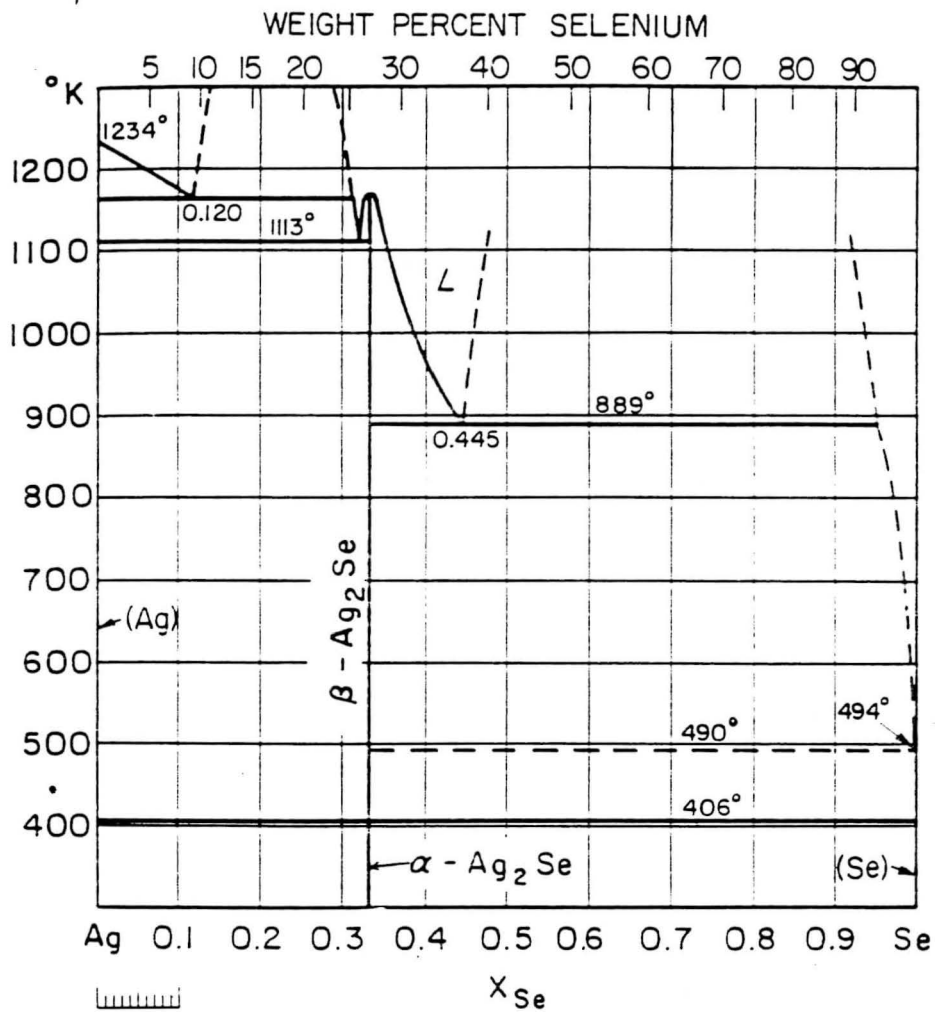
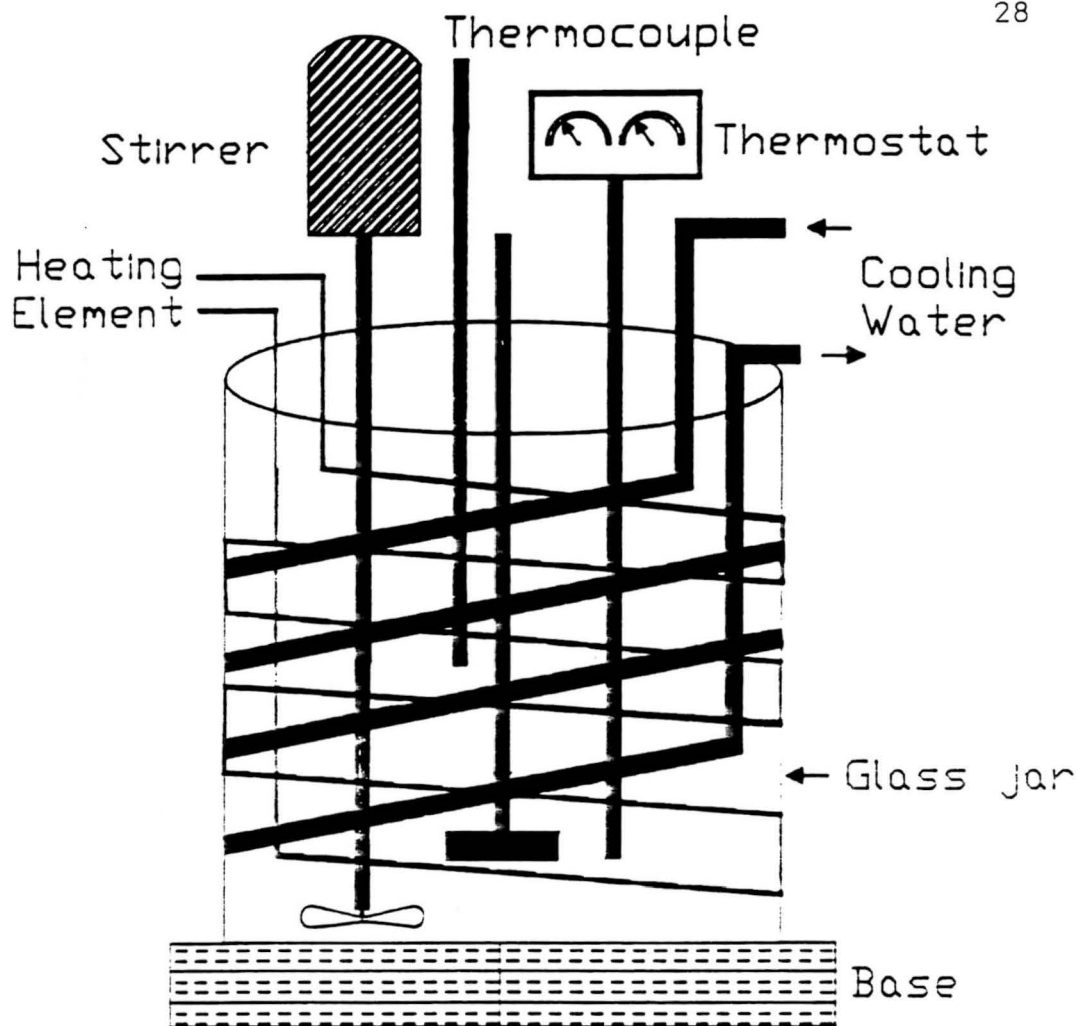
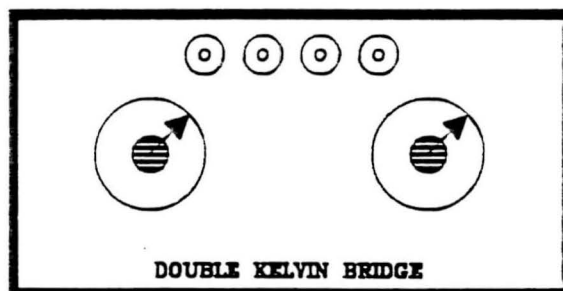


Figure 1. SILVER-SELENIUM SYSTEM



(a)



(b)

Figure 2. a. Blue M high temperature bath
b. Double Kelvin bridge

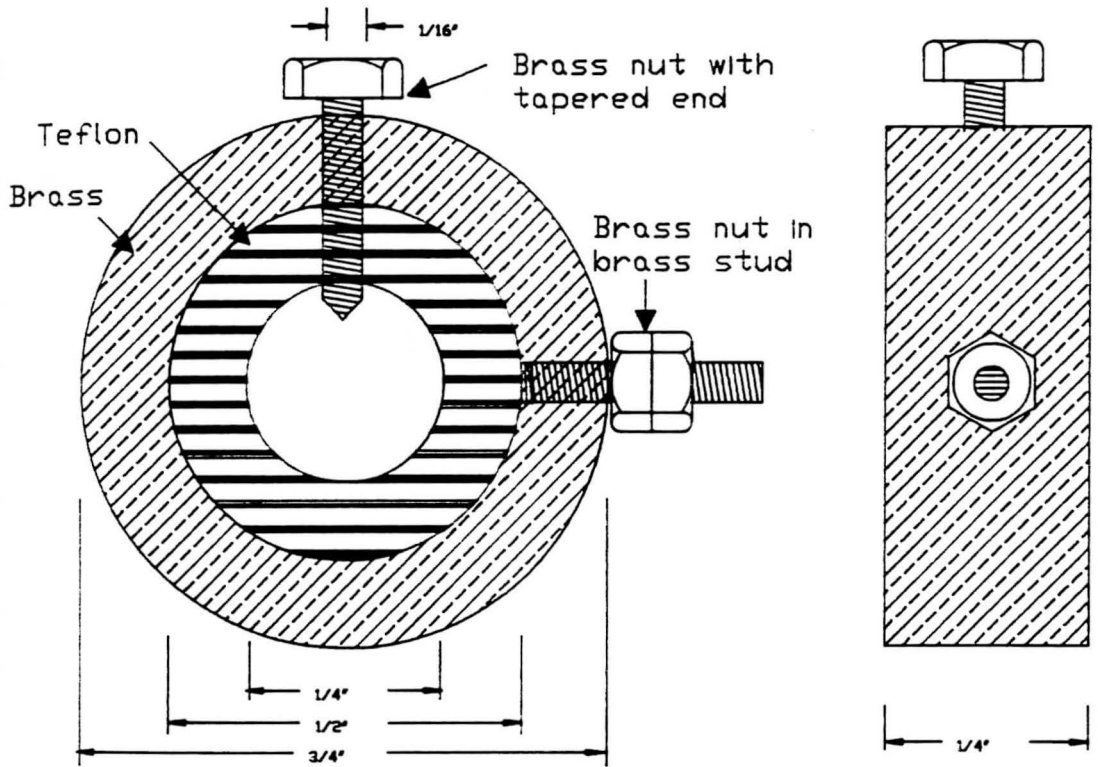


Figure 3. View of specimen holder

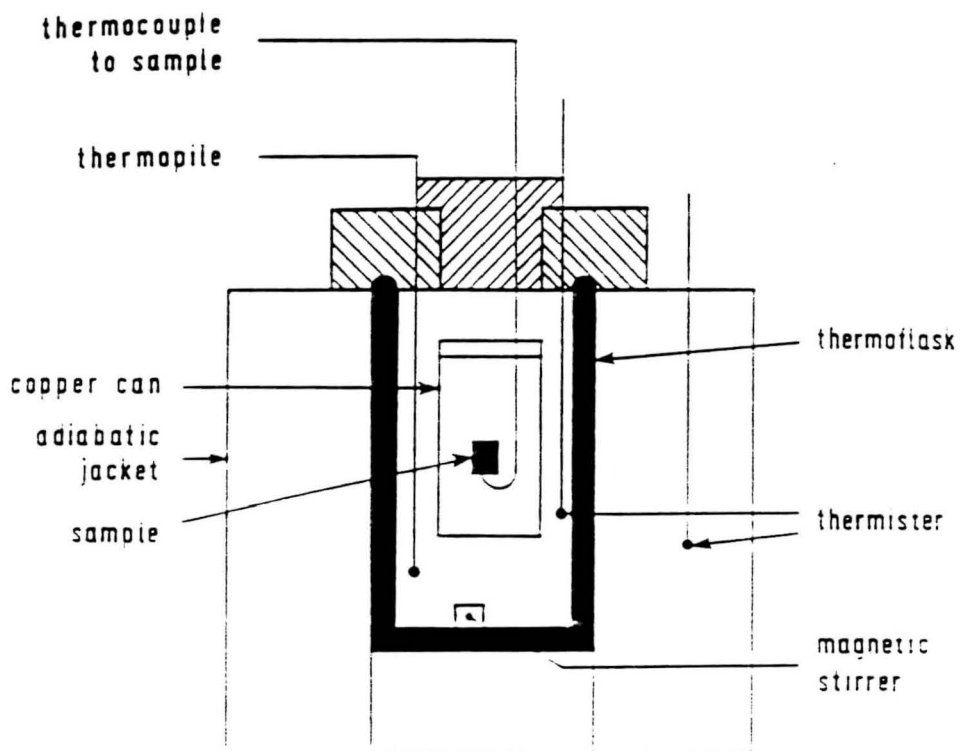


Figure 4. Modified Olsen Calorimeter

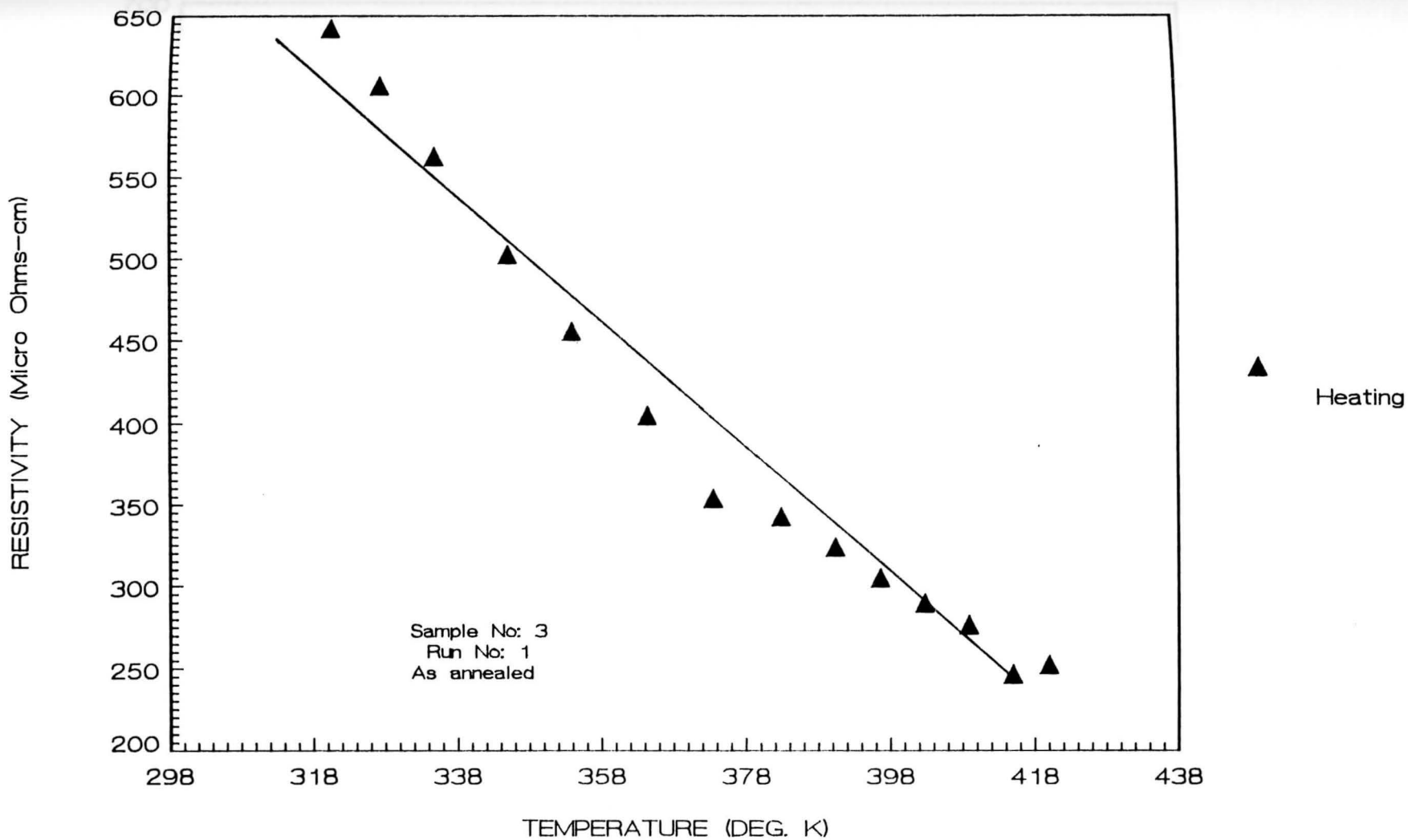


Figure 5. Variation of resistivity as a function of temperature

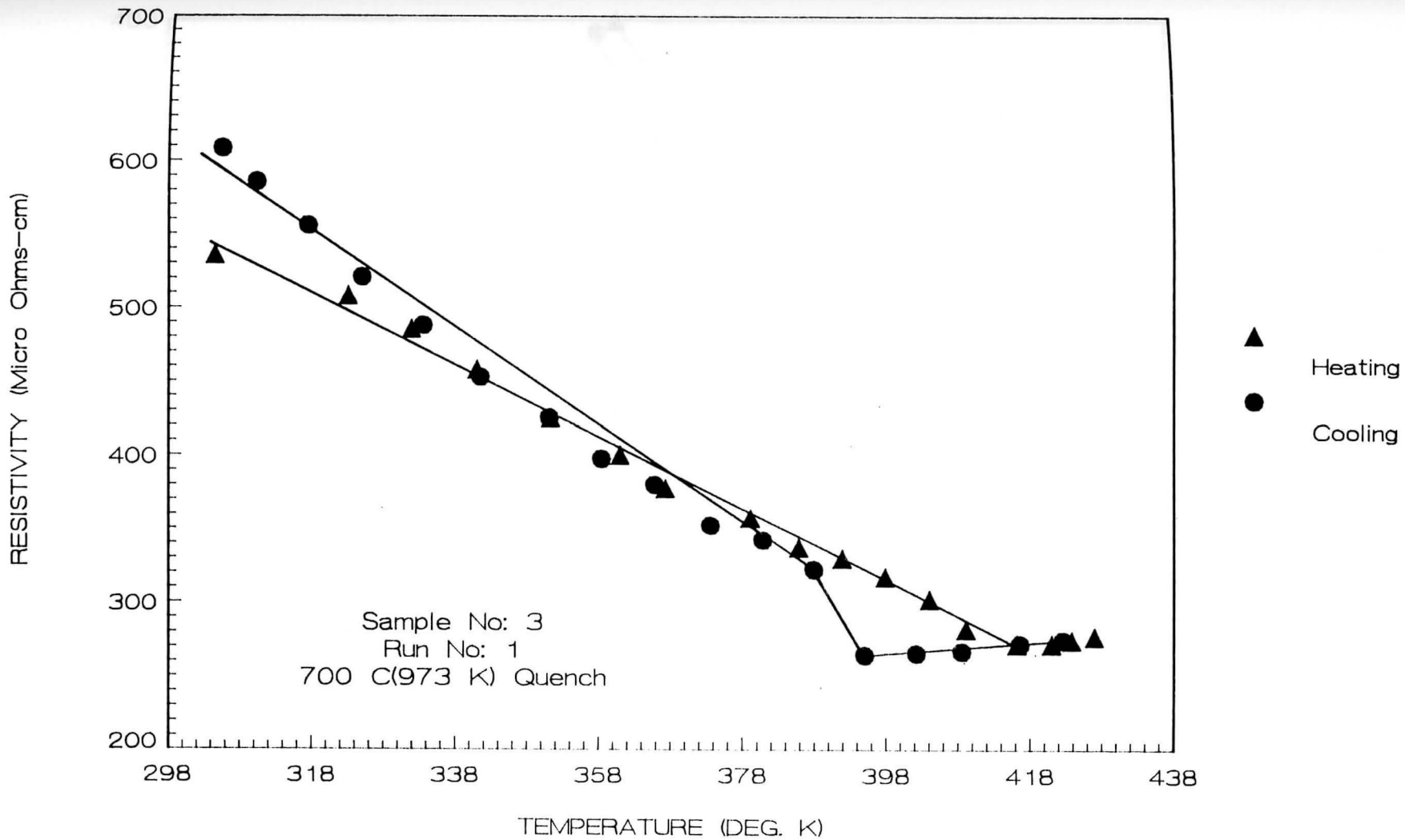


Figure 6. Variation of resistivity as a function of temperature

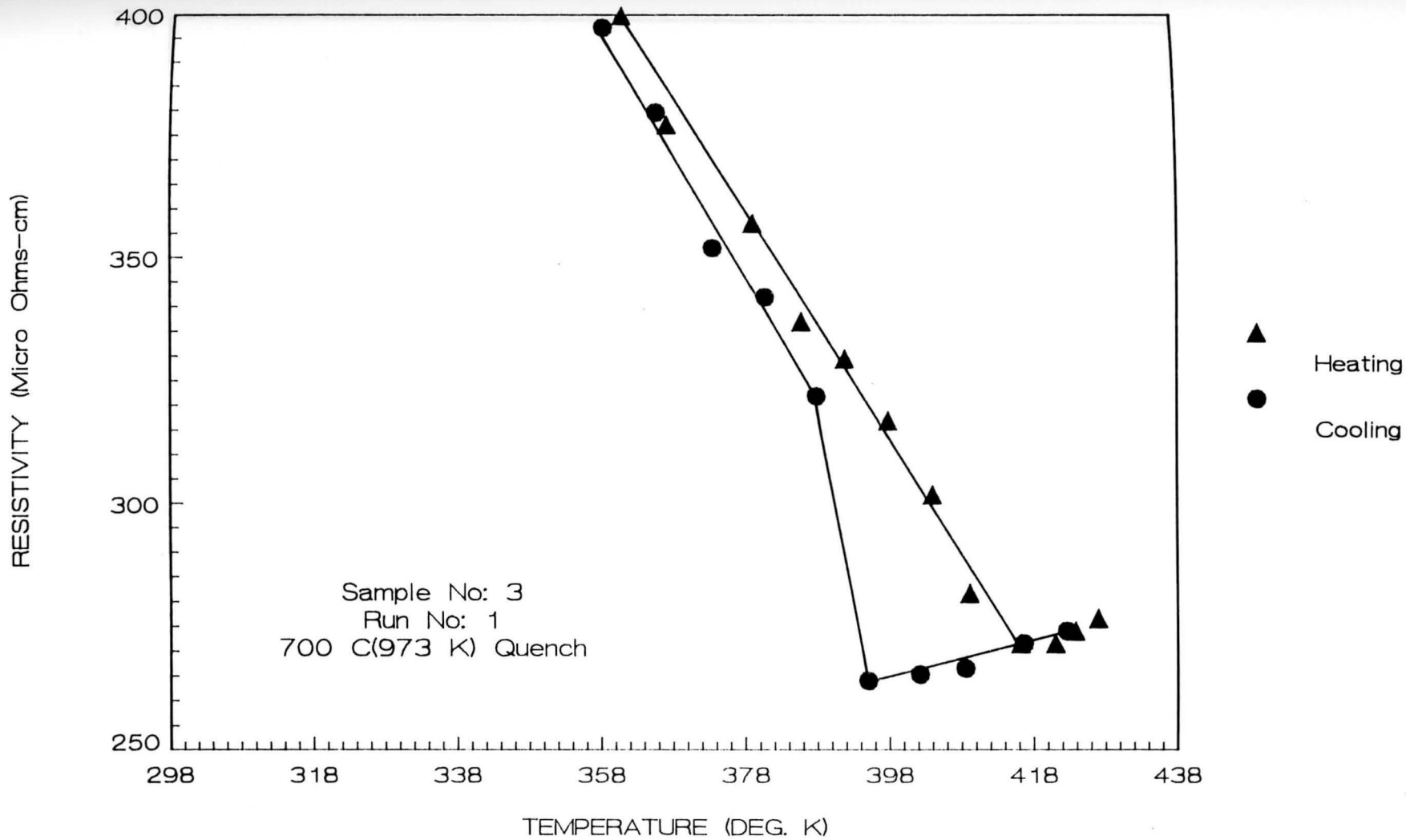


Figure 6a. Variation of resistivity as a function of temperature

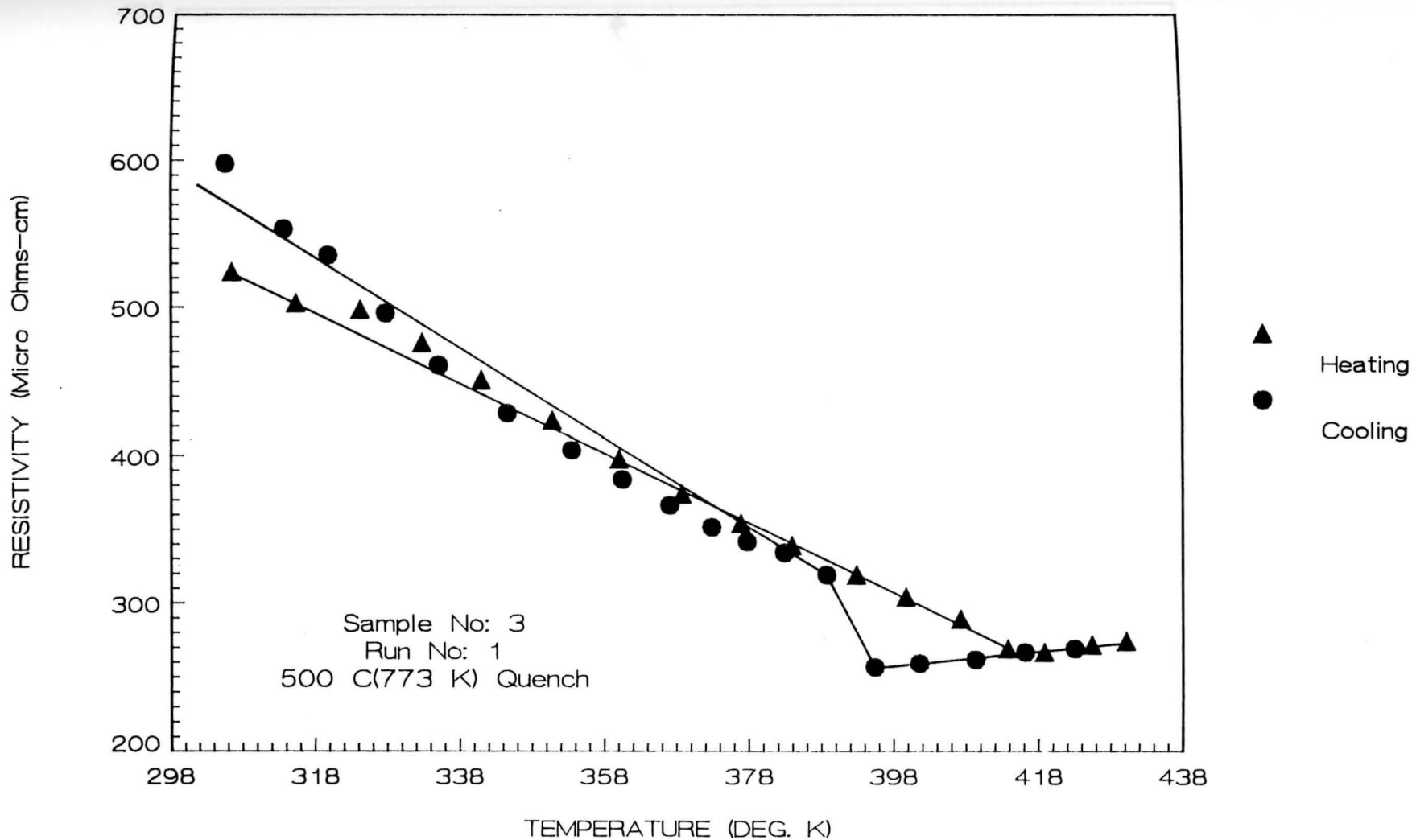


Figure 7. Variation of resistivity as a function of temperature

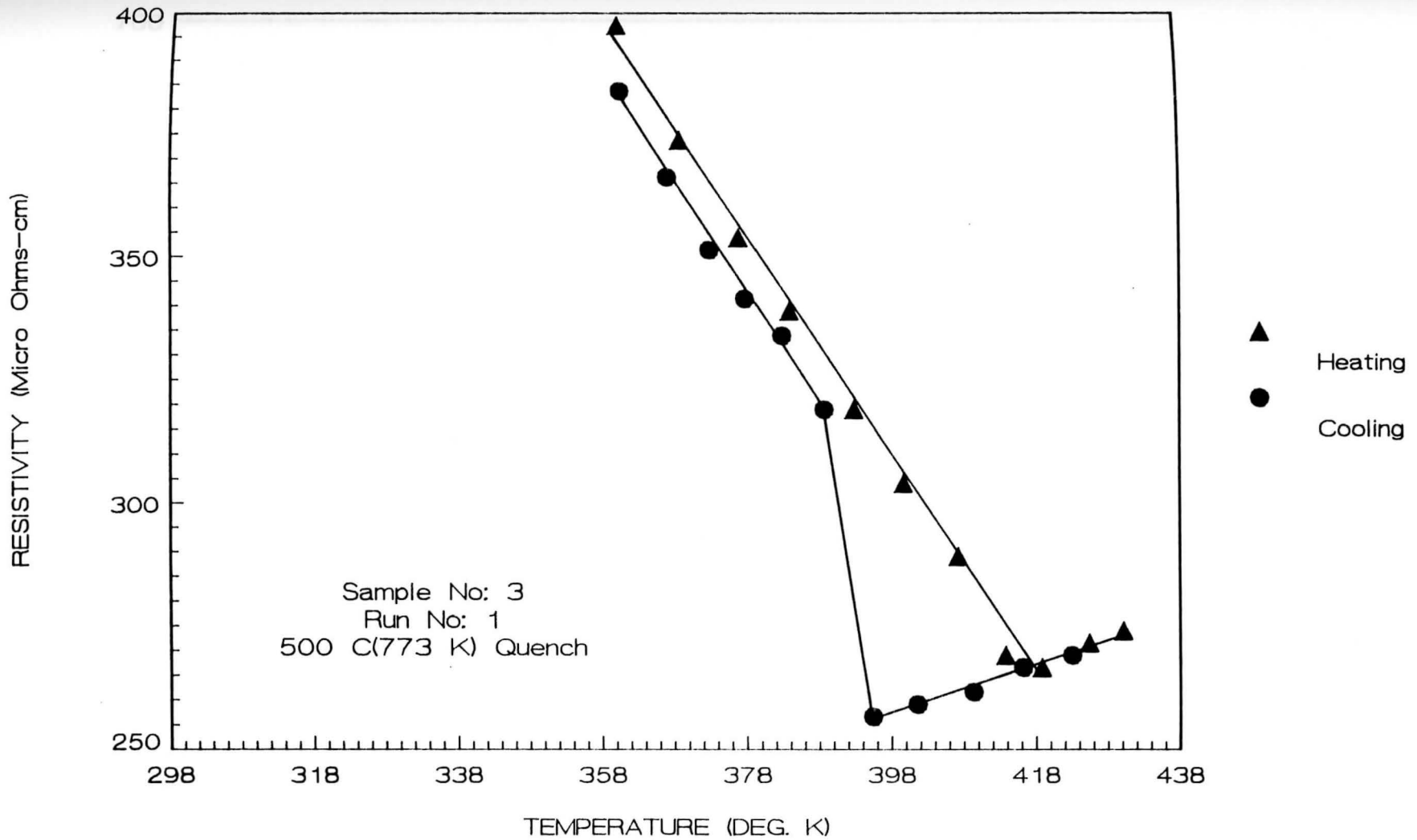


Figure 7a. Variation of resistivity as a function of temperature

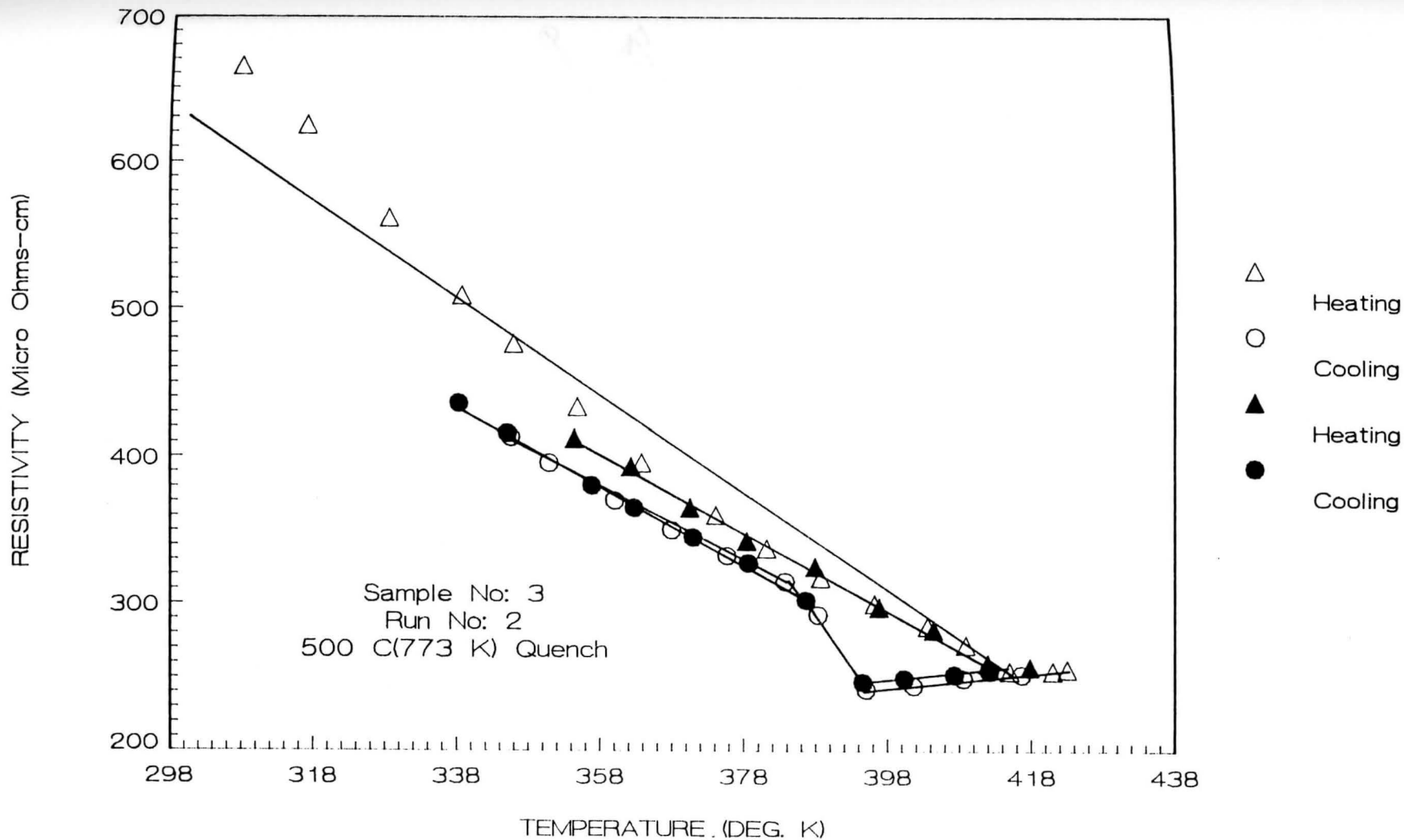


Figure 8. Variation of resistivity as a function of temperature

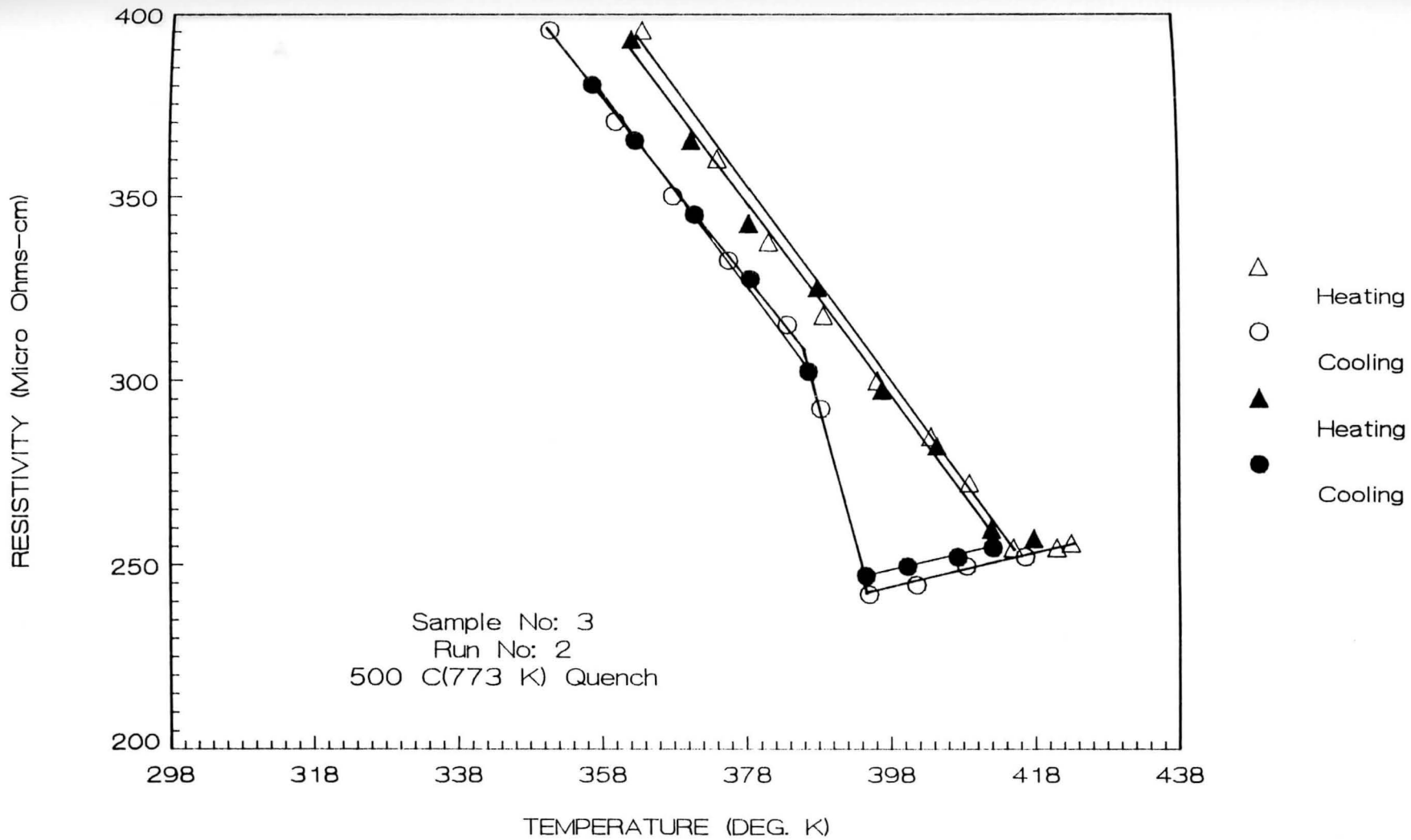


Figure 8a. Variation of resistivity as a function of temperature

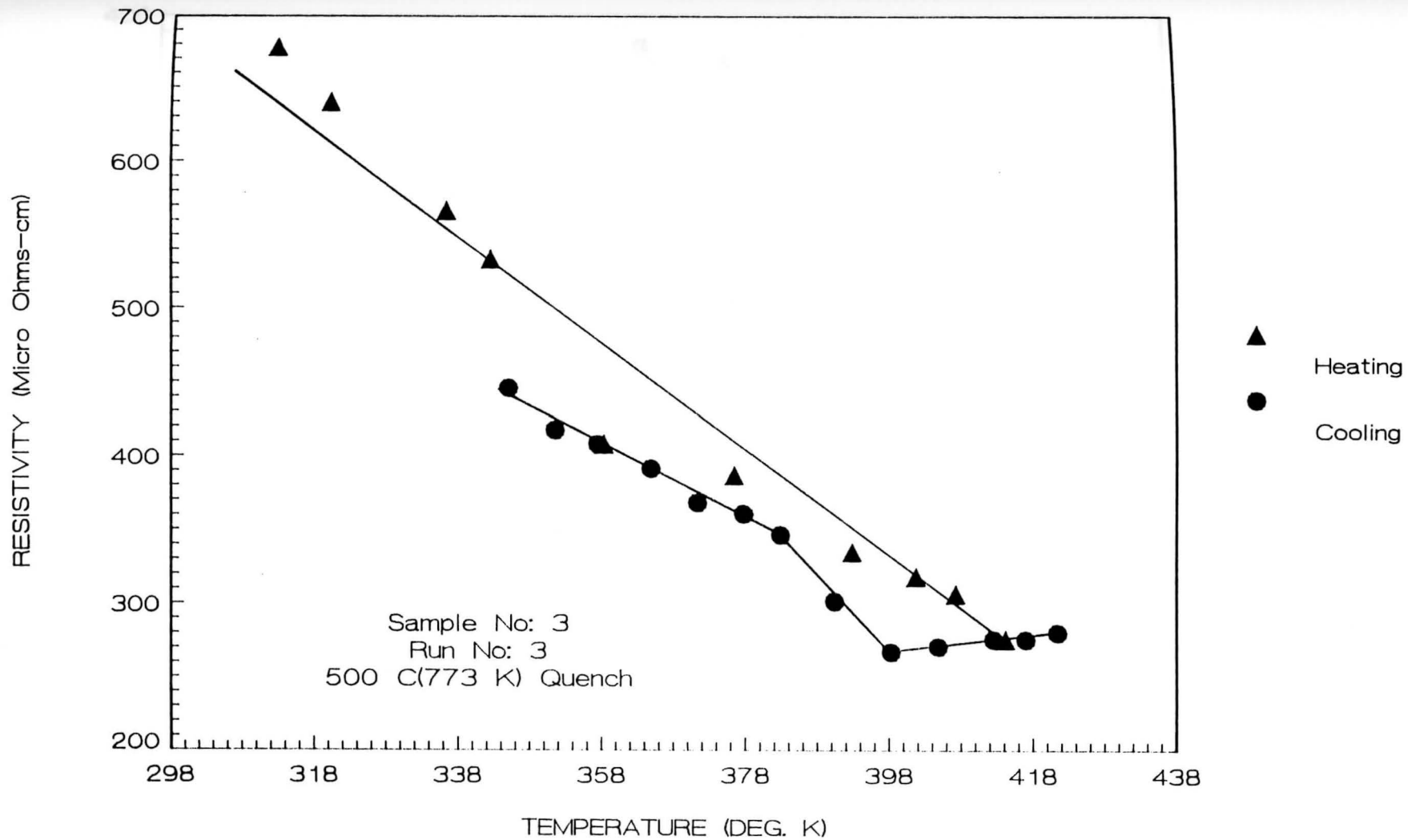


Figure 9. Variation of resistivity as a function of temperature

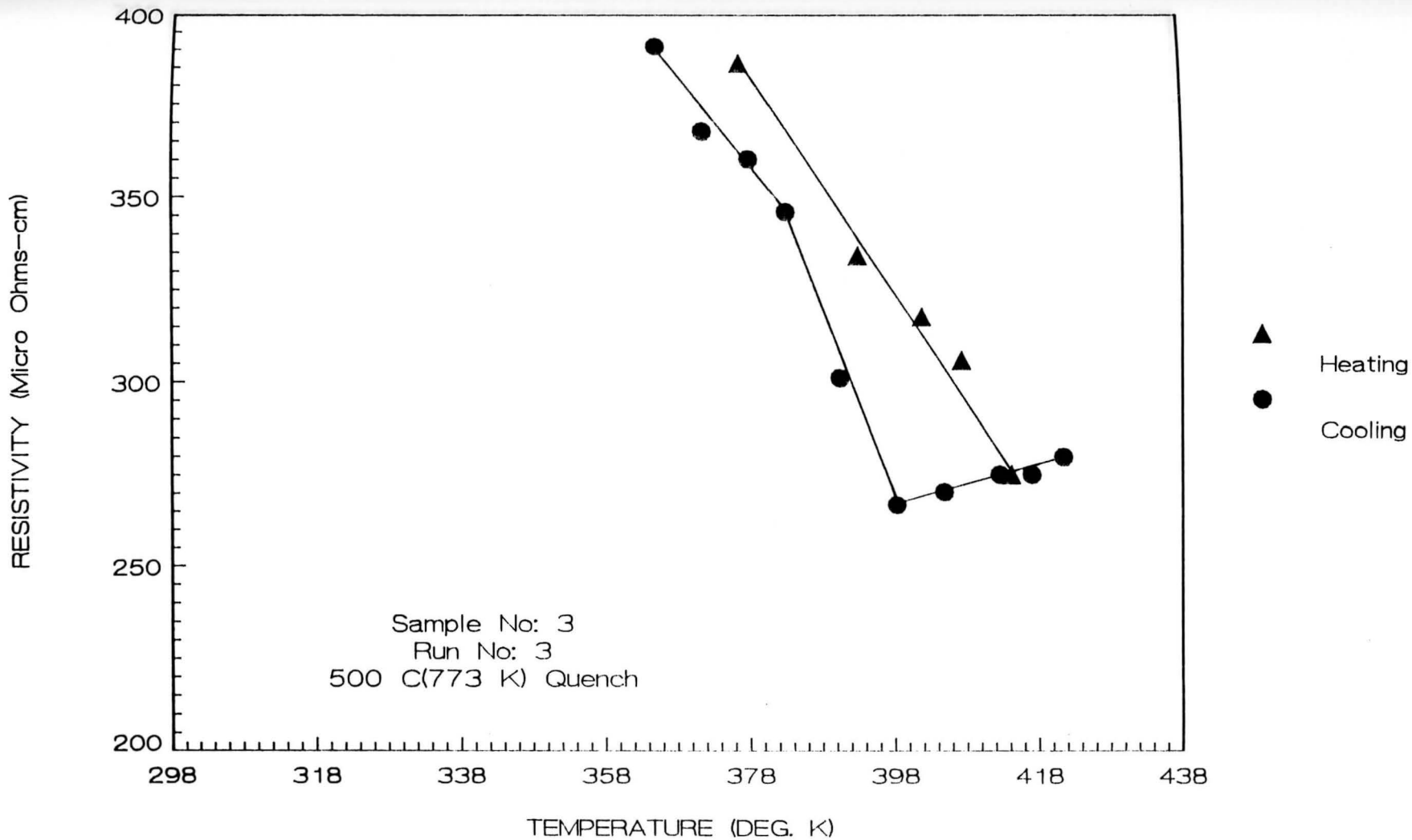


Figure 9a. Variation of resistivity as a function of temperature

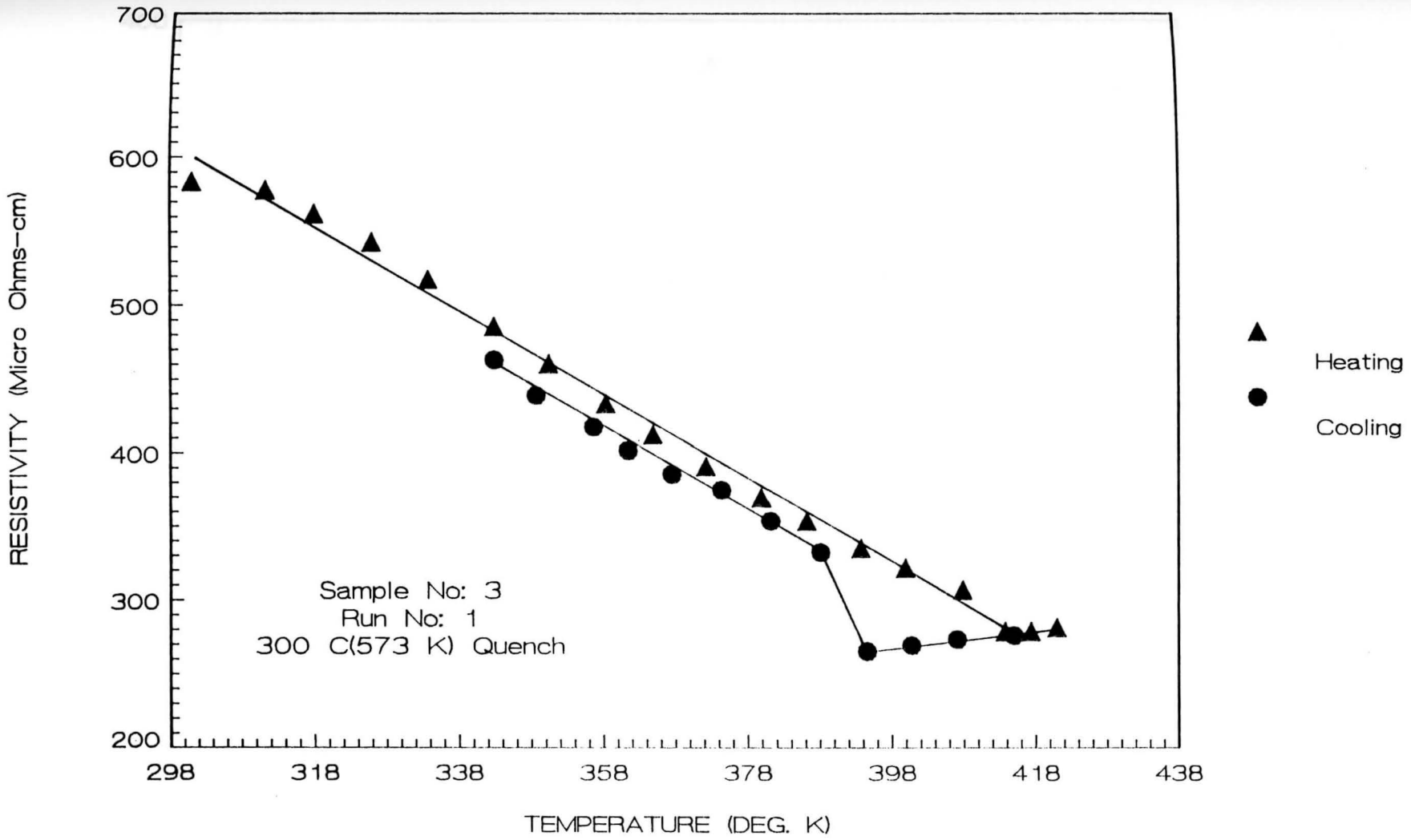


Figure 10. Variation of resistivity as a function of temperature

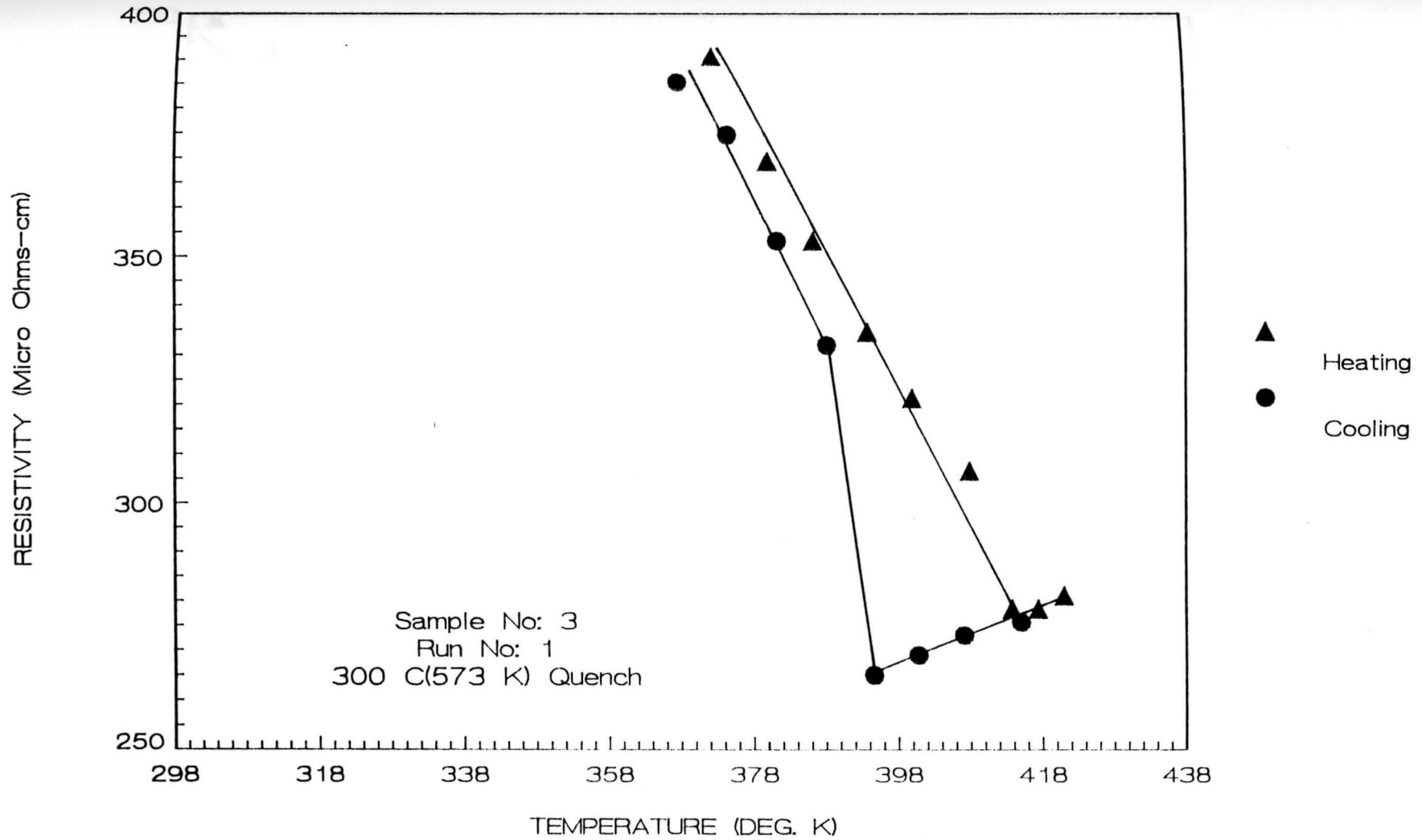


Figure 10a. Variation of resistivity as a function of temperature

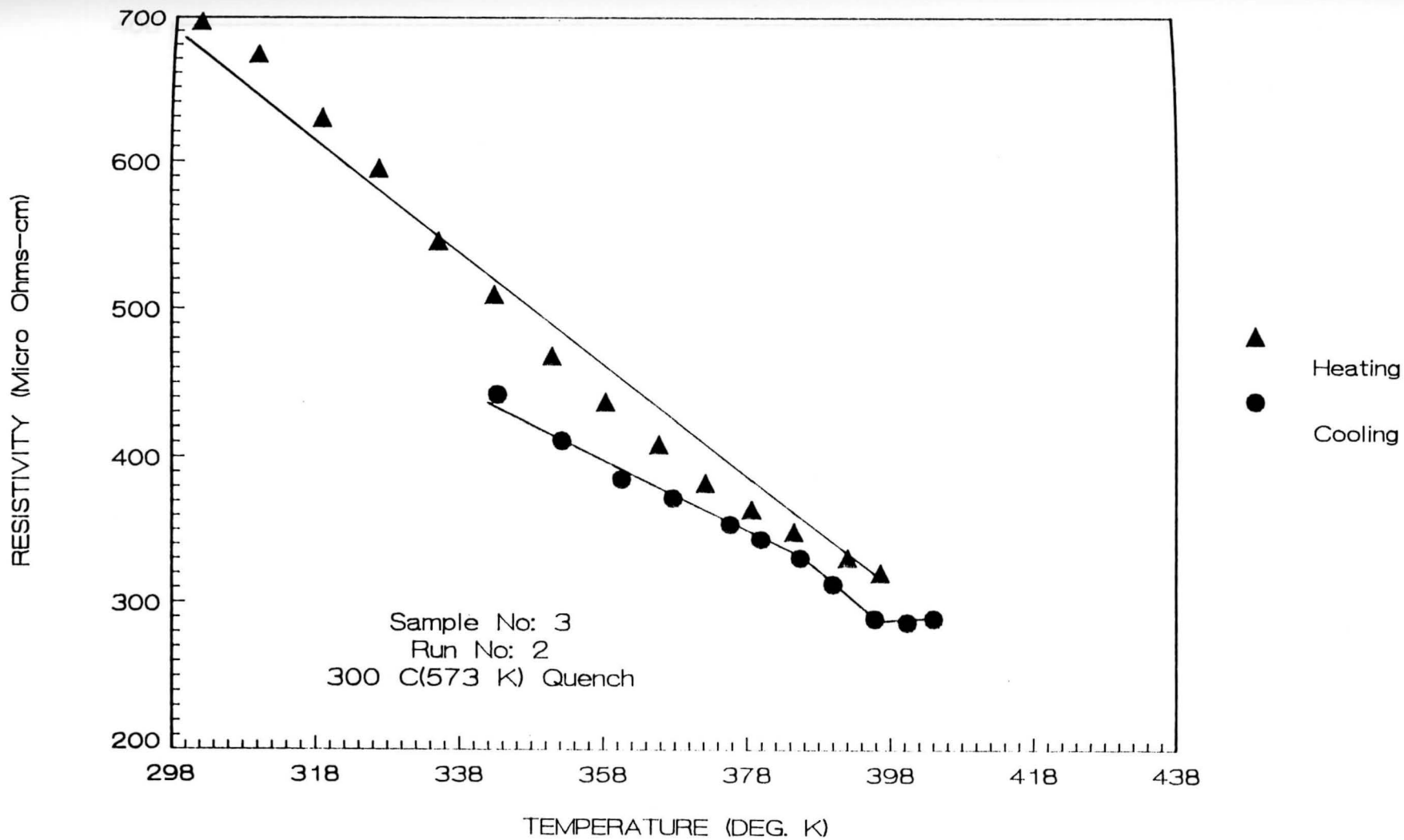


Figure 11. Variation of resistivity as a function of temperature

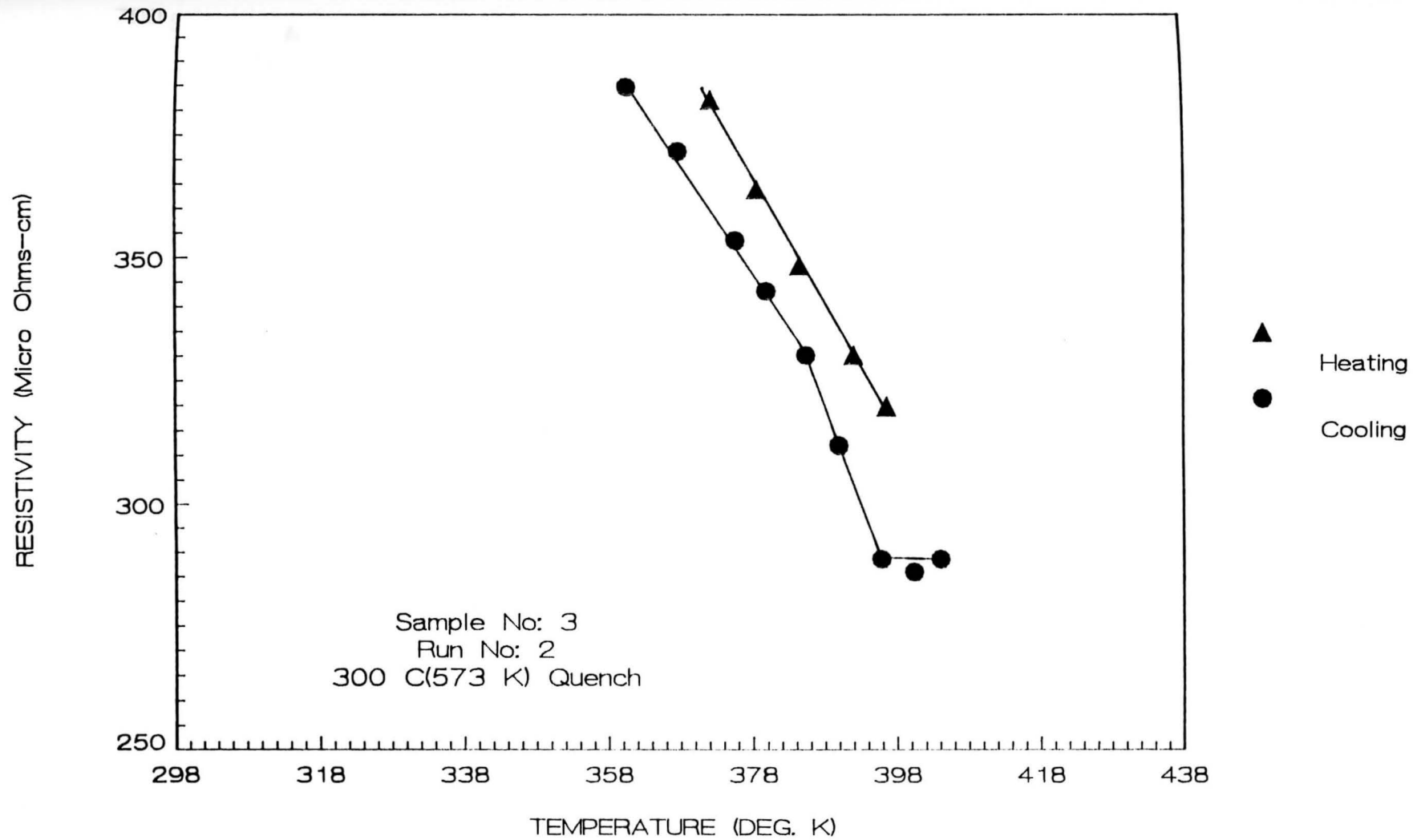


Figure 11a. Variation of resistivity as a function of temperature

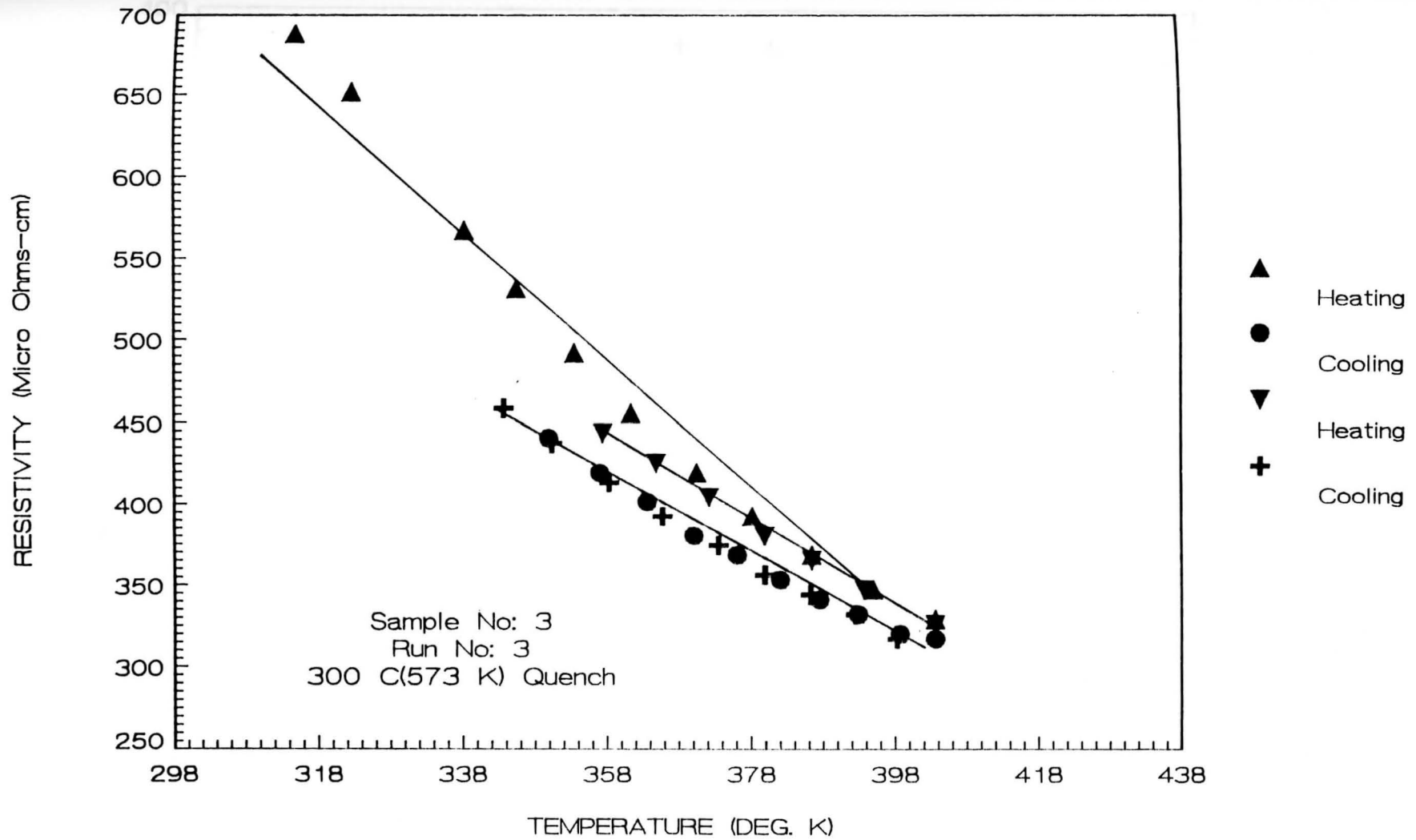


Figure 12. Variation of resistivity as a function of temperature

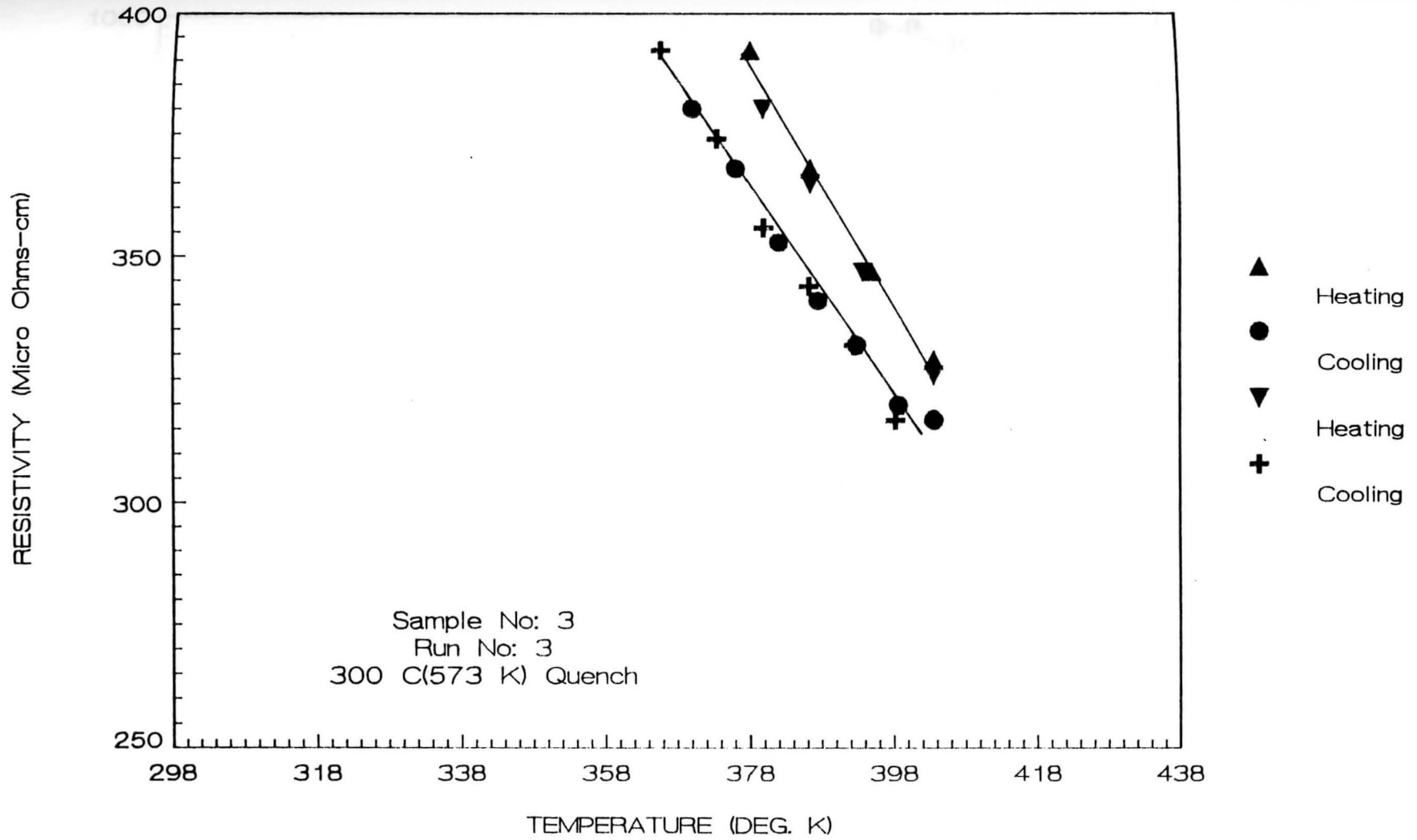


Figure 12a. Variation of resistivity as a function of temperature

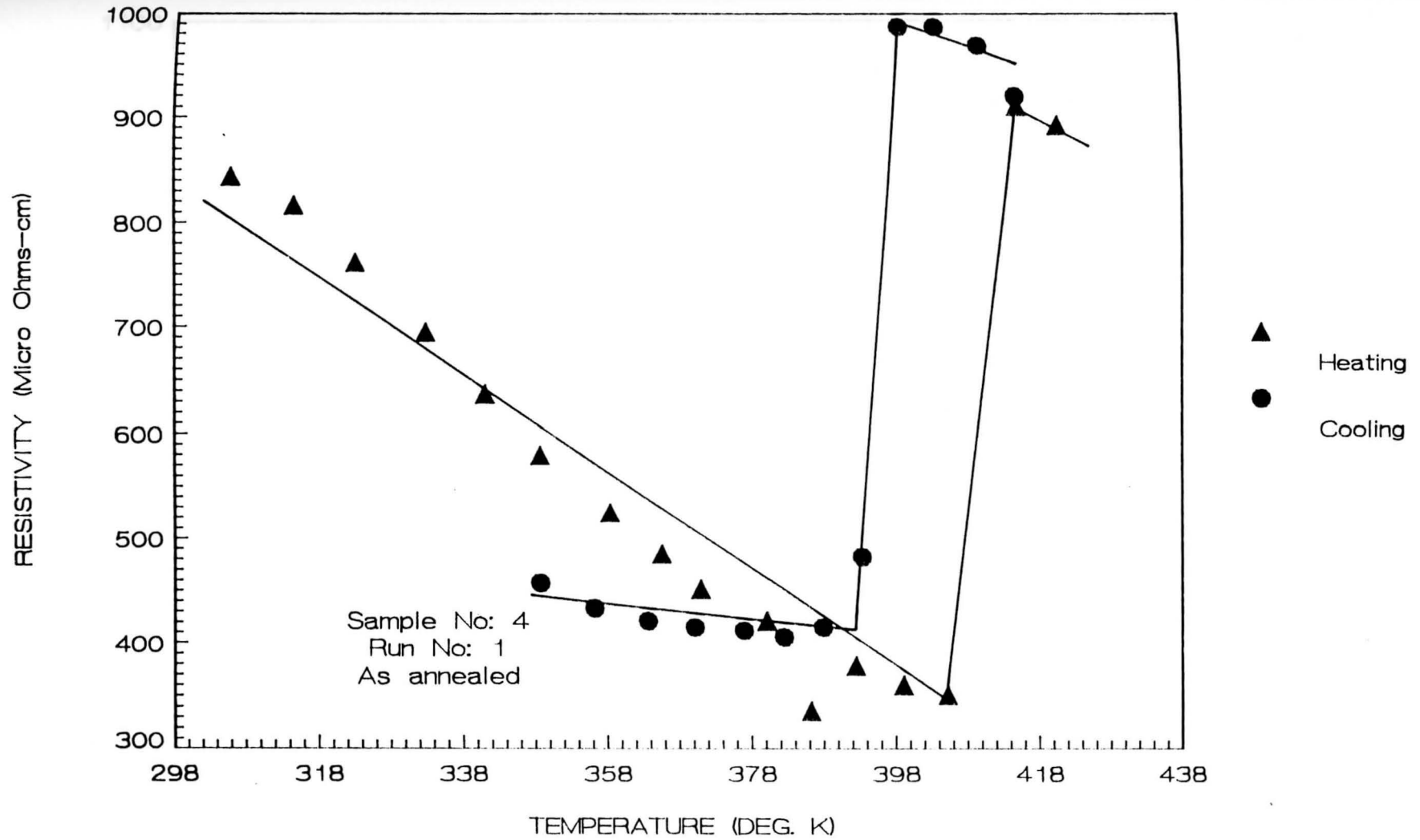


Figure 13. Variation of resistivity as a function of temperature

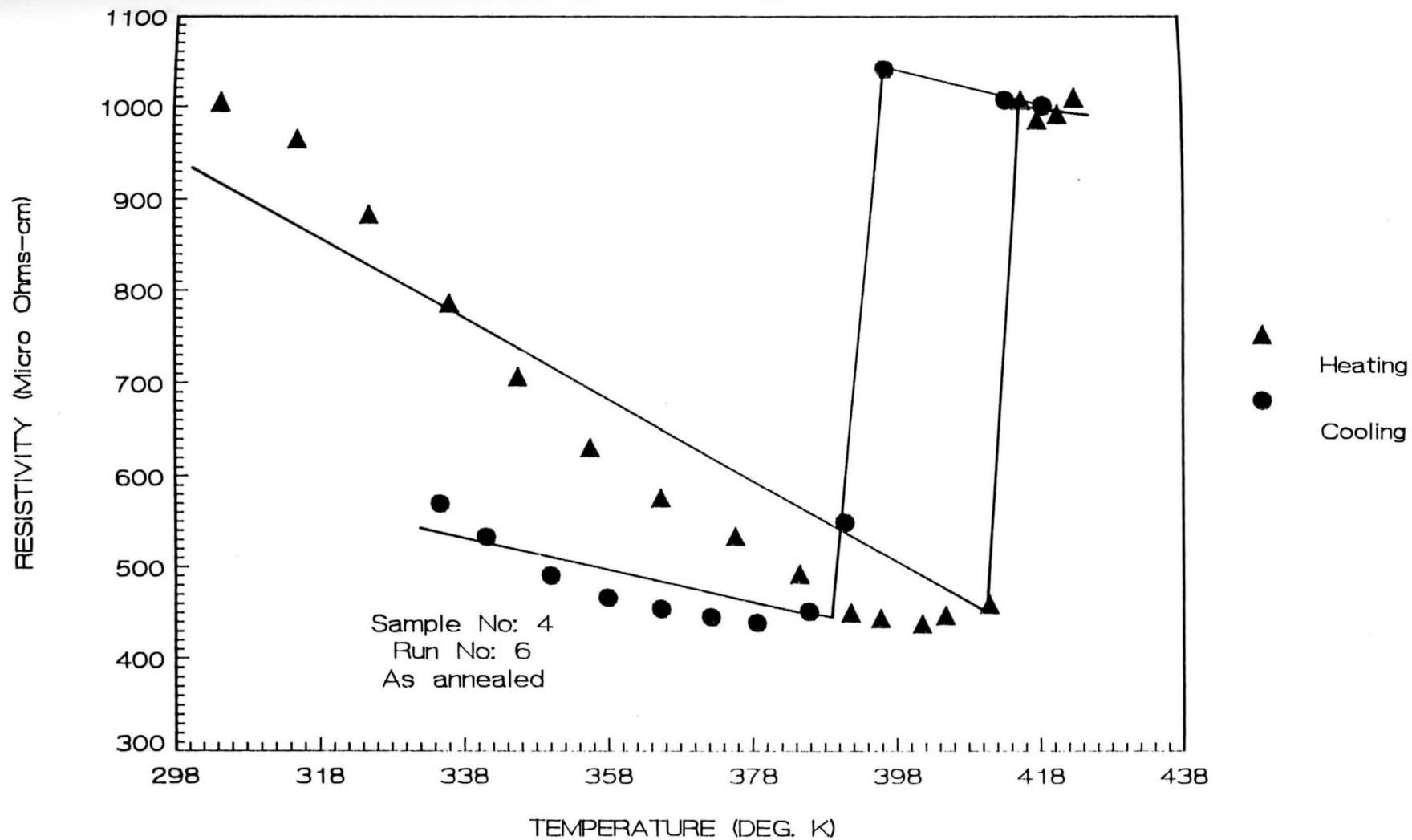


Figure 14 .Variation of resistivity as a function of temperature

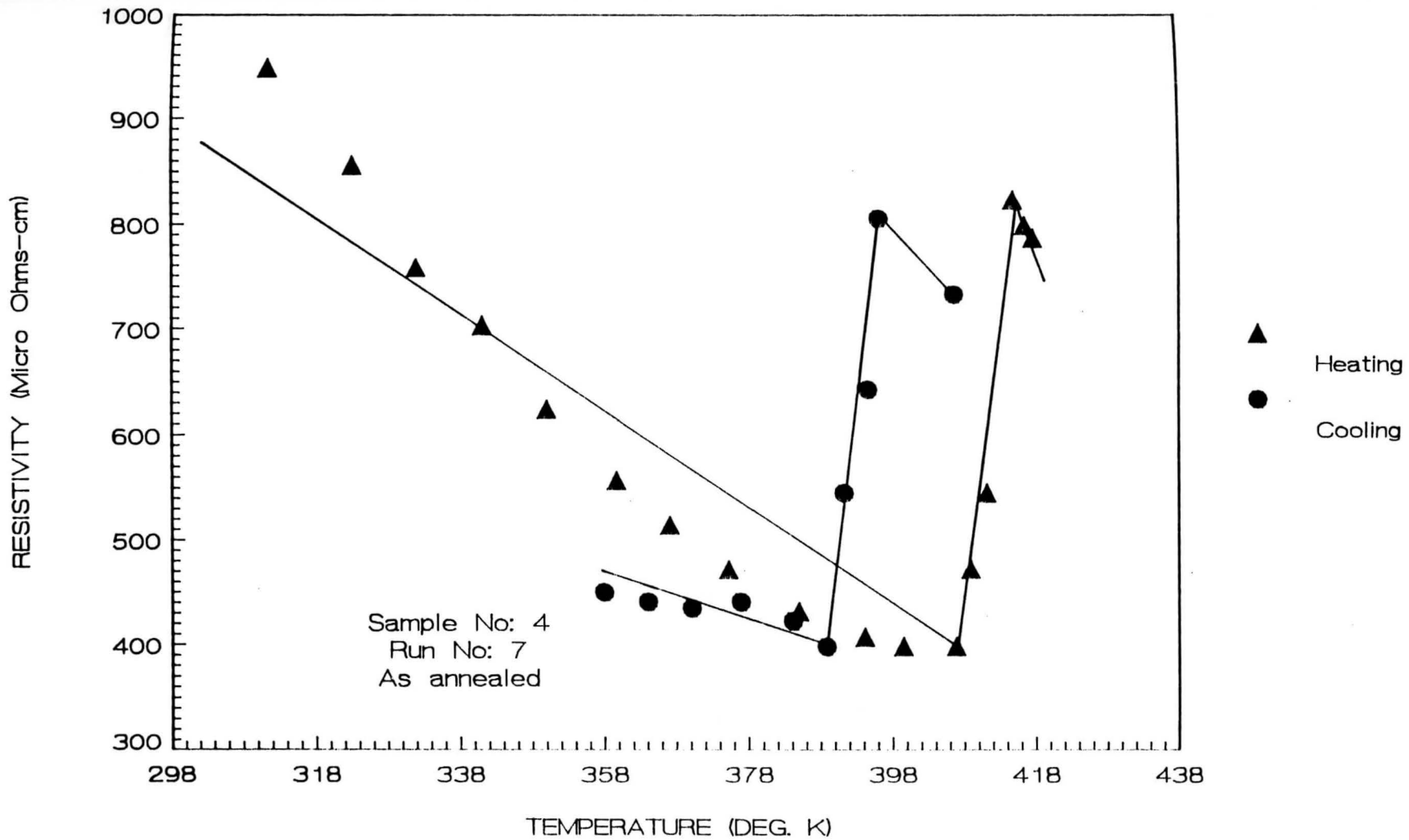


Figure 15. Variation of resistivity as a function of temperature

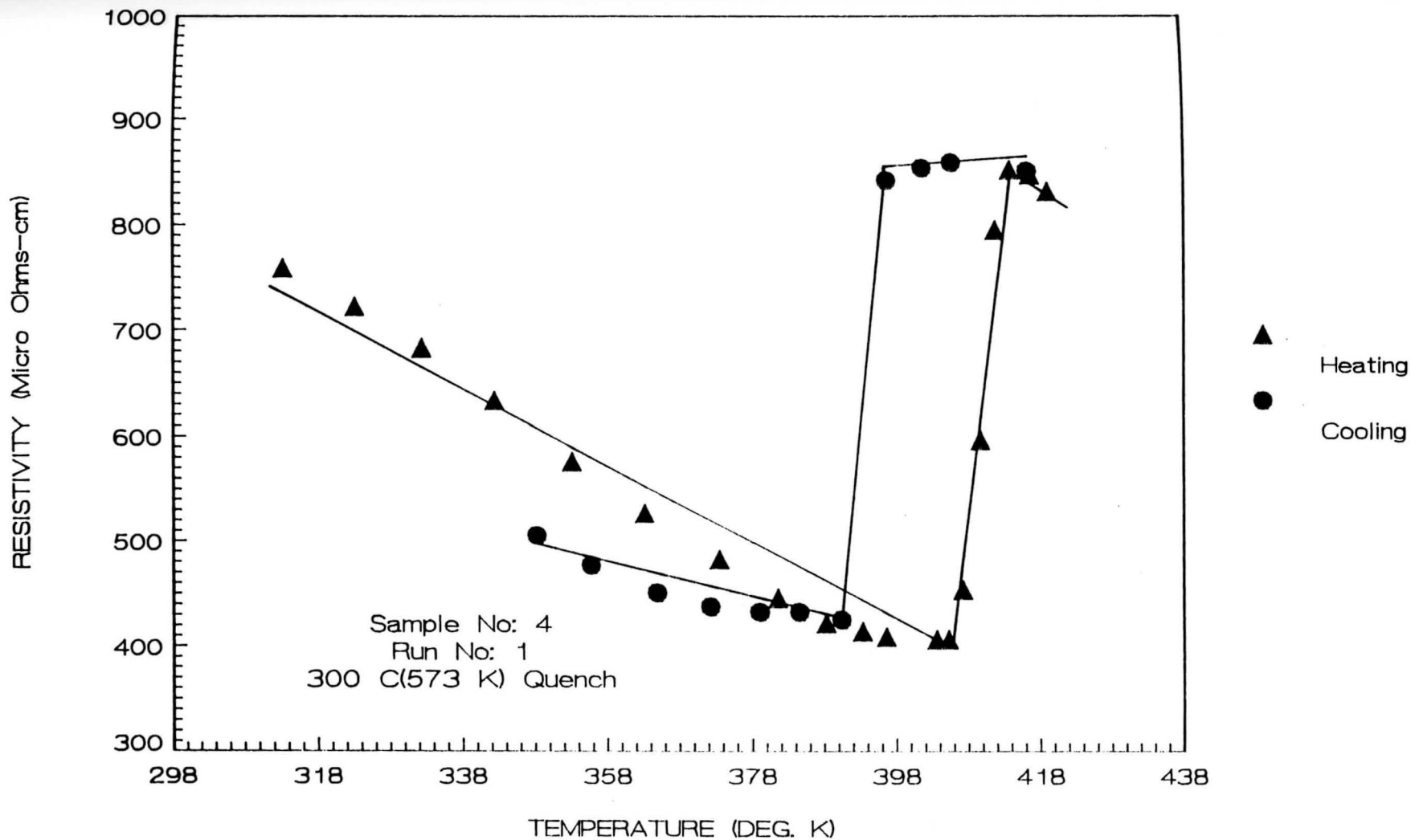


Figure 16. Variation of resistivity as a function of temperature

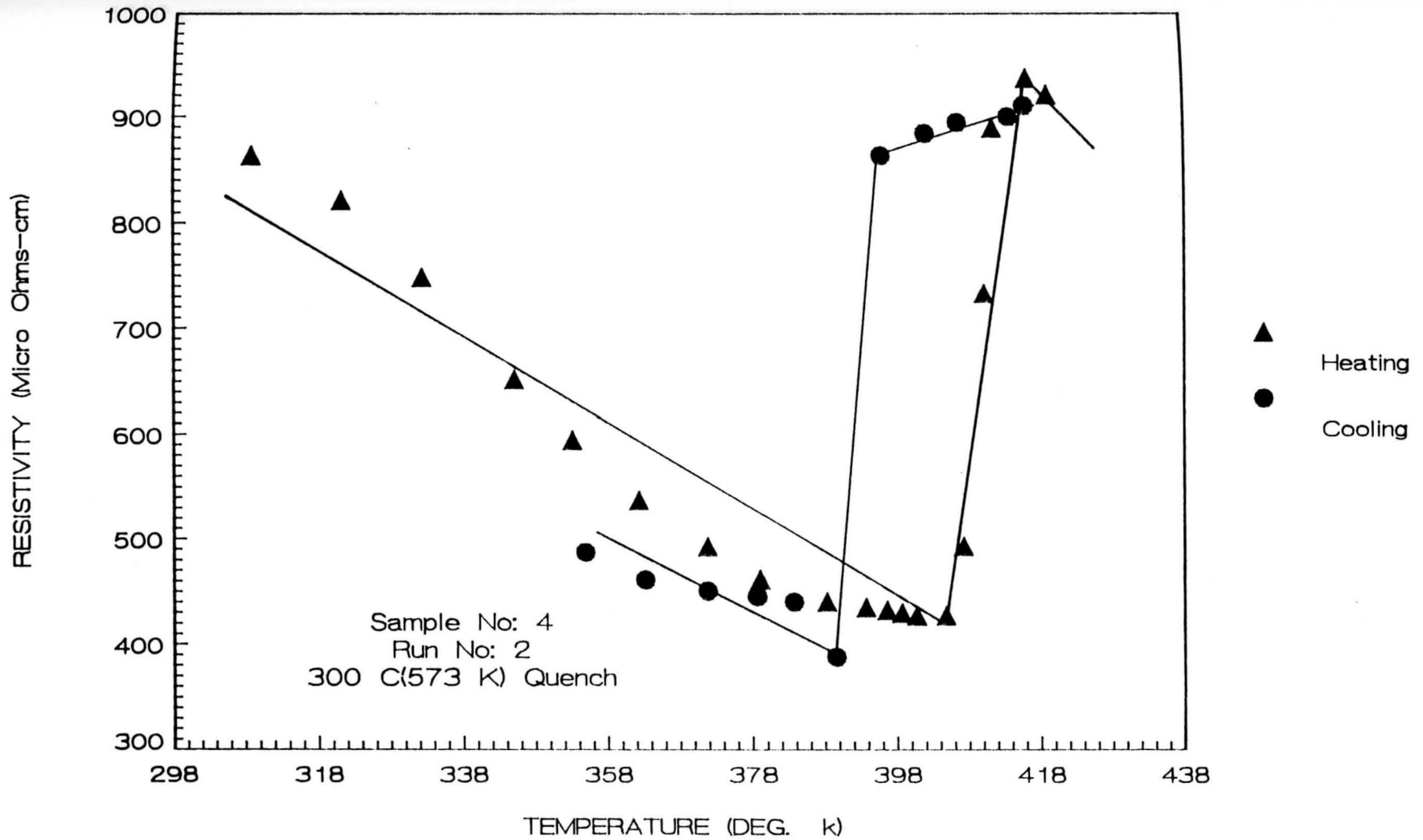


Figure 17. Variation of resistivity as a function of temperature

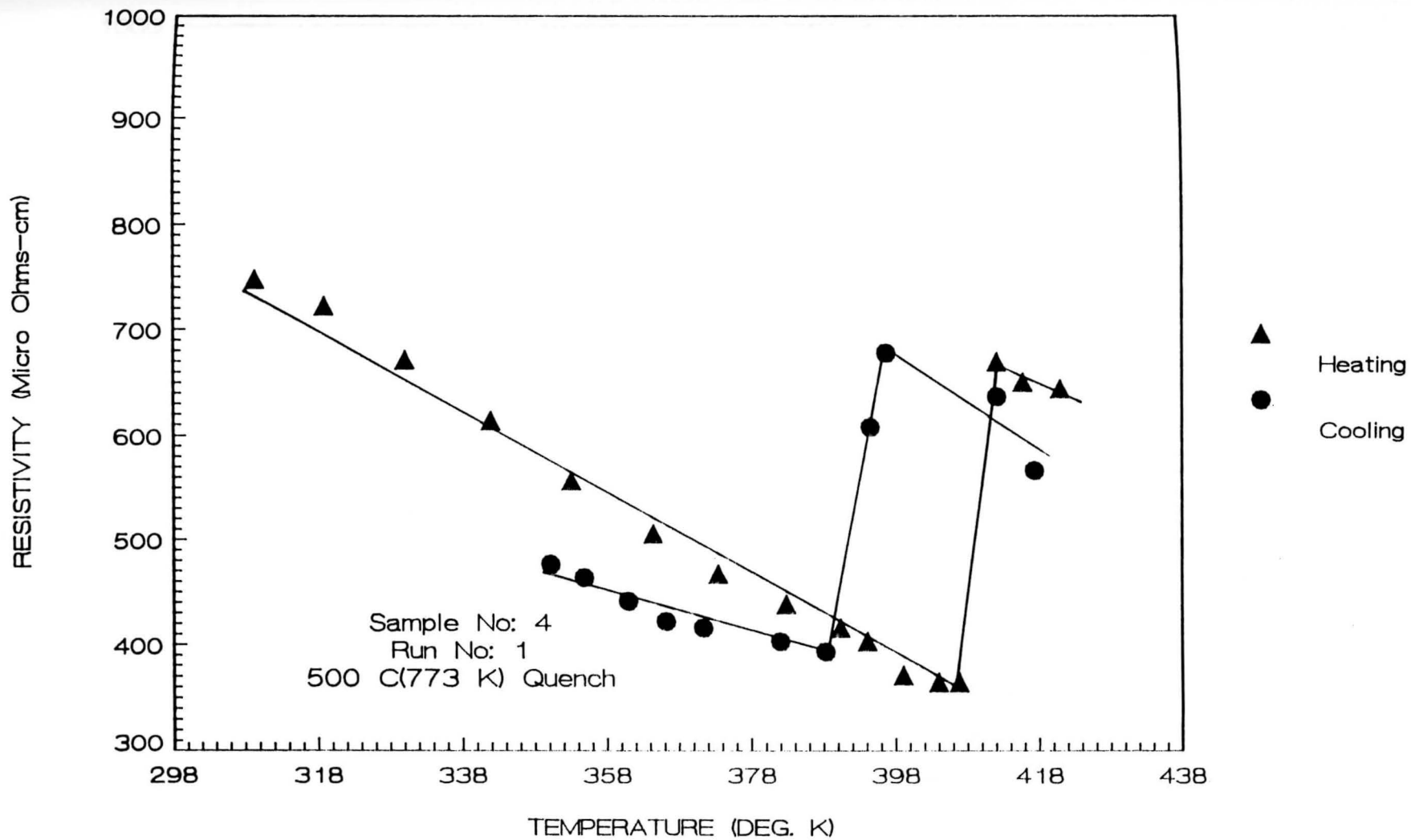


Figure 18. Variation of resistivity as a function of temperature

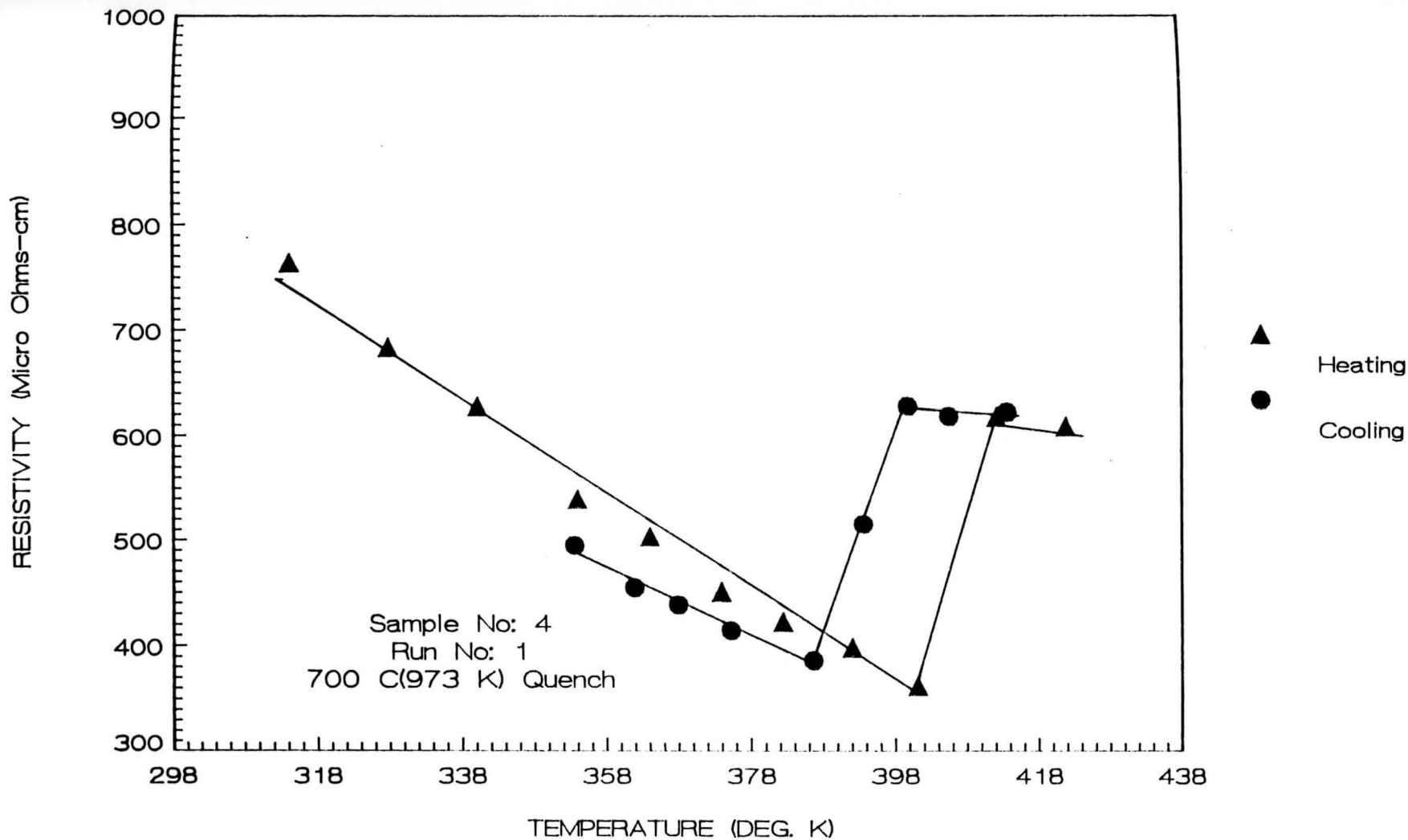


Figure 19. Variation of resistivity as a function of temperature

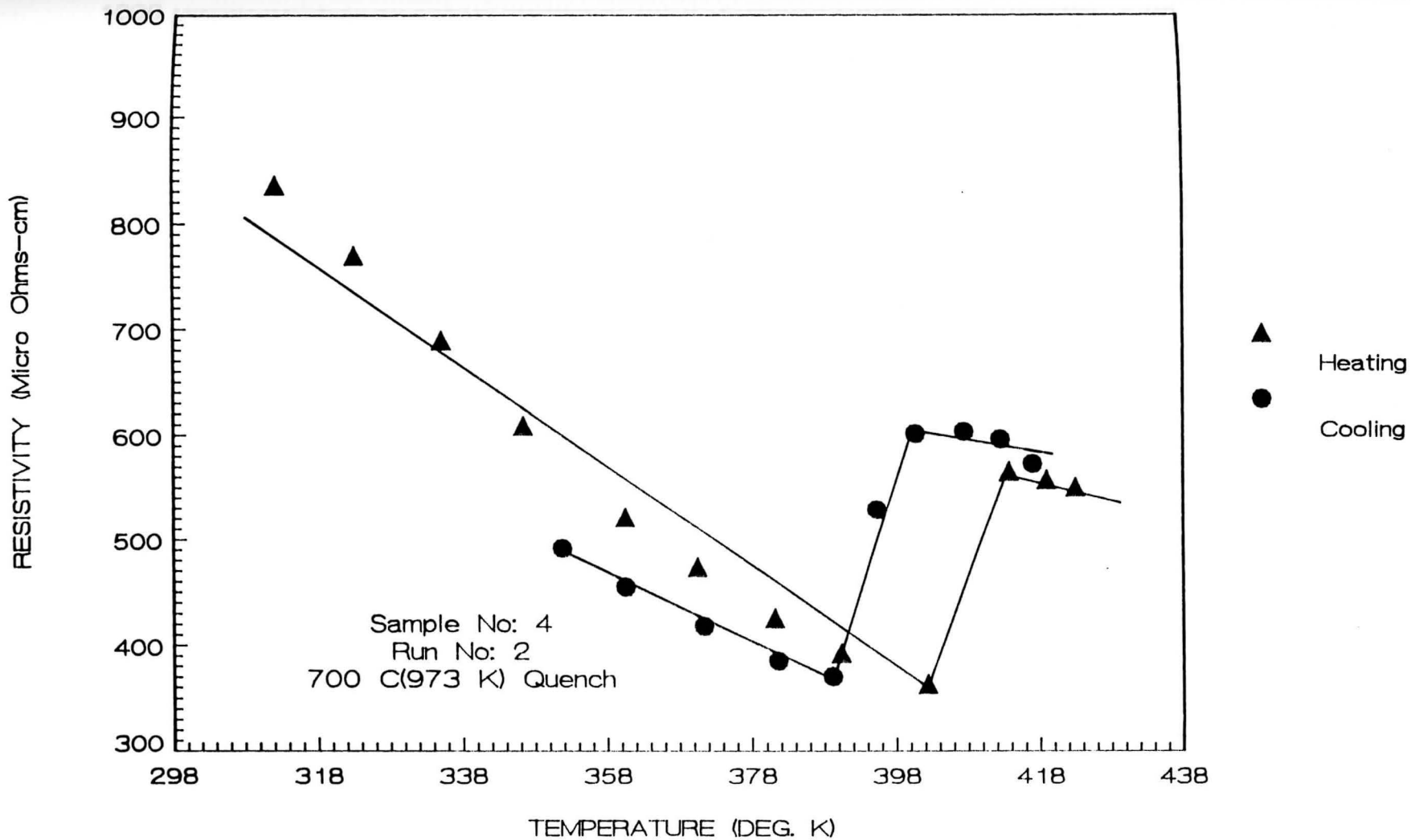


Figure 20. Variation of resistivity as a function of temperature

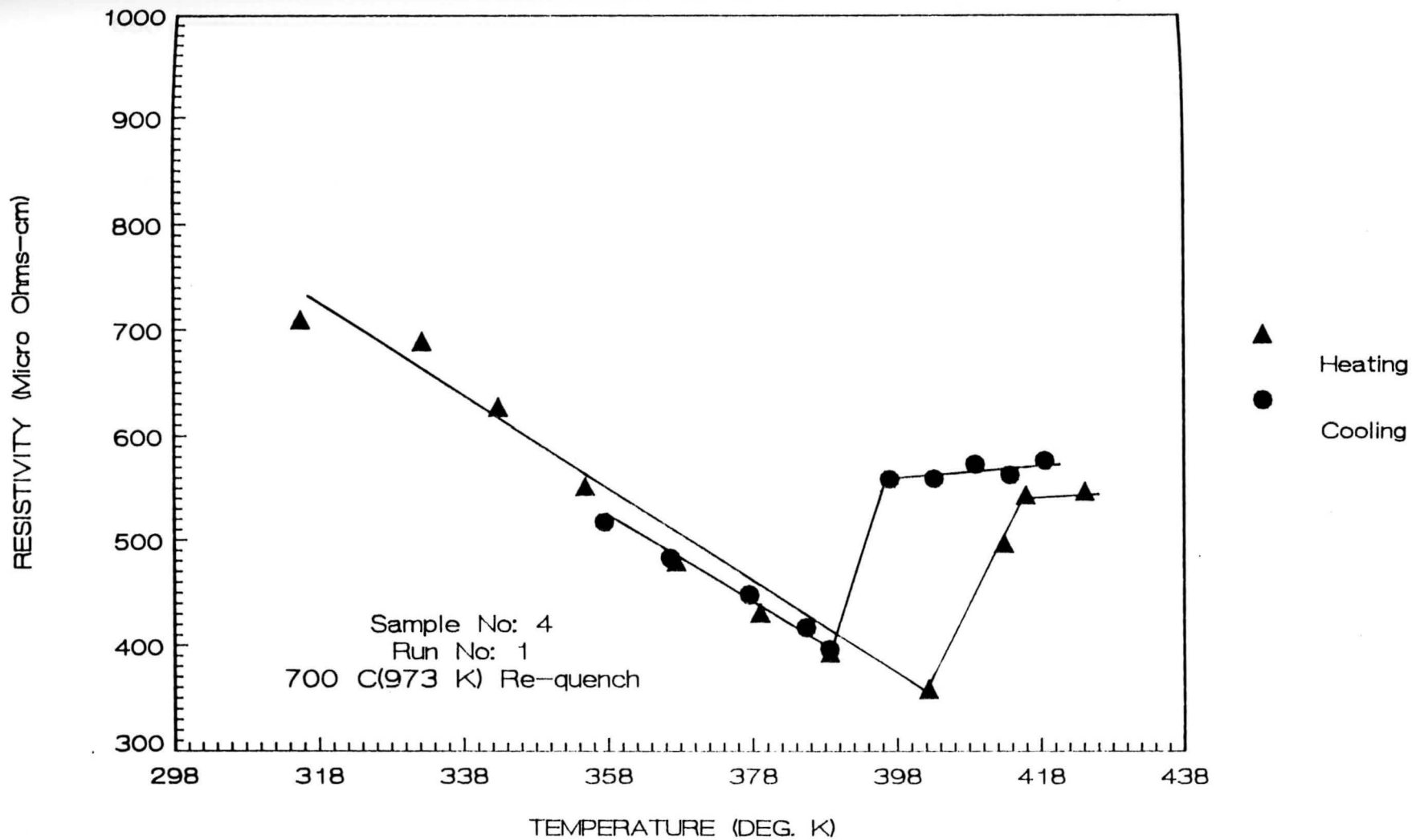


Figure 21. Variation of resistivity as a function of temperature

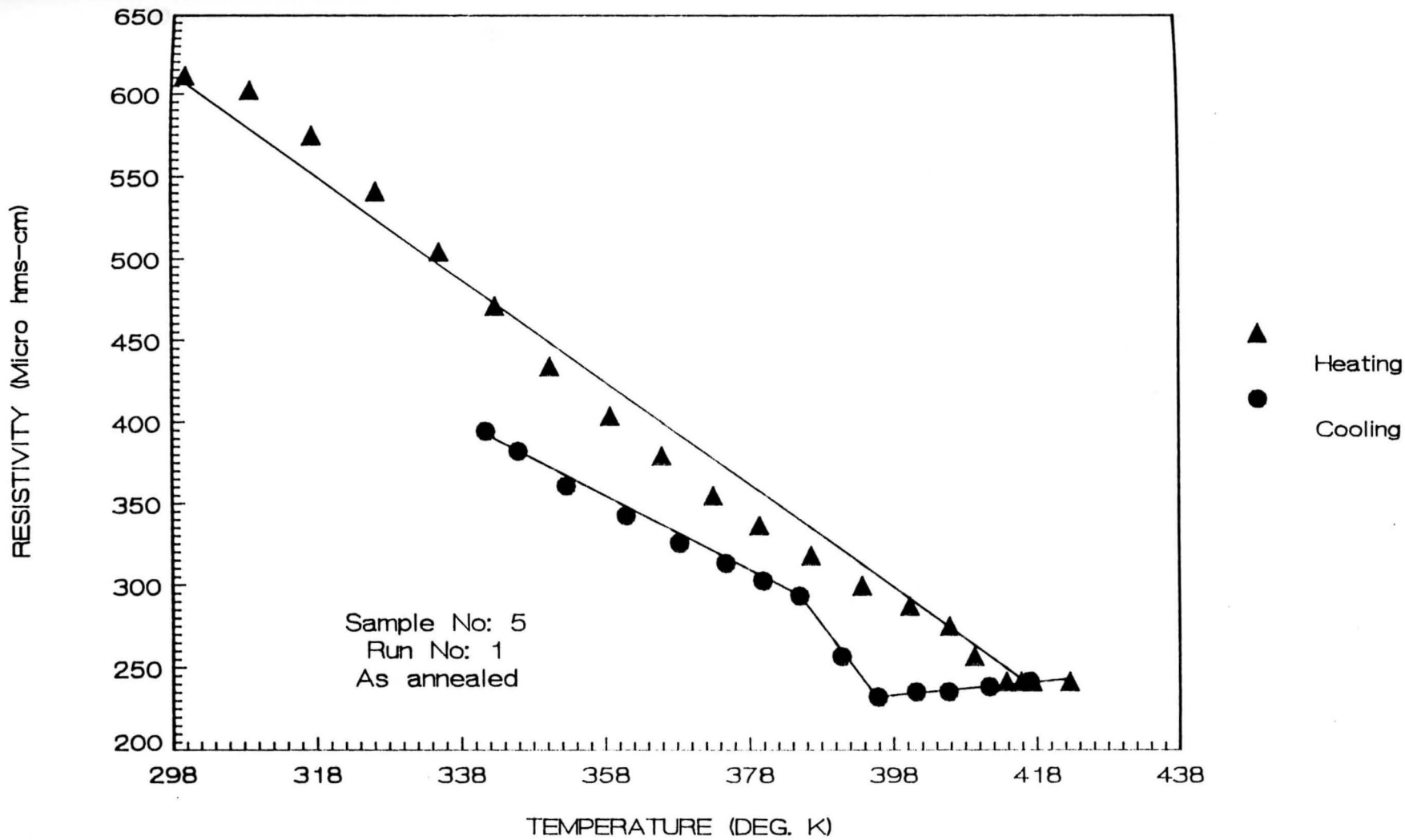


Figure 22. Variation of resistivity as a function of temperature

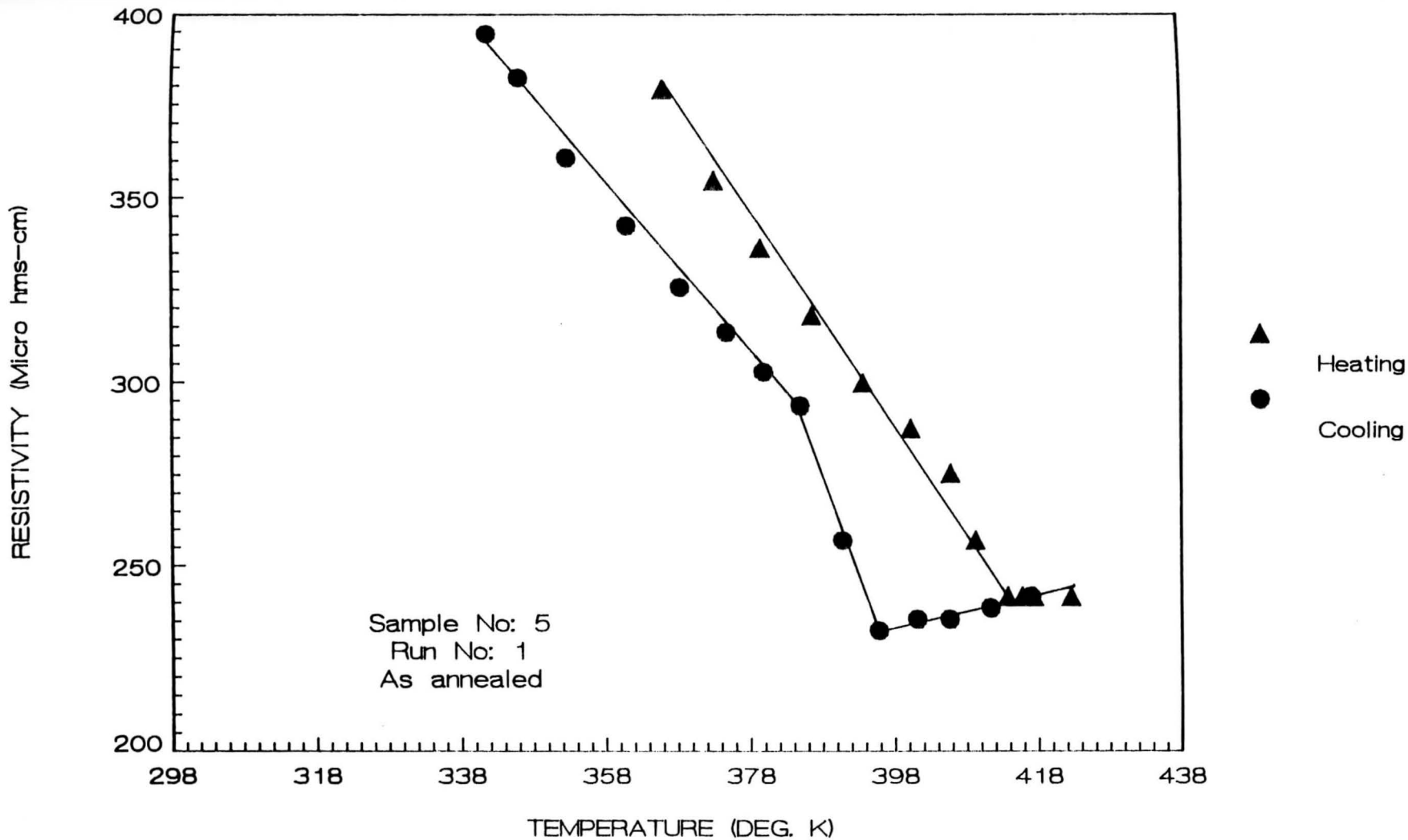


Figure 22a. Variation of resistivity as a function of temperature

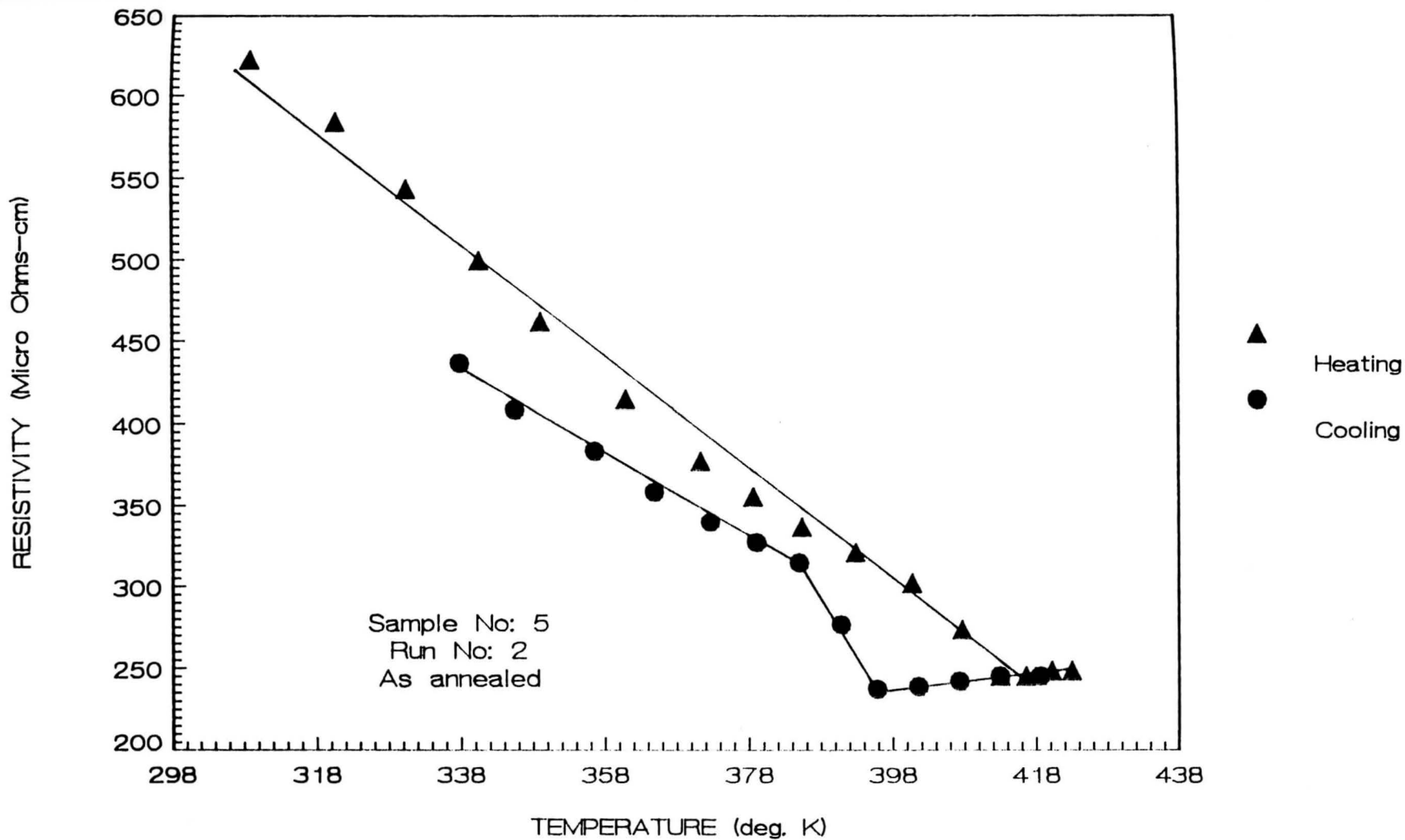


Figure 23. Variation of resistivity as a function of temperature

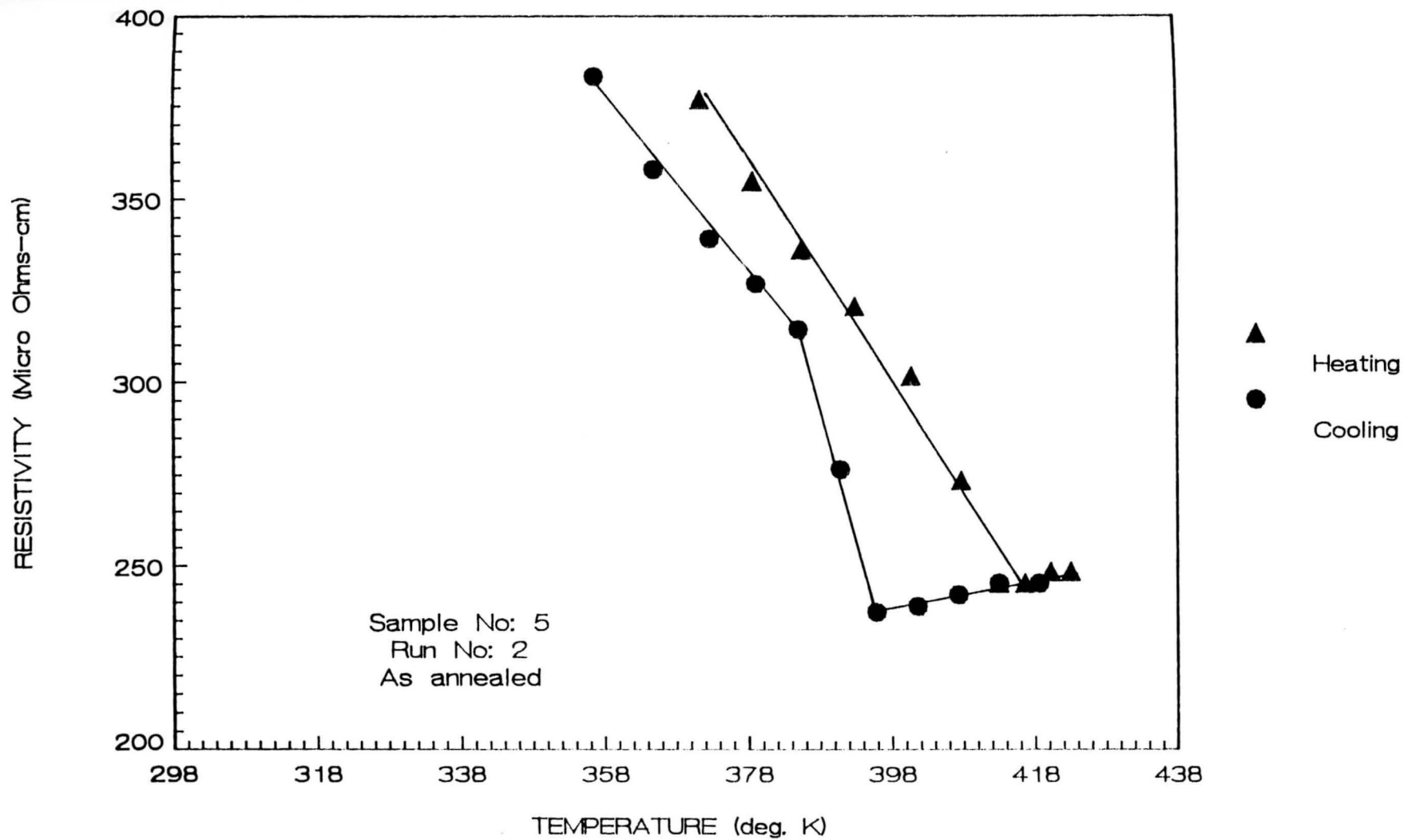


Figure 23a. Variation of resistivity as a function of temperature

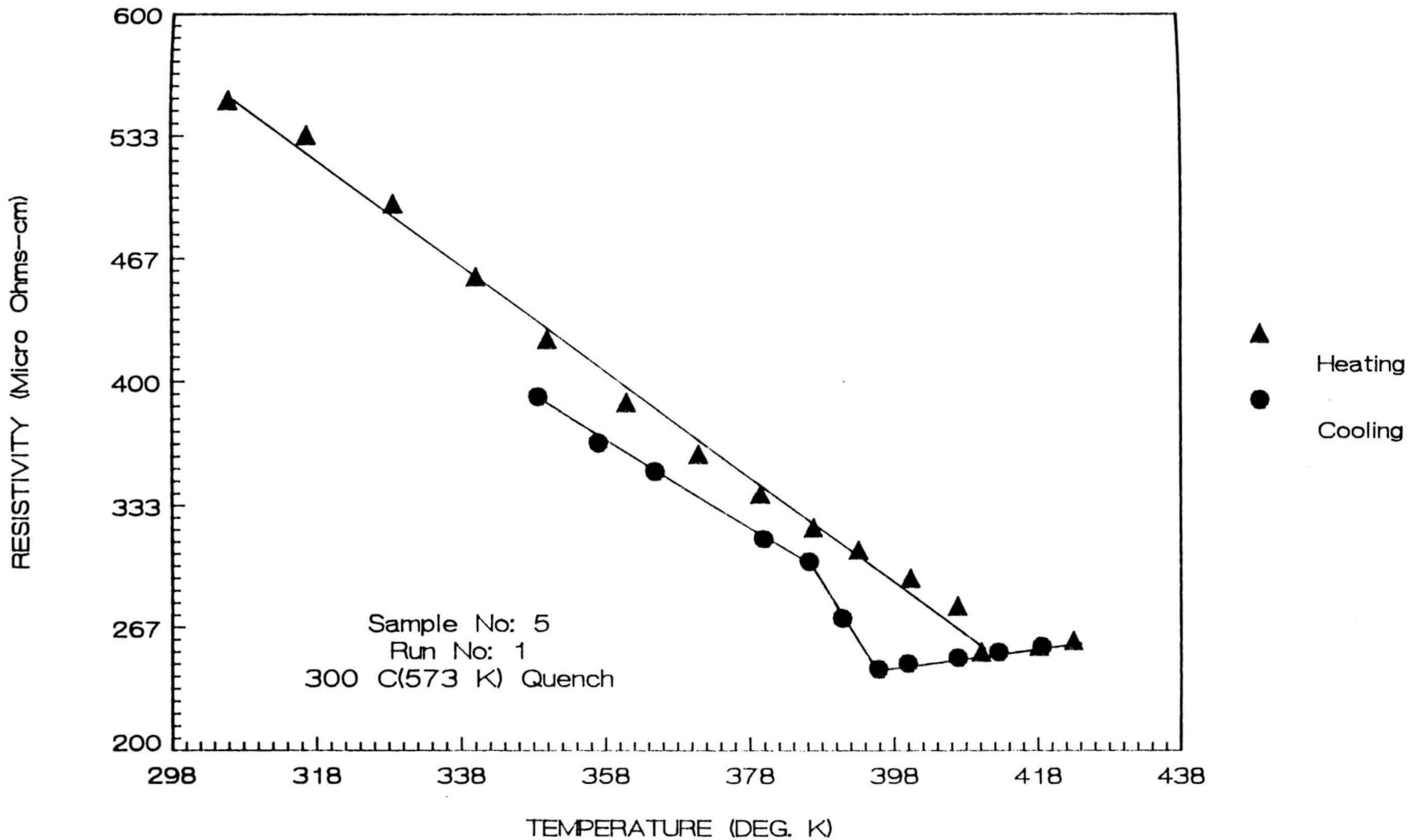


Figure 24. Variation of resistivity as a function of temperature

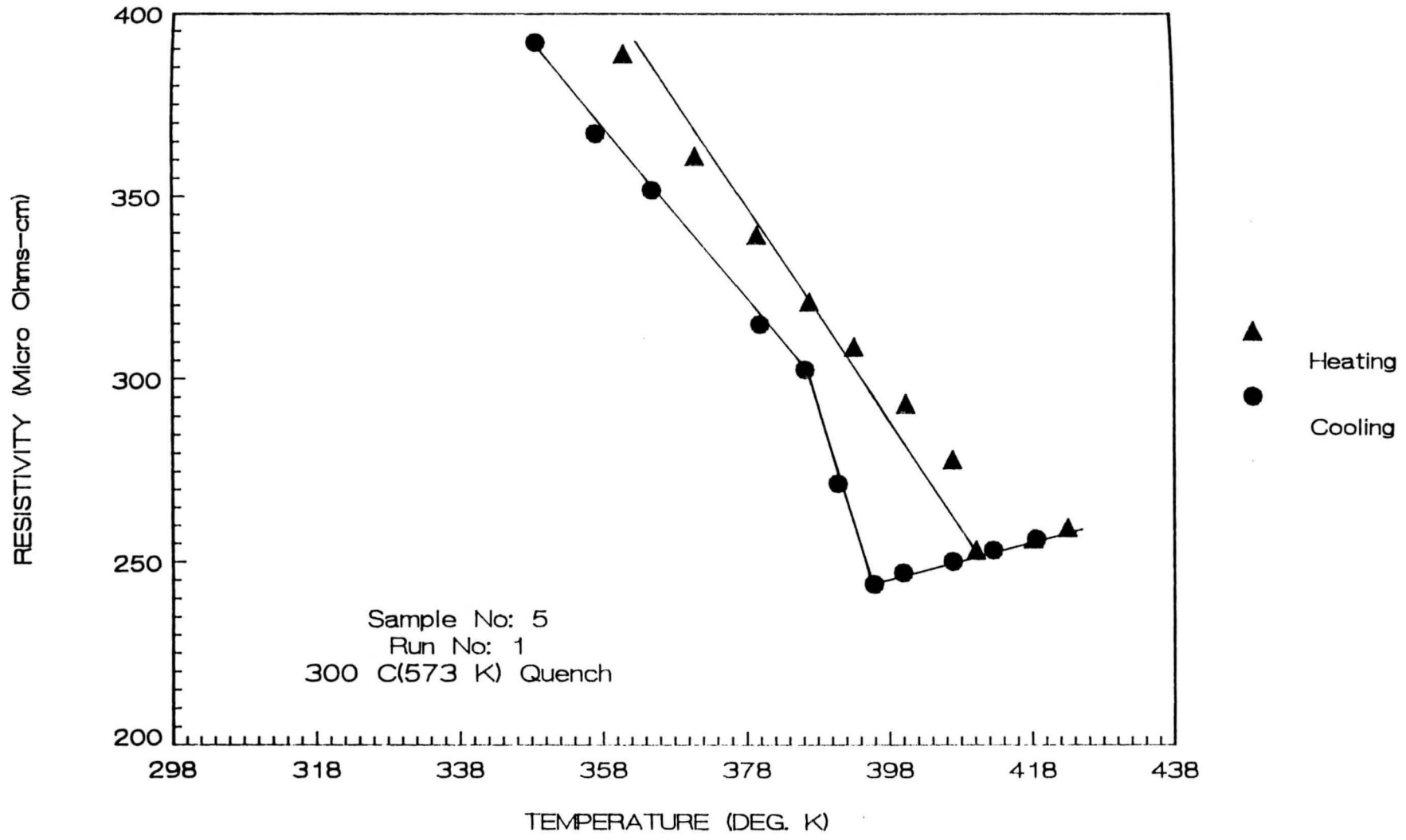


Figure 24a. Variation of resistivity as a function of temperature

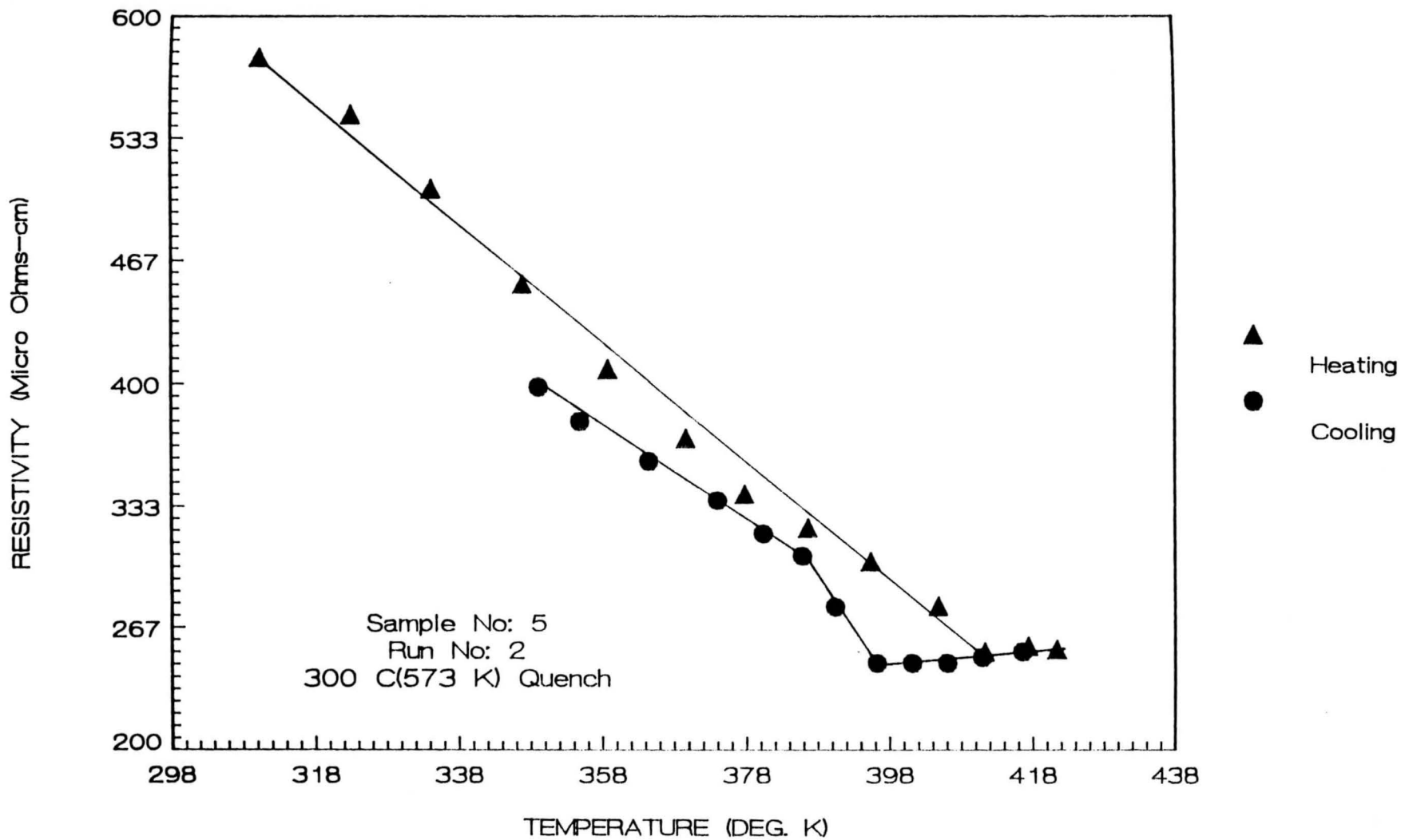


Figure 25. Variation of resistivity as a function of temperature

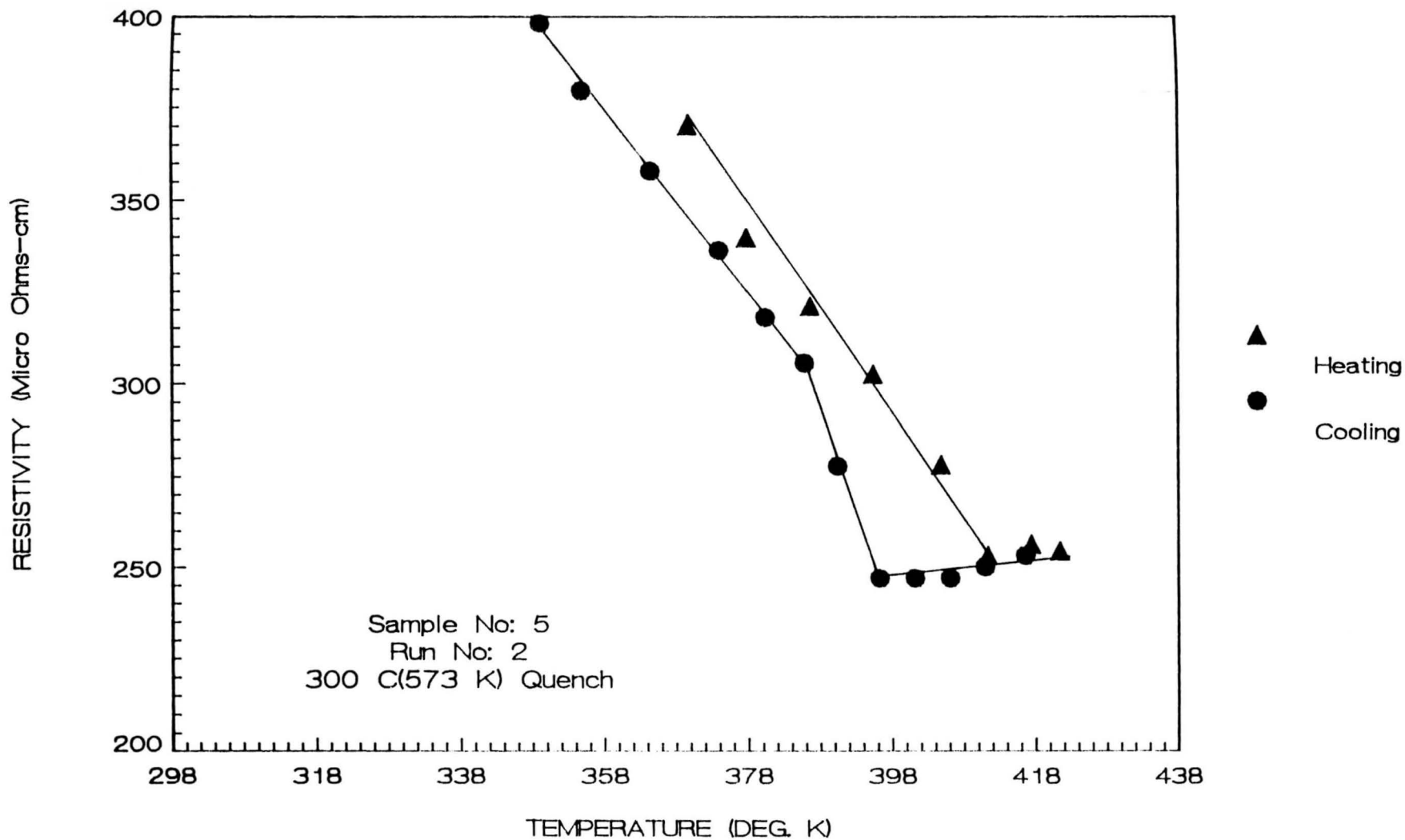


Figure 25a. Variation of resistivity as a function of temperature

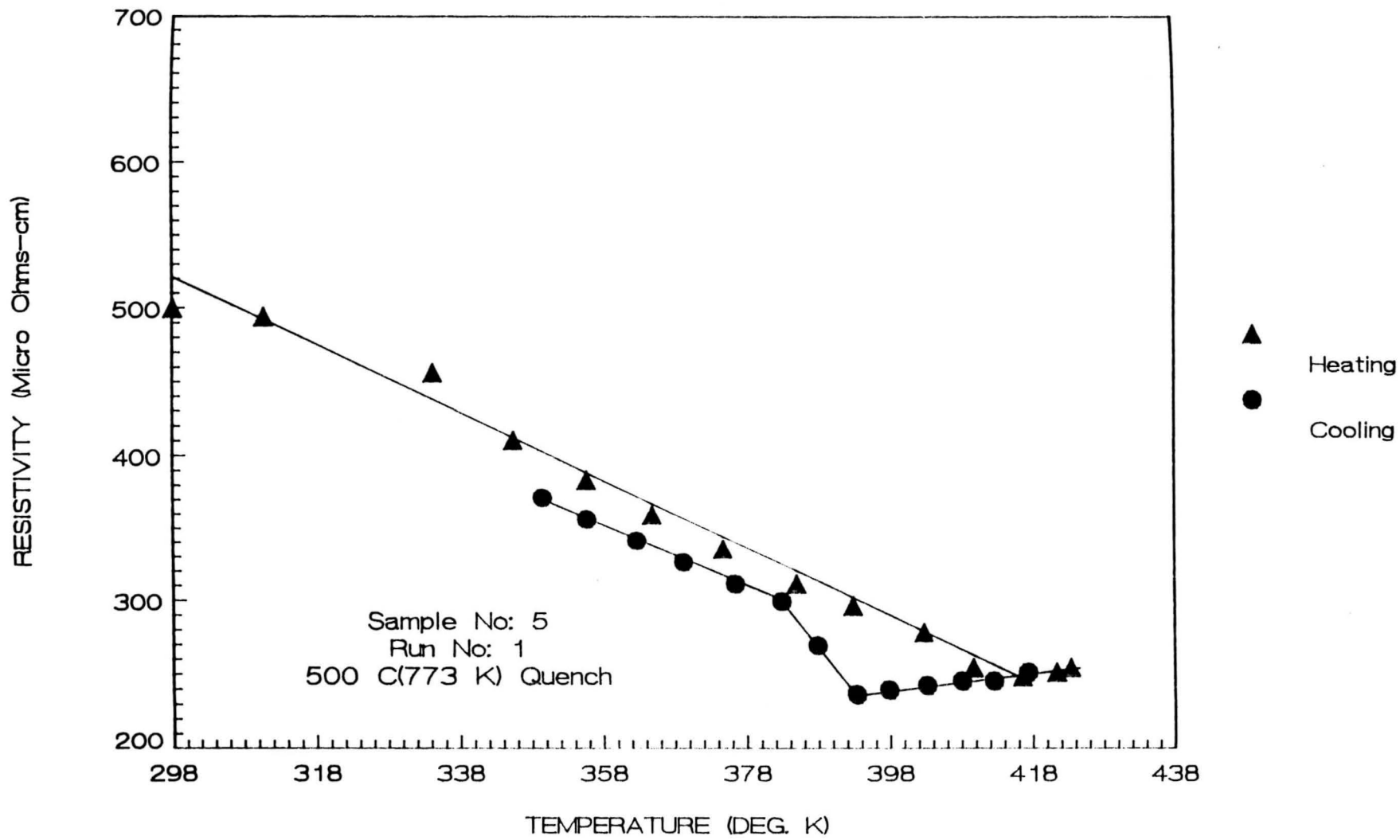


Figure 26. Variation of resistivity as a function of temperature

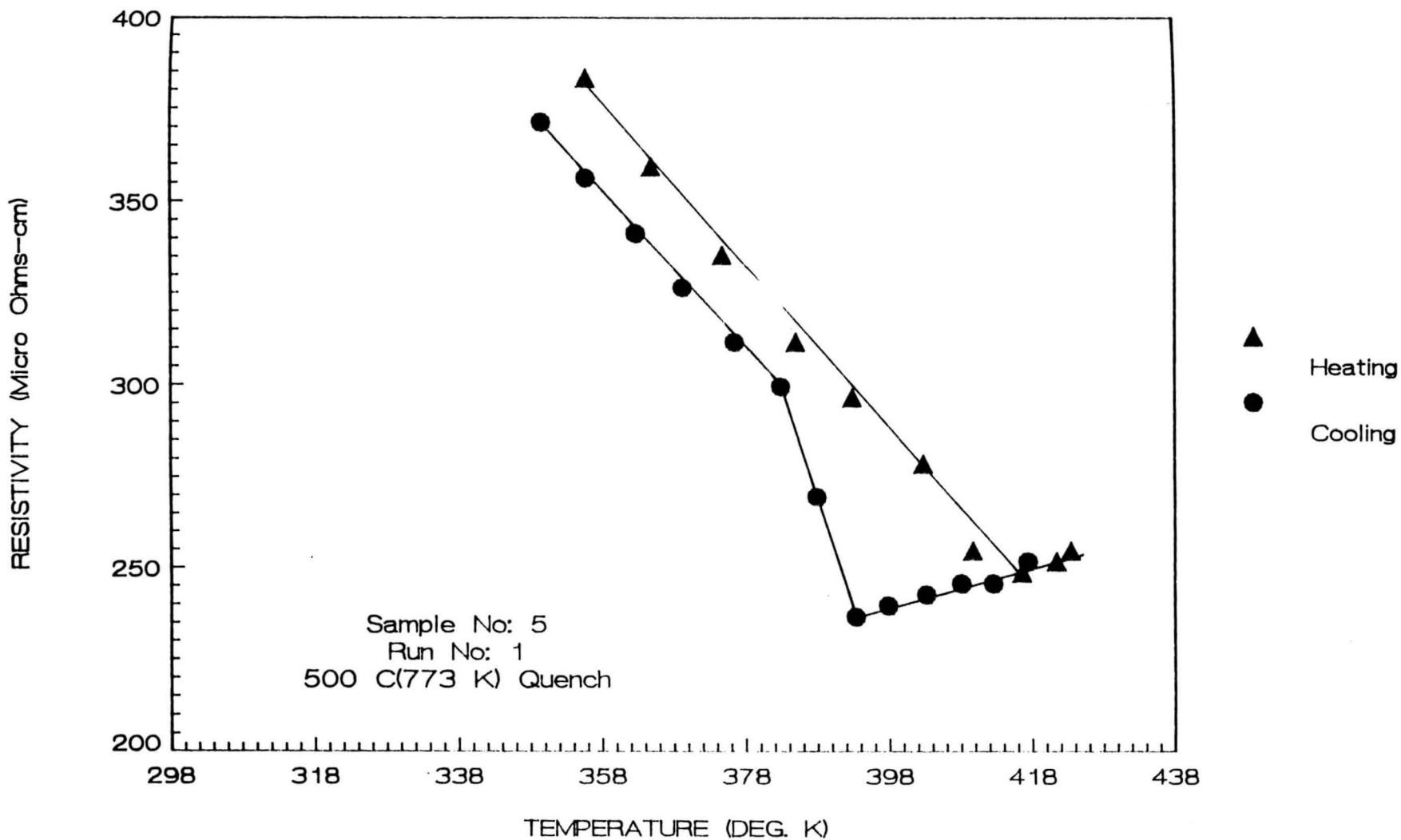


Figure 26a. Variation of resistivity as a function of temperature

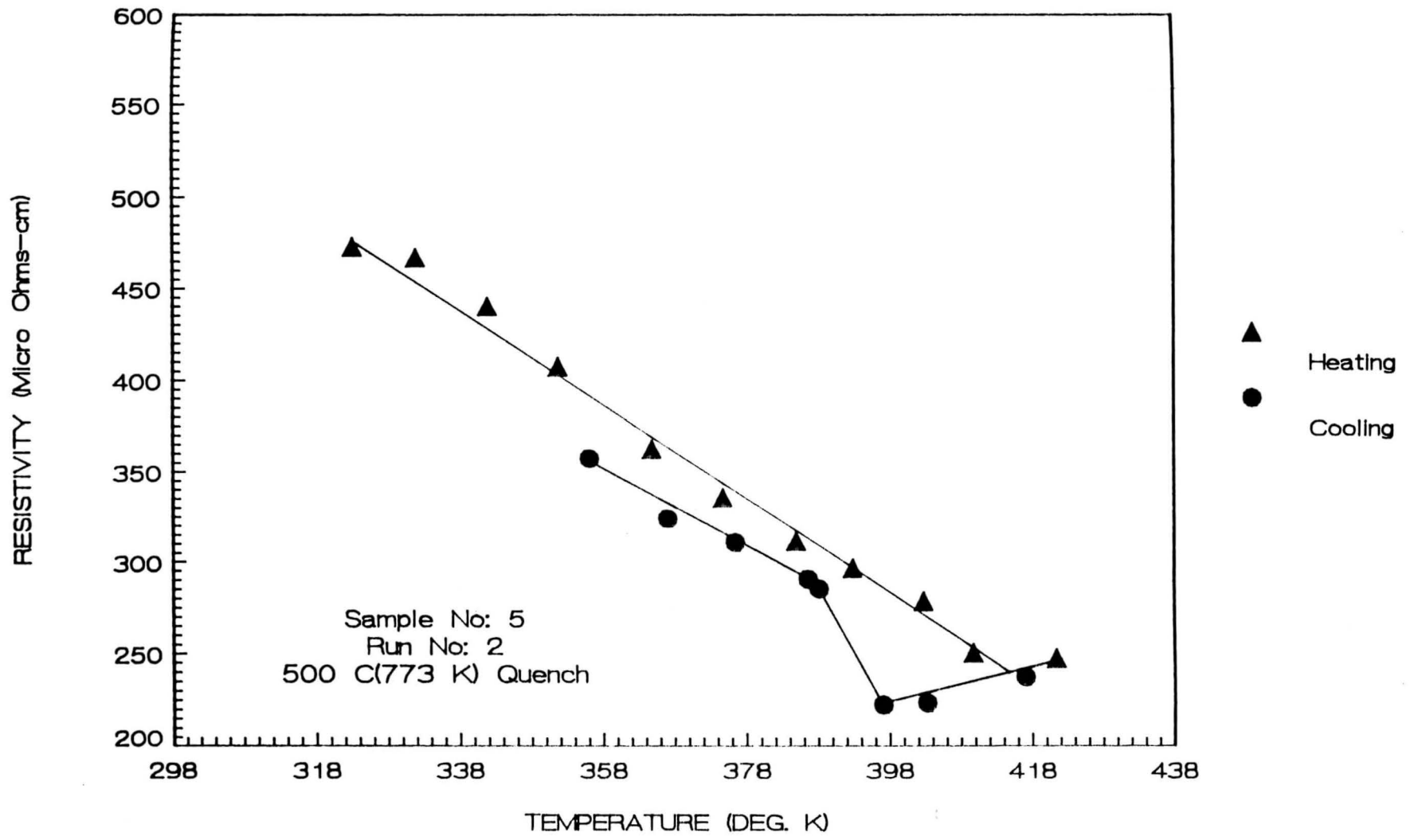


Figure 27. Variation of resistivity as a function of temperature

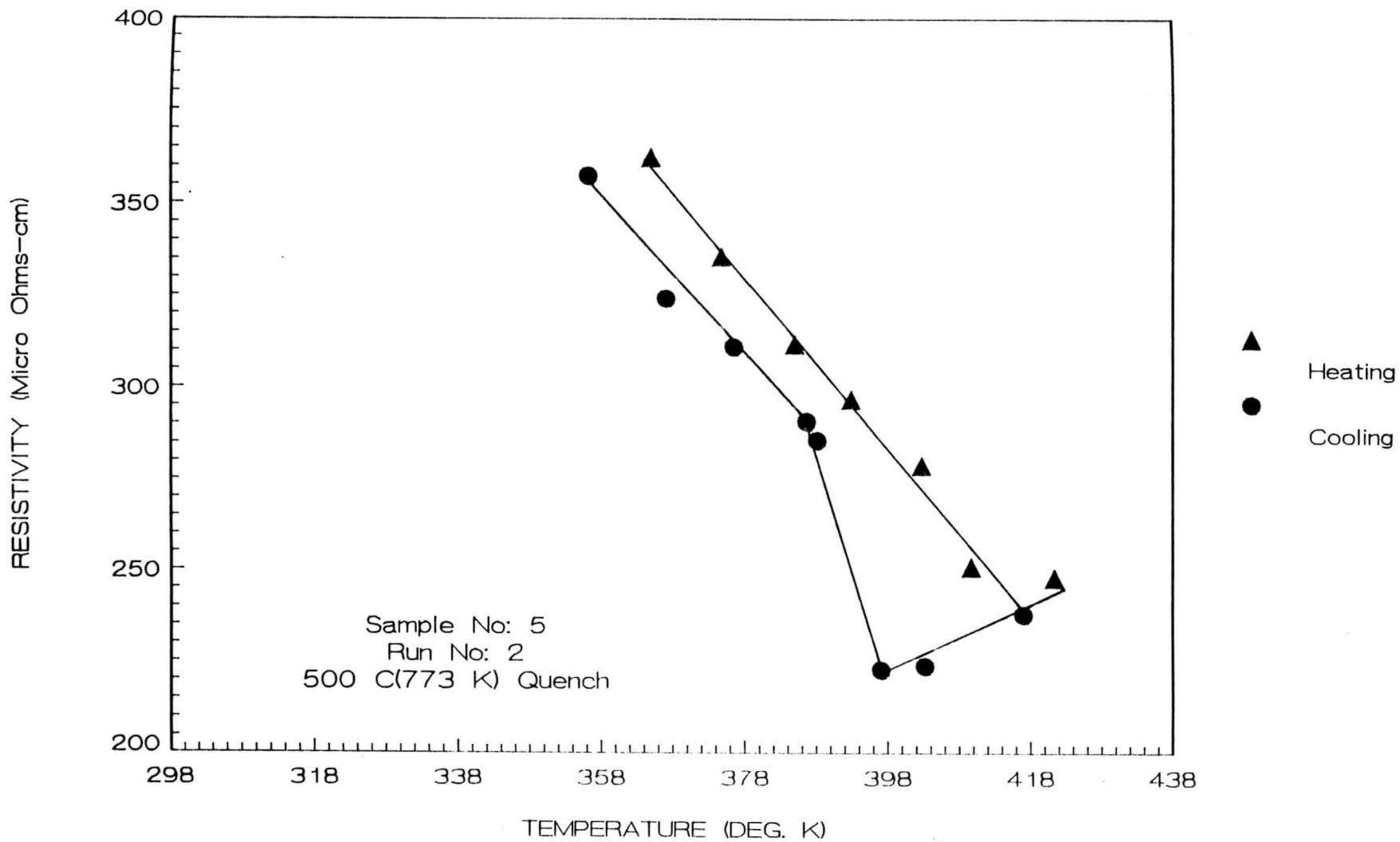


Figure 27a. Variation of resistivity as a function of temperature

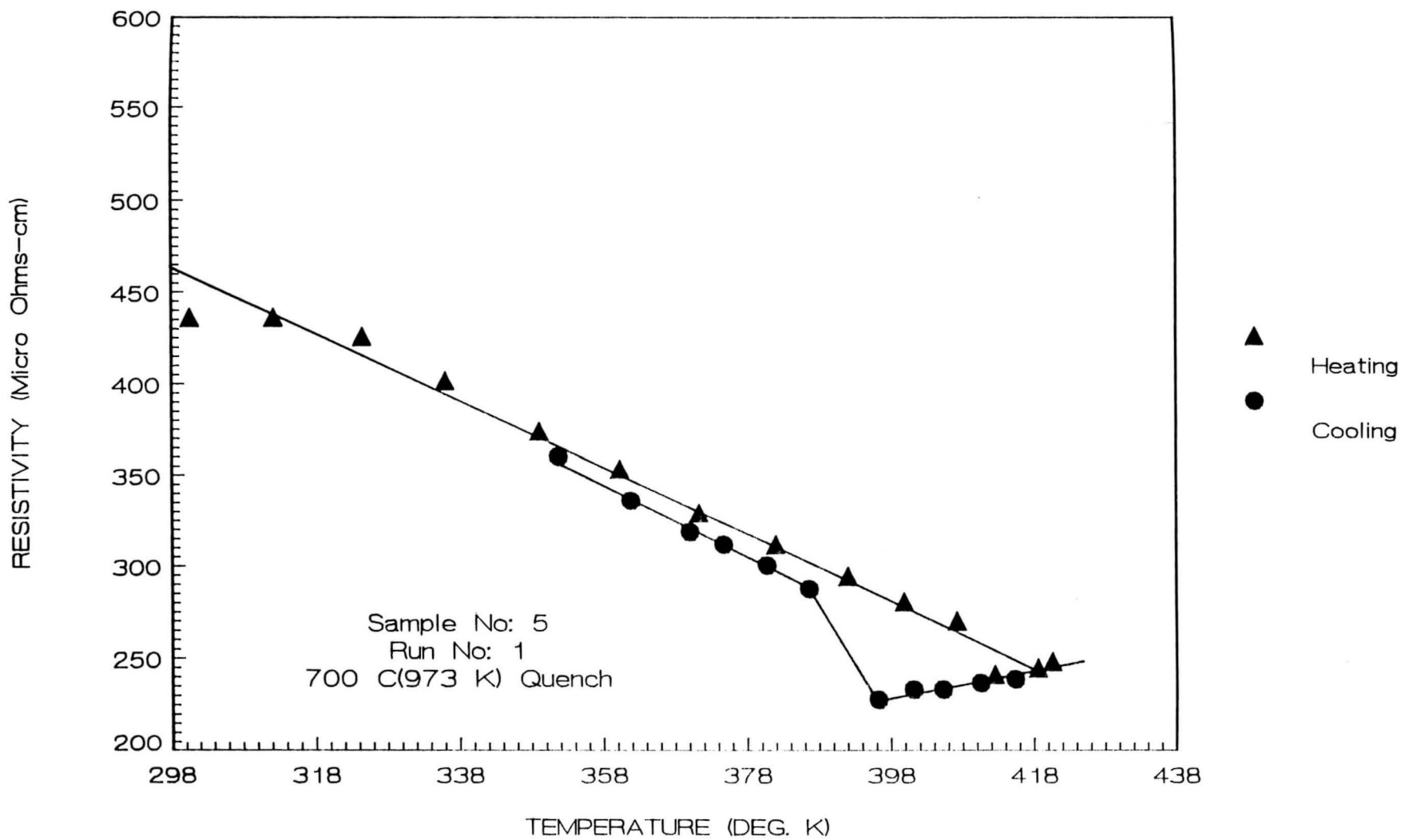


Figure 28. Variation of resistivity as a function of temperature

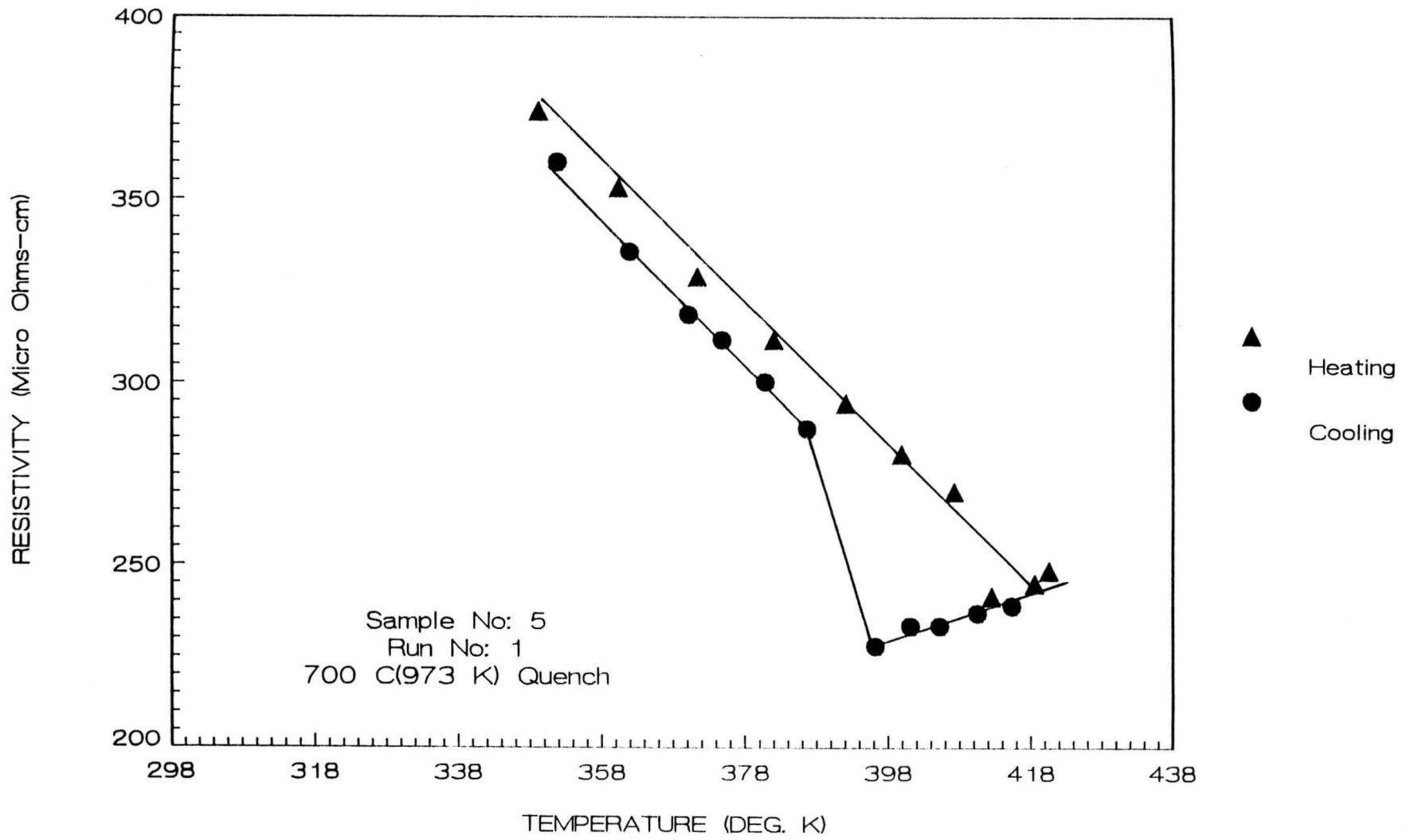


Figure 28a. Variation of resistivity as a function of temperature

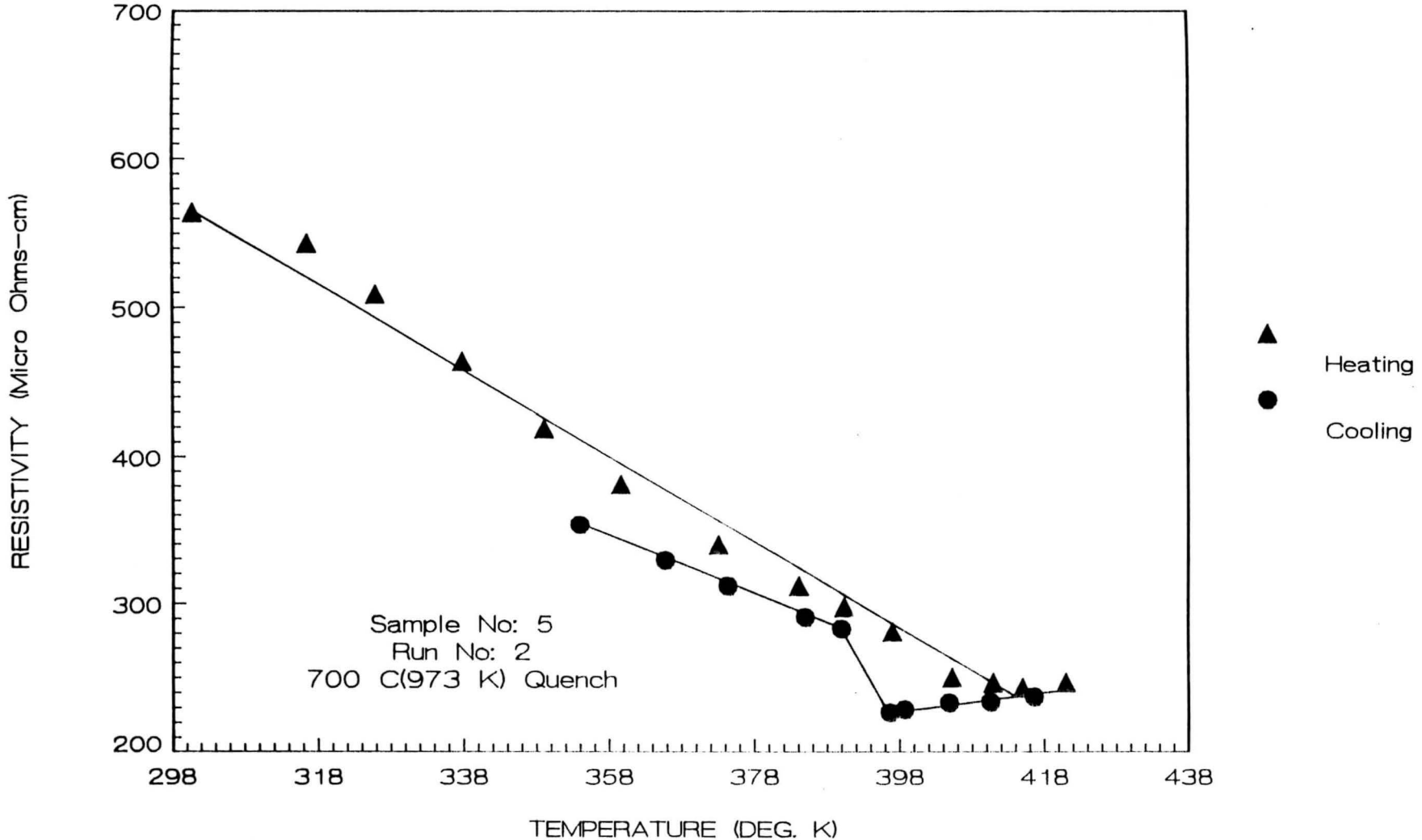


Figure 29. Variation of resistivity as a function of temperature

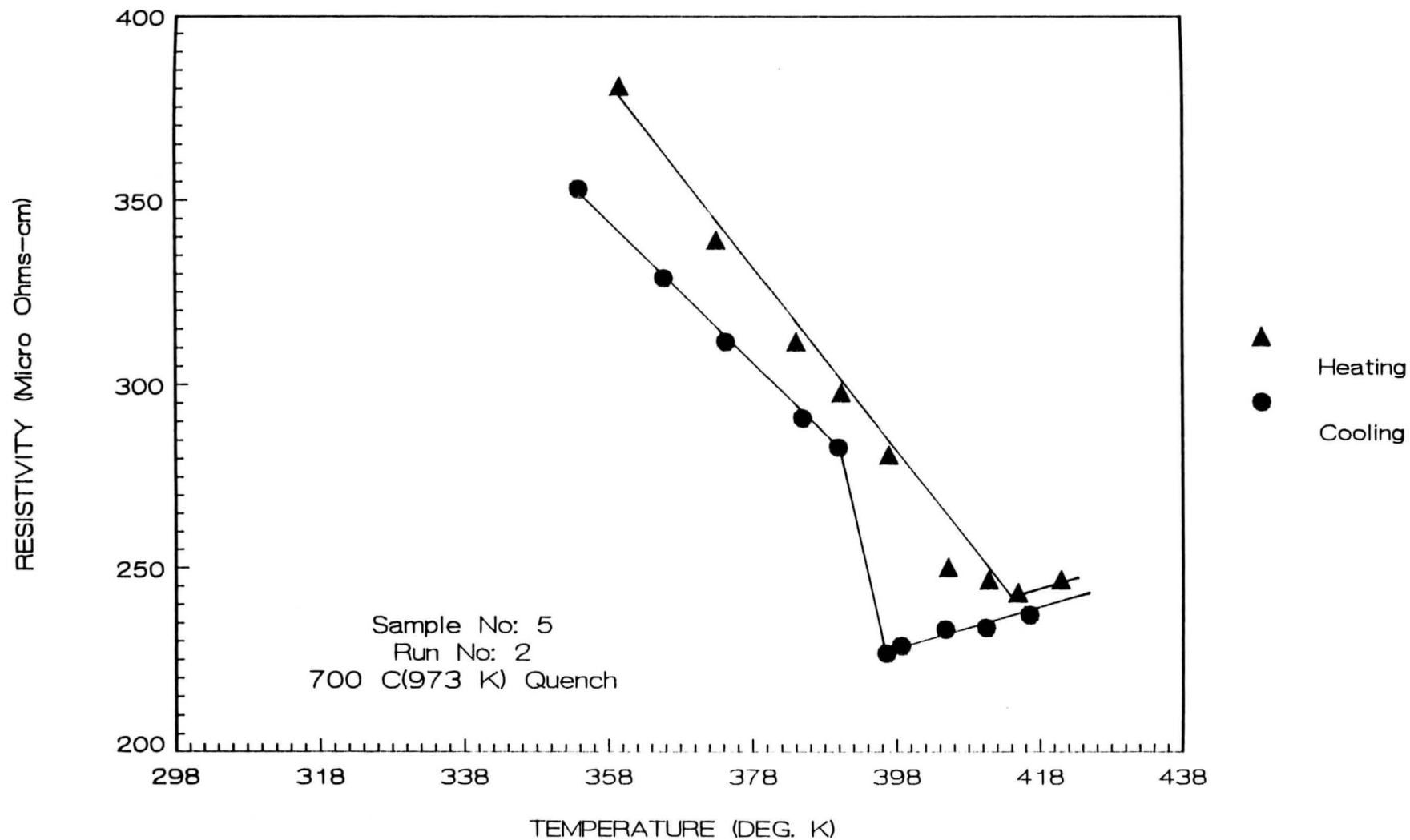


Figure 29a. Variation of resistivity as a function of temperature

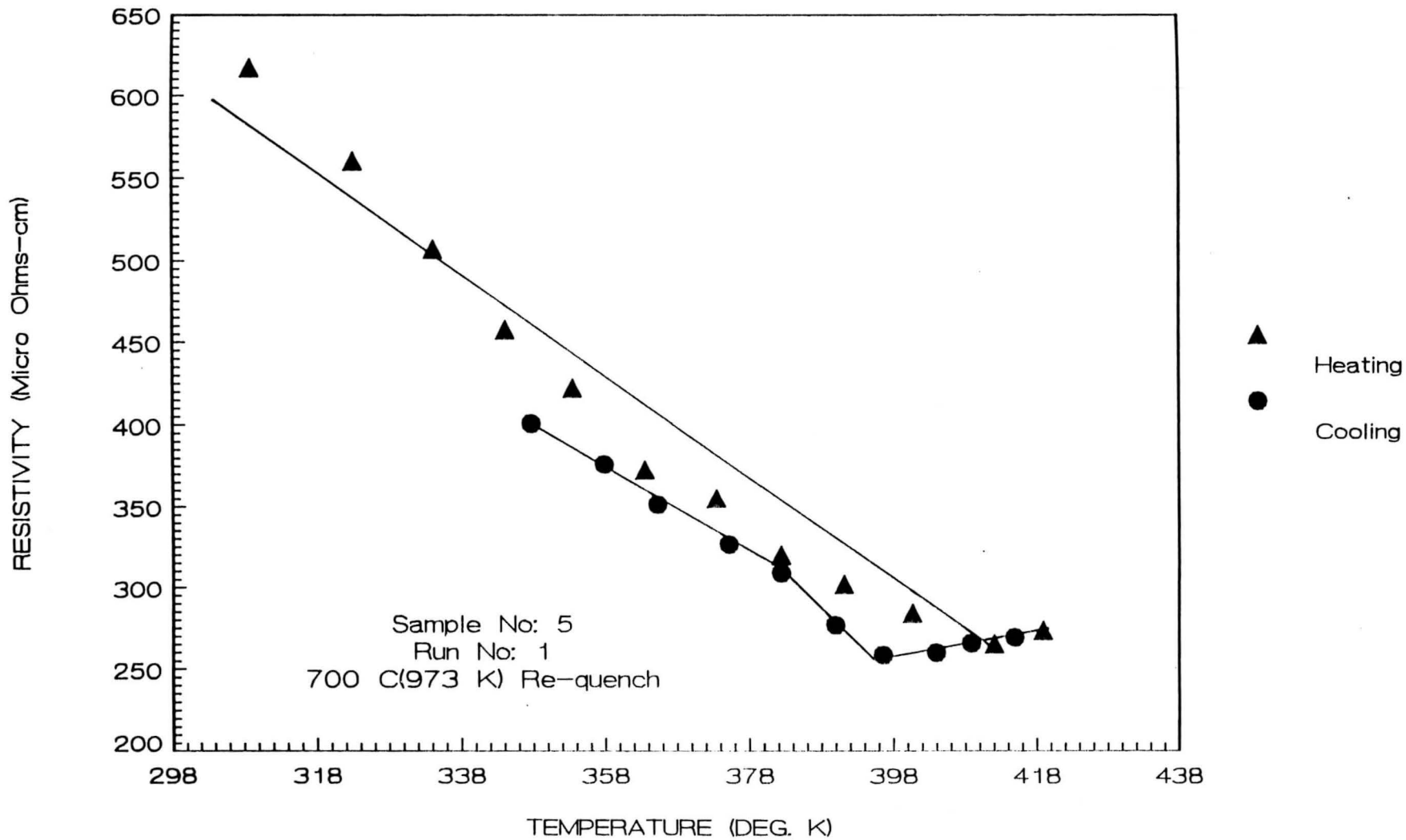


Figure 30. Variation of resistivity as a function of temperature

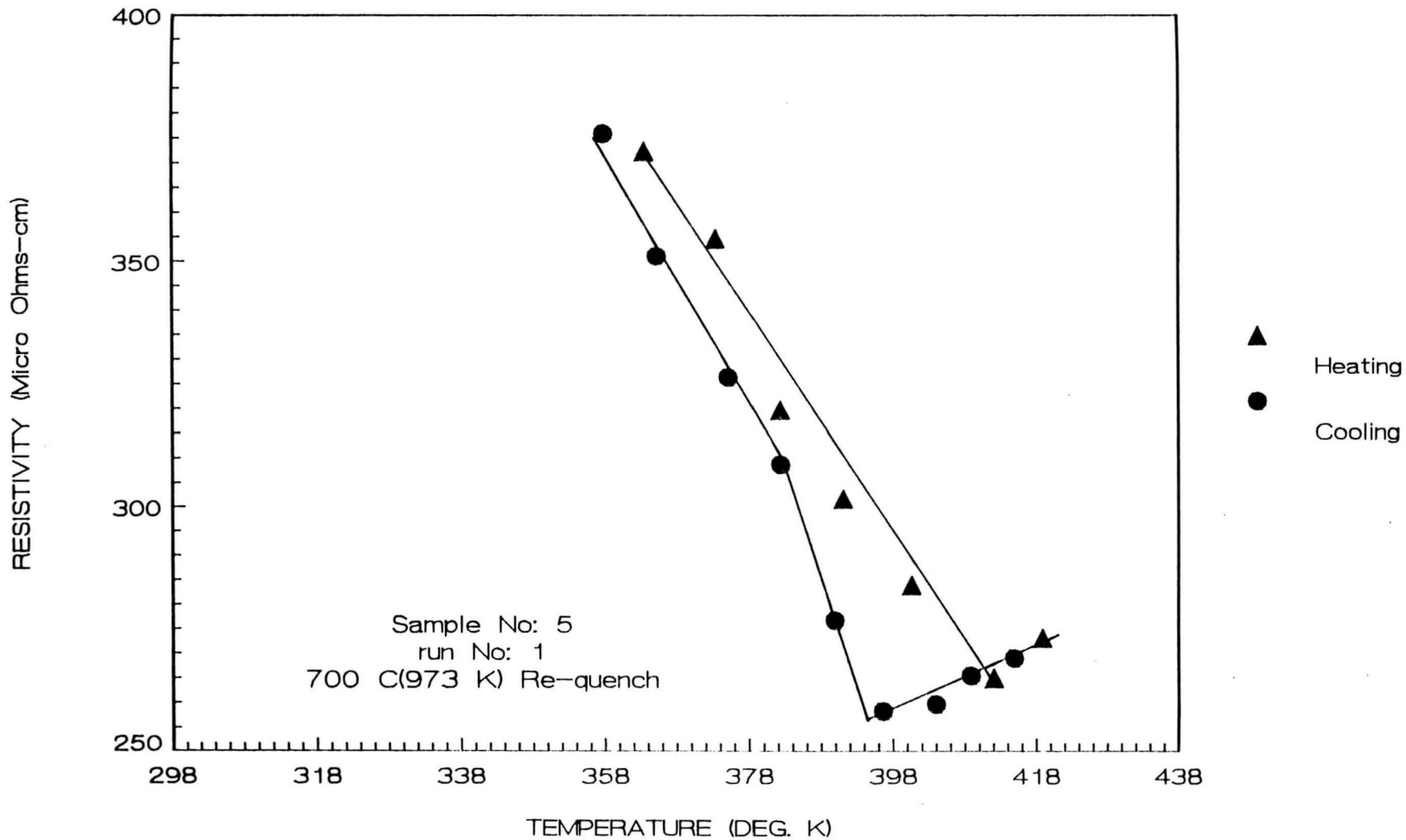


Figure 30a. Variation of resistivity as a function of temperature

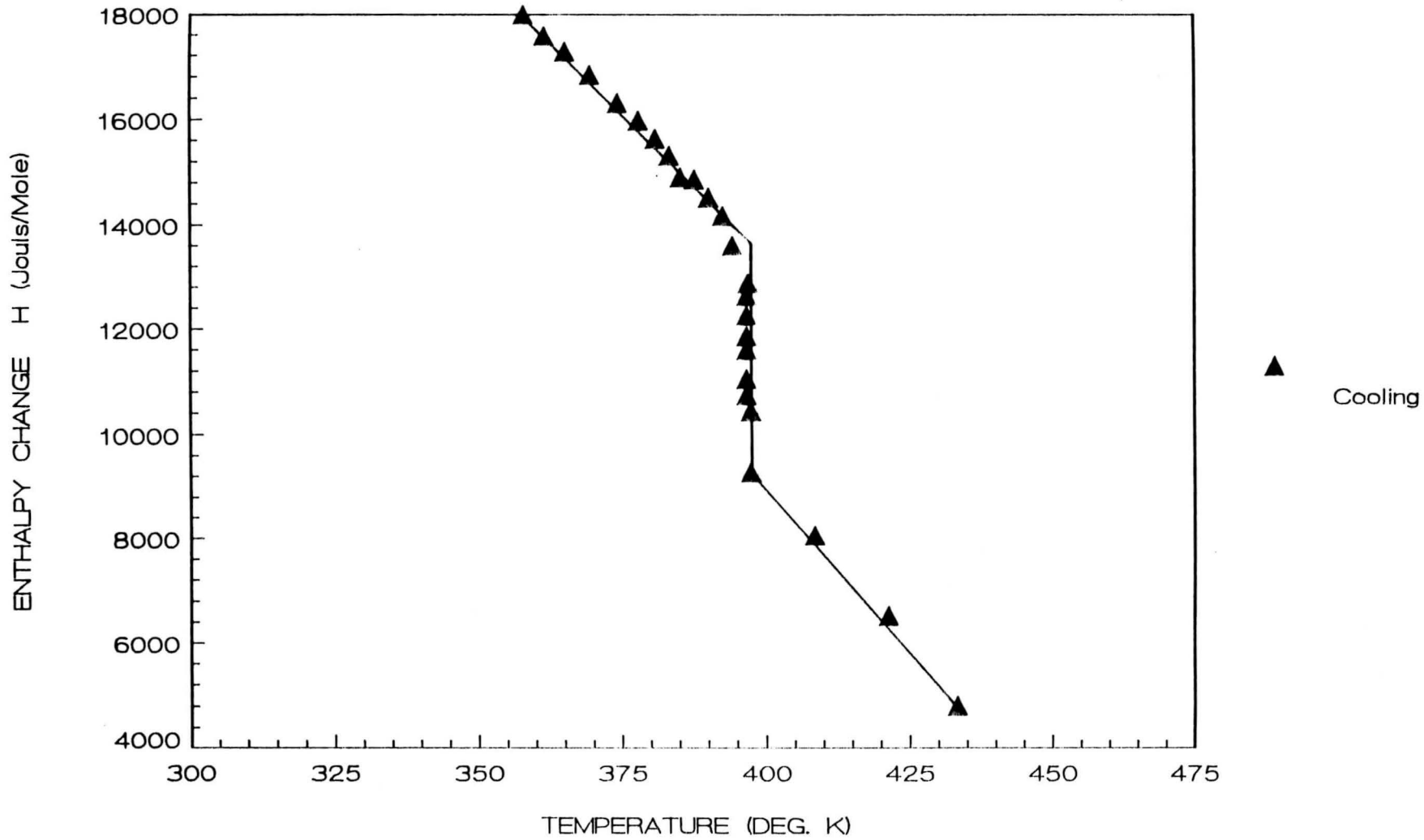


Figure 31. Enthalpy change as a function of temperature

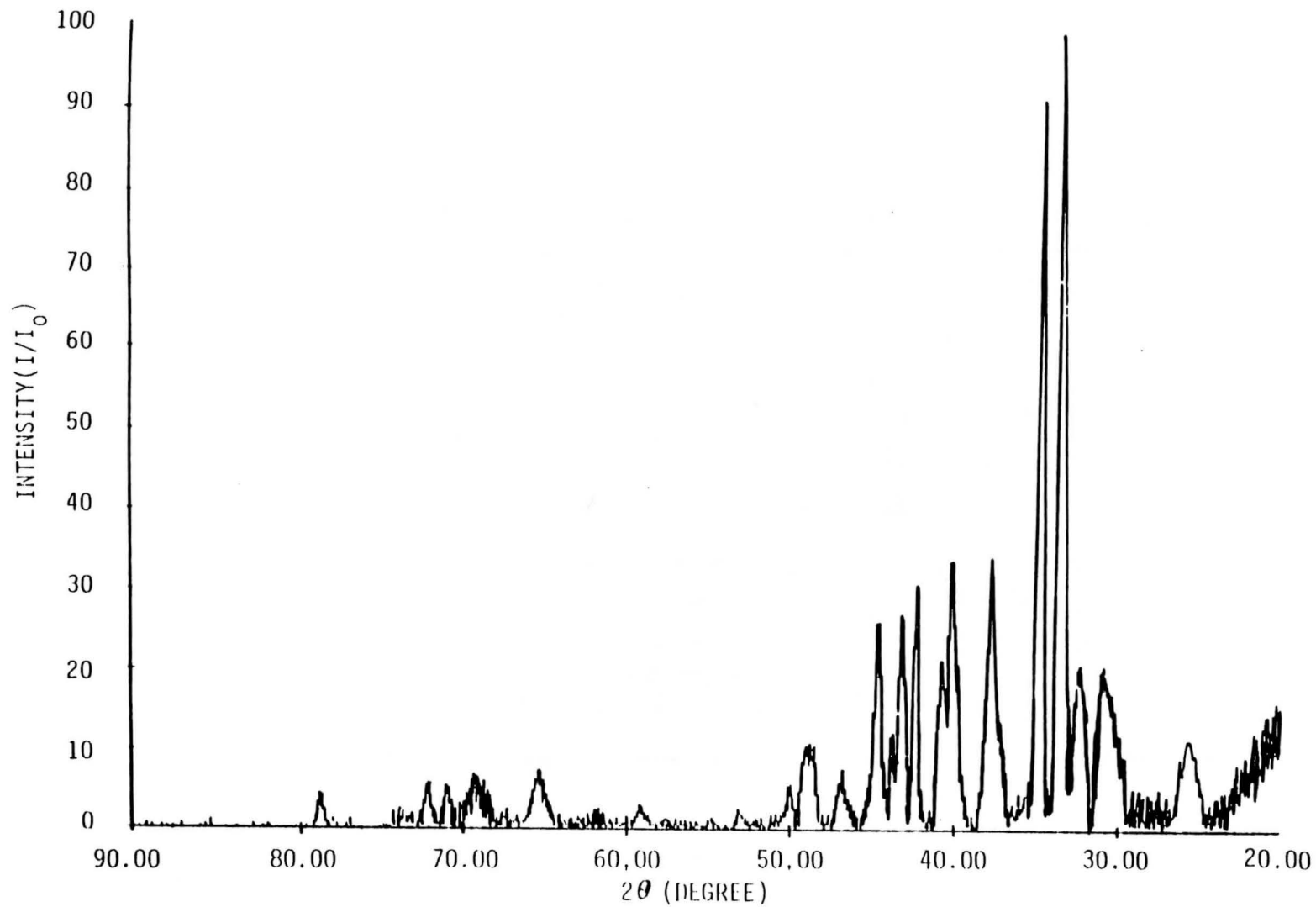


Figure 32. X-ray diffraction pattern of Ag_2Se at 25°C (298°K)

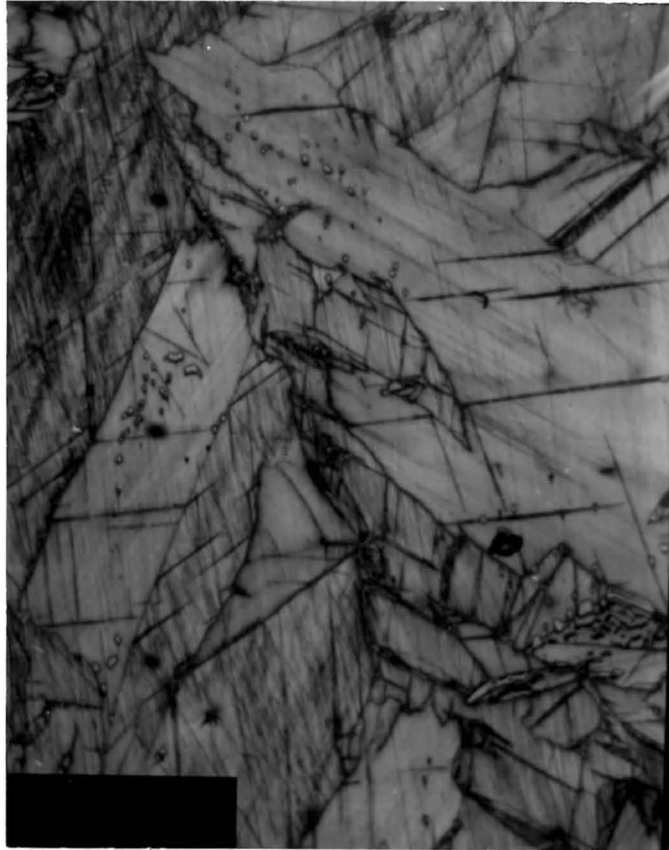


Fig. 33- Photomicrograph shows the twin
boundaries in different crystal grains
Sample No: 3
Treatment: 300°C (573°K) quench
Etching Reagent: Saturated solution of
 $K_2Cr_2O_7$ with 0.2% H_2SO_4
Magnification: 500X



Fig. 34- Photomicrograph shows transformation product which is needle shaped
Sample No: 3
Treatment: 300°C (573°K) quench
Etching Reagent: Saturated solution of $K_2Cr_2O_7$ with 0.2% H_2SO_4
Magnification: 500X



Fig. 35- Photomicrograph shows transformation product which is needle shaped
Sample No: 3
Treatment: 300°C (573°K) quench
Etching Reagent: Saturated solution of $K_2Cr_2O_7$ with 0.2% H_2SO_4
Magnification: 500X

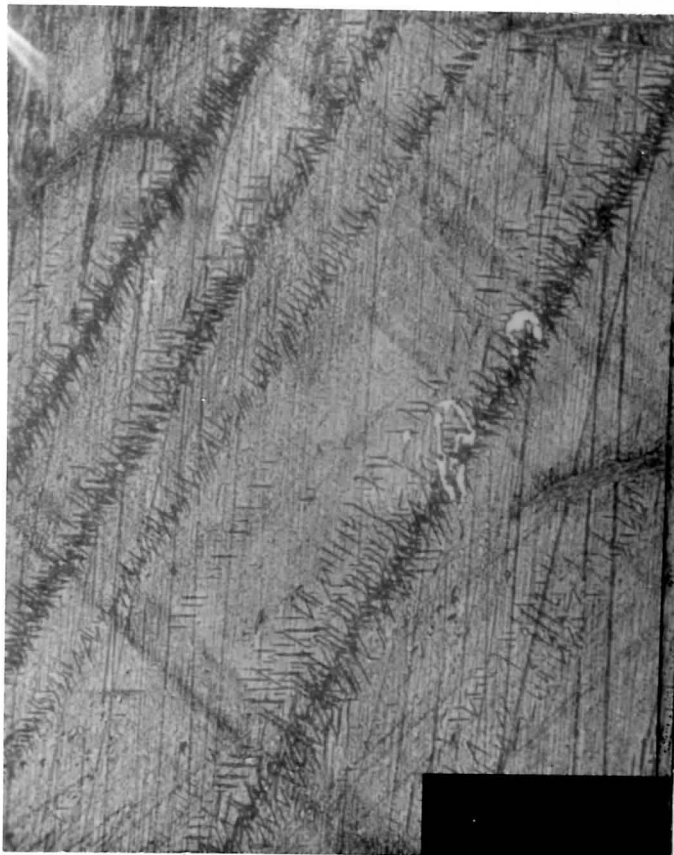


Fig. 36- Photomicrograph shows both twin traces
and needle shaped transformation product
in grains
Sample No: 4
Treatment: As annealed
Etching Reagent: Saturated solution of
 $K_2Cr_2O_7$ with 0.2% H_2SO_4
Magnification: 500X

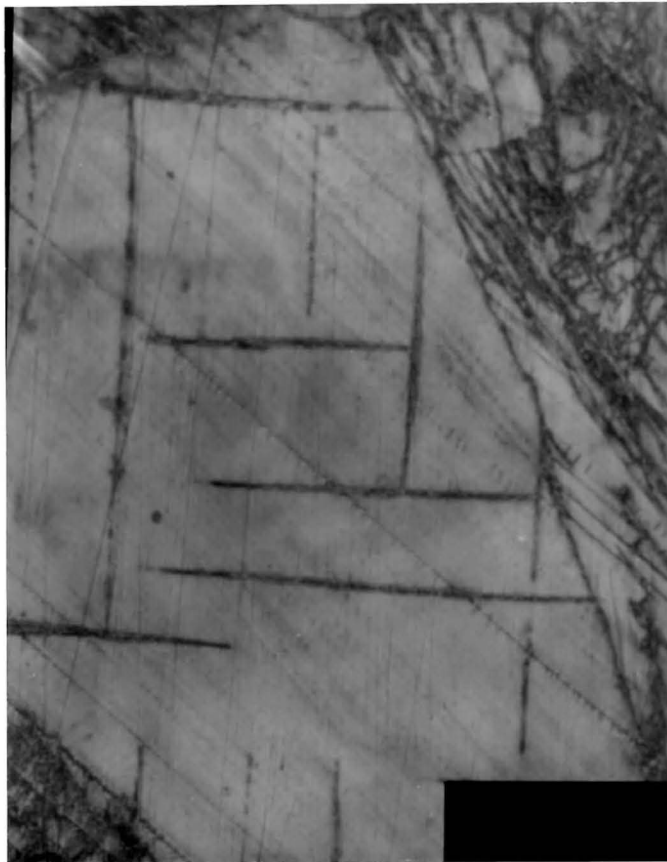


Fig. 37- Photomicrograph clearly shows traces of twin lamellae with adjoining midrib
Sample No: 4
Treatment: As annealed
Etching Reagent: Saturated solution of $K_2Cr_2O_7$ with 0.2% H_2SO_4
Magnification: 500X

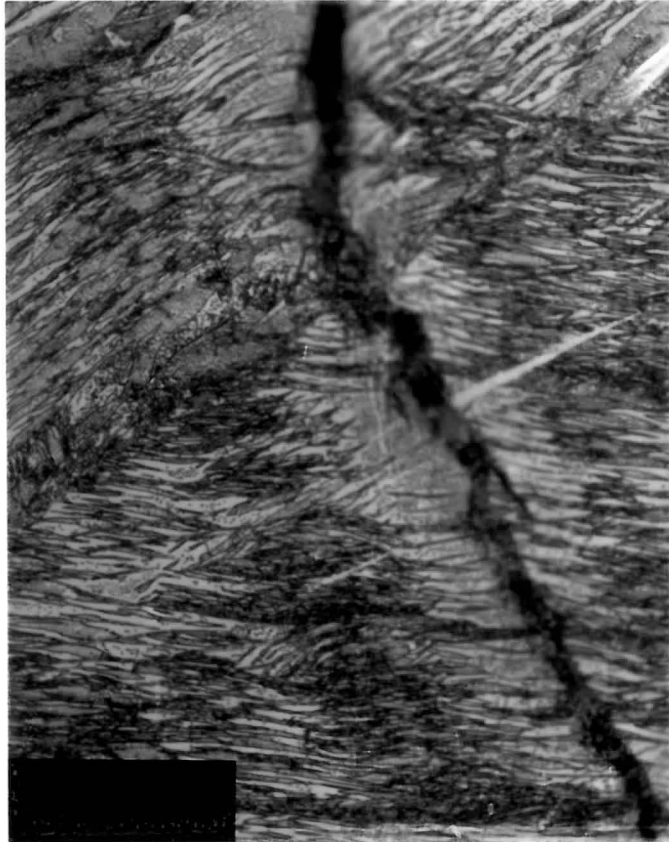


Fig. 38- Photomicrograph clearly shows traces of twin lamellae with adjoining midrib
Sample No: 5
Treatment: 700°C (973°K) quench
Etching Reagent: Saturated solution of $K_2Cr_2O_7$ with 0.2% H_2SO_4
Magnification: 500X



Fig. 39- Photomicrograph clearly shows traces of twin lamellae with adjoining midrib
Sample No: 5
Treatment: 700°C (973°K) quench
Etching Reagent: Saturated solution of $K_2Cr_2O_7$ with 0.2% H_2SO_4
Magnification: 500X



Fig. 40- Photomicrograph shows both twin traces and needle shaped transformation product in grains

Sample No: 5

Treatment: 700°C (973°K) quench

Etching Reagent: Saturated solution of

$K_2Cr_2O_7$ with 0.2% H_2SO_4

Magnification: 500X

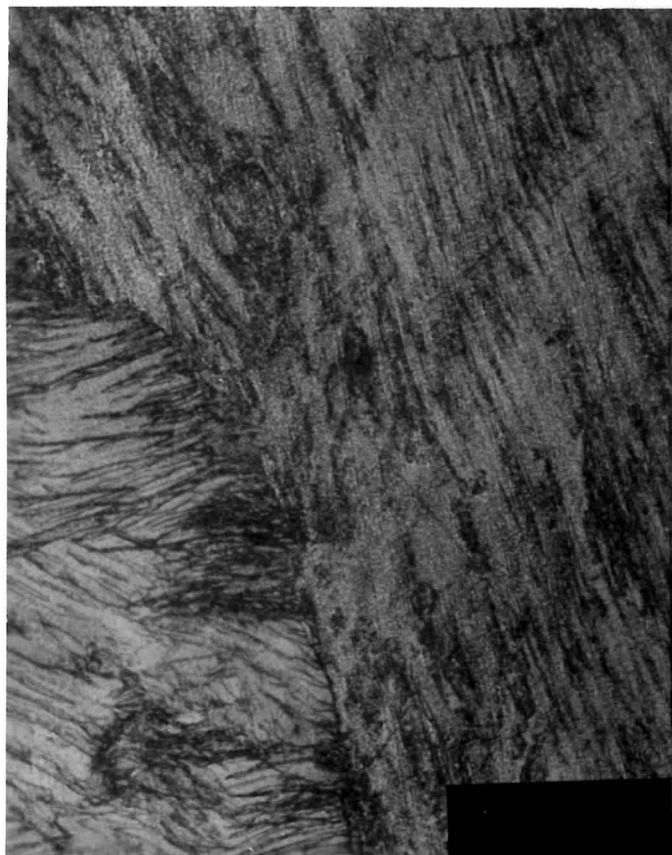


Fig. 41- Photomicrograph shows both twin traces and needle shaped transformation product in grains

Sample No: 5

Treatment: 700°C (973°K) quench

Etching Reagent: Saturated solution of $K_2Cr_2O_7$ with 0.2% H_2SO_4

Magnification: 500X

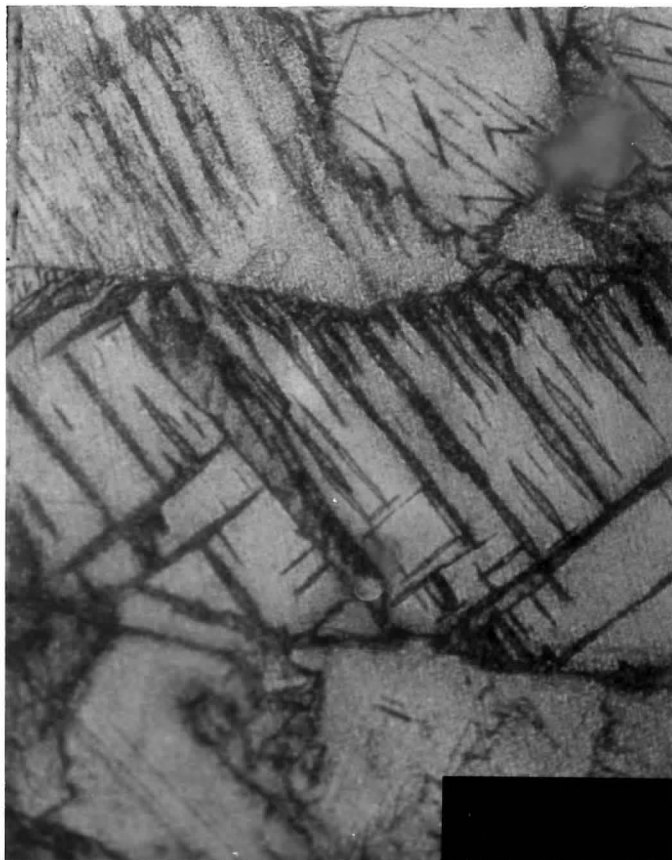


Fig. 42- Photomicrograph clearly shows twin
lamaellae with adjoining midrib
Sample No: 5
Treatment: 700°C (973°K) quench
Etching Reagent: Saturated solution of
 $K_2Cr_2O_7$ with 0.2% H_2SO_4
Magnification: 500X

CHAPTER IV

DISCUSSION

Silver-selenide exhibits many interesting properties. Several interesting results were found in this investigation by metallographic, thermodynamic, resistivity, and X-ray studies. This investigation was based on silver-selenide inter-metallic compound prepared from highly pure silver and selenium metals. It undergoes a first order phase transformation from cubic to orthorhombic.

Silver-selenide inter-metallic compound undergoes a diffusionless phase transformation at about 122 °C (395 °K) on cooling and about 134 °C (407 °K) on heating. It is clear from thermodynamic results that in addition to the above results, 95% of the transformation is completed spontaneously at about 123.16 °C (396.16 °K). Beyond this stage, transformation slows down due to an instability introduced by the large volumetric change associated with the phase transformation. Finally, the transformation is completed at about 124 °C (397 °K). These results are further substantiated by resistivity studies. The enthalpy of phase transformation is determined to be 1050 cal/mole. This value is higher than the average value listed by Hultgreen (1). The possible reason could be the use of different methods in the preparation of Ag_2Se . The specific

heat and enthalpy changes are listed in tables 8 and 9.

The resistivity study was carried out using three samples. Samples 3 and 5 did not show any phase transformation upon heating, but did show transformation upon cooling at about 122 °C (395 °K). Sample 4 showed transformation upon heating at about 134 °C (407 °K) and upon cooling at about 122 °C (395 °K). The reason samples 3 and 5 did not transform upon heating is not well understood at this present time and further investigation is necessary.

The transformation temperature, on cooling, of samples 3, 4, and 5 agrees well with that of the sample used for thermodynamic studies.

A study was initiated to investigate the effect of quenched-in vacancies on all three samples. Phase transformation appears, on cooling, almost at the same temperature in annealed and quenched samples. This indicates that the transformation was not influenced by the quenching operation even from different quenching temperatures.

The change in resistivity at the phase transformation temperature on cooling was not the same in annealed and quenched samples. The resistivity change for sample 4, in as-annealed condition, was about 580 Micro ohm-cm in the heating and cooling cycles, and for samples 3 and 5 were about 59 Micro ohm-cm in the cooling cycle. Also, the resistivity change for sample 4, for 700 °C quench, was about 265 Micro ohm-cm in the heating and cooling cycles, and for samples 3 and 5 were about 57 Micro ohm-cm in the cooling cycle. The above results seem to indicate that the strain

accompanying the volume change upon transformation on cooling is gradually accommodated by the atomic adjustment provided by the quenched-in vacancies.

It is interesting to note that holding the sample at a higher temperature for a length of time did decrease the resistivity change associated with the phase transformation but not the transformation temperature. Further attempts were made to see the effect of different quenching sequences. The results indicate that the vacancy concentration quenched-in at higher temperature with those of quenched-in at lower temperature or vice versa did not produce any significant change in the phase transformation kinetics. So, it can be concluded that the defect structure in this case does not change the phase transformation kinetics.

X-ray studies were carried out to determine the crystal structure of the low temperature phase. After calculations, an orthorhombic unit cell was found with lattice parameters: $a = 4.333 \text{ \AA}$, $b = 7.062 \text{ \AA}$, and $c = 7.764 \text{ \AA}$. The high temperature phase has been reported to be cubic with lattice parameter $a = 4.98 \text{ \AA}$. The volume change accompanying the phase transformation is about 40%, with the low temperature phase having the larger volume.

The metallographic results do exhibit several important characteristic features of the phase transformation products in the low temperature phase (figures 33 through 42). It can be seen in the above photographs that the transformation product falls into two structural modifications. The first type consists of twin related lamellae. Within each

lamaellae there are secondary twins in a direction perpendicular to the original twin (figures 33 and 38). Some variations of the twin traces can be seen in figure 40. It appears that the transformation twin starts in different directions at the same time. The second type of structure consists of needle-shaped transformation products originating from a grain boundary (figures 41 and 42). The above structural modifications do exist in certain areas together at the same time (figure 36). Here the needle-shaped products originate at the twin boundary and radiate out in a particular direction at right angle to the twin boundary in a parallel fashion. This observation seems to suggest that the needles in this picture are indeed secondary twins within the twin lamaellae as seen earlier.

CHAPTER V

CONCLUSION

This investigation directly results in the determination of the following parameters:

1. The crystal structure and the lattice parameters of the low temperature phase.
2. The resistivity values of annealed and quenched samples.
3. The thermodynamic properties in the temperature range of 181 °C (454 °K) to 75 °C (348 °K) from which the enthalpy of phase transformation and the specific heat have been determined.

From the above results the following characteristics of phase transformation are determined:

4. Silver-selenide intermetallic compound undergoes a first order phase transformation from cubic to orthorhombic at 122 °C (395 °K) on cooling.
5. The phase transformation is martensitic in nature with athermal characteristics.
6. The volume change accompanying the phase transformation is about 40% with the low temperature phase having the larger volume.
7. The phase transformation temperature is fixed and unaffected by point defects introduced by the

quenching operation.

8. The resistivity change accompanying the phase transformation does increase with the increase in the quenching temperature. It is simply due to the increase in the quenched-in vacancies. However, this increase in the vacancy concentration does not influence the transformation temperature.
9. The transformation products on cooling consist of two sets of twins. The first set includes relatively large twin lamellae and the second set consists of sets of twins within a twin lamellae.

APPENDIX
LIST OF SYMBOLS

LIST OF SYMBOLS

SYMBOL	DEFINITION	UNITS
K	Characteristic Radiation of X-ray Tube	None
	Wavelength of X-ray	$^{\circ}\text{A}$
a, b, and c	Lattice Parameters of A, B, and C axis	$^{\circ}\text{A}$
2θ	Angle	Degree
T_s	Starting temperature of Transformation	Kelvin
T_f	Ending Temperature of Transformation	Kelvin
T_c	Mean Transformation Temperature During Cooling	Kelvin
T_h	Mean Transformation Temperature During heating	Kelvin
$\Delta\rho_{tc}$	Resistivity Change During Phase Transformation for Cooling Curve	μ Ohm-cm
$\Delta\rho_{th}$	Resistivity Change During Phase Transformation for Heating Curve	μ Ohm-cm
ΔH	Enthalpy Change	J/mole
C_p	Specific Heat	J/mole $^{\circ}\text{K}$

REFERENCES

- 1 Hultgreen, R., Selected Values of the Thermodynamics Properties of Binary Alloys, 1973, P. 95
- 2 Earley, J. W., Description and Synthesis of Selenide Mineral, V. 35, 1950, P. 377
- 3 Boetcher, A. G., Z. Angew. Phys., V. 7, 1955, P. 487
- 4 Junod, P., Helv. Phys. Acta., V. 32, 1959, P. 567
- 5 Conn, J. B., J. Electrochem Society, V. 107, 1960 P. 977
- 6 Cho, C. L., Kristallografiya, V. 7, 1962, P. 66-71
- 7 Pinsker, Z. G., Soviet Physics Crys., V. 7, 1962, P. 52-57
- 8 Sharma, S. K., Physics Letters, V. 9, 1964, P. 218-219
- 9 Akiyama, K., National Technical Report, V. 8, 1962, P. 241-250
- 10 Wyckoff, B. W. G., Crystal Structures, V. 1, Chap. 4, 1948, P. 34
- 11 Pellini, G., Gazz. Chim. Ital., V. 45, 1915, P. 533-539
- 12 Bellati, M., Atti. Ist. Veneto, V. 7, 1888, P. 1051
- 13 Walsh, P. N., J. Physics Chemistry, V. 66, 1962, P. 1546
- 14 Bear, Y., Z. Naturforsch, V. 17, 1962, P. 886-9
- 15 Villars, P., Pearson's Handbook of Crystallographic Data for Intermetallic Phases, V. 2, 1985, P. 882
- 16 Roy, R., Economic Geology, V. 54, 1959, P. 1278-80